GUERAP:
General Unwanted Energy Rejection Analysis Program User's Manual

Honeywell, Inc.

OCTOBER 1972

AD755353

GUERAP:

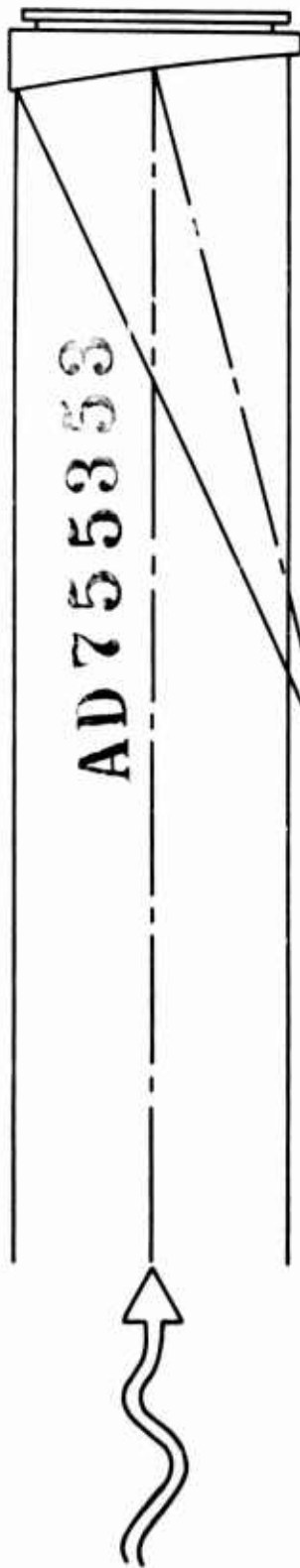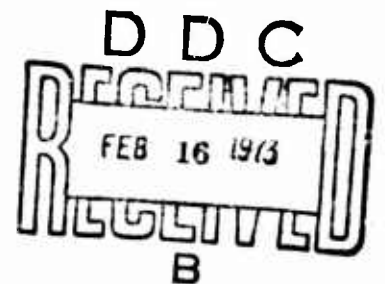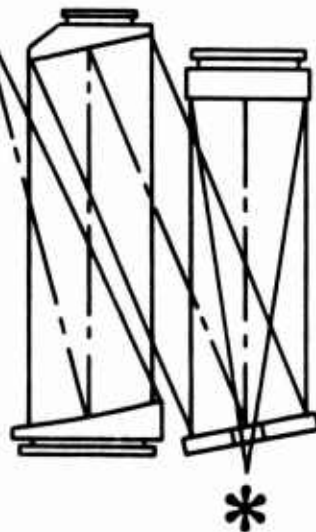## General Unwanted Energy Rejection Analysis Program

USER'S MANUAL

FOR
USAF SPACE AND MISSILE
SYSTEMS ORGANIZATION
EL SEGUNDO, CALIFORNIA

*

Honeywell

D D C
RECEIVED
FEB 16 1973
B

127

DOCUMENT CONTROL DATA - R & D

(Security classification of title, body of abstract and indexing annotation must be entered when the overall report is classified)

1. ORIGINATING ACTIVITY *(Corporate author)*	2a. REPORT SECURITY CLASSIFICATION
Honeywell Inc. Aerospace Division St. Petersburg, Florida	Unclassified
	2b. GROUP

3. REPORT TITLE

GUERAP: General Unwanted Energy Rejection Analysis Program
User's Manual

4. DESCRIPTIVE NOTES *(Type of report and inclusive dates)*

User's Manual

5. AUTHOR(S) *(First name, middle initial, last name)*

Tien S. Chou

6. REPORT DATE	7a. TOTAL NO. OF PAGES	7b. NO. OF REFS
5 October 1972	127	5
8a. CONTRACT OR GRANT NO. SAMSO F04701-71-C-0377	9a. ORIGINATOR'S REPORT NUMBER(S) UERTD TM 3366-008	
b. PROJECT NO.		
c.	9b. OTHER REPORT NO(S) *(Any other numbers that may be assigned this report)*	
d.	SAMSO TR No. 72-314, Vol I	

10. DISTRIBUTION STATEMENT

Approved for public release; distribution unlimited.

11. SUPPLEMENTARY NOTES	12. SPONSORING MILITARY ACTIVITY
	USAF Space and Missile Systems Organization El Segundo, California

13. ABSTRACT

This report documents a significant new optical system analysis tool, the General Unwanted Energy Rejection Analysis Program (GUERAP). This computer code is able to efficiently and accurately measure the off-axis rejection characteristics of a given optical system or baffle. It is applicable to a wide spectrum of systems, such as radiometers, star trackers and sensors, optical system baffles, optical test chambers, spacecraft sun and Earth shields, etc.

In addition to being a powerful off-axis rejection analysis tool, the GUERAP can also be used to evaluate on-axis image quality for most optical systems, including those with very complex geometry, and for the evaluation of the effect of both internal and external emission energy on infrared systems.

DD FORM 1473
1 NOV 65

i

14 KEY WORDS	LINK A		LINK B		LINK C	
	ROLE	WT	ROLE	WT	ROLE	WT
GUERAP - General Unwanted Energy Rejection Analysis Program						
Energy Rejection Analysis						
Optical System Simulation						
Radiometer Simulation						
Scattering						
Diffraction						
Thermal Emission						

GUERAP

(GENERAL UNWANTED ENERGY REJECTION ANALYSIS PROGRAM)

USER'S MANUAL

Prepared by

T. S. Chou
Surveillance Section

Honeywell

AEROSPACE DIVISION
ST PETERSBURG, FLORIDA

iii

TABLE OF CONTENTS

TABLE OF CONTENTS (Continued)

LIST OF ILLUSTRATIONS

LIST OF ILLUSTRATIONS (Continued)

LIST OF TABLES

Section 1

INTRODUCTION

The statistical approach to the solution of radiant energy transfer among surfaces of a system, commonly known as the Monte Carlo Method, makes it possible to attack difficult problems which are not amenable to conventional analytical or computer methods such as Fourier Transform techniques. Monte Carlo methods represent radiant energy flux statistically as rays which can be traced through the system according to a set of probability distribution functions. Although the ray representation of the radiant energy is similar to that of a photon characterization, it is treated in this method as merely a statistical representation.

A distinct disadvantage of the method is the extremely large number of calculations necessary to simulate a fairly complicated system with a reasonable degree of accuracy. With the advent of high speed digital computers, however, it has become a feasible tool in a wide variety of problems.

With the general radiation analysis in mind, the GUERAP (General Unwanted Energy Rejection Analysis Program) was written specifically for tracing radiant energy through systems with extremely high attenuation. Since the number of rays necessary to analyze a system normally is directly proportional to its attenuation, the "brute force" Monte Carlo method becomes impractical in tracing rays through systems with high attenuations, e. g., $> 10^6$.

Many rays are required for a high attenuation system because all but a handful of the rays generated are lost in the system, without contributing anything to the net energy at points of interest, e.g., a detector. The situation can be drastically improved if rays are directed to follow predetermined paths toward the points of interest.

This is accomplished by dividing the angular probability density distribution function of an emerging ray into multiple sections. Each section is represented by a ray whose direction is randomly selected within the angular confine of the section. The total energy of the original ray is distributed among the several rays according to their "share" of the total probability distribution function. This method is commonly known as the Importance Sampling or Expected Value Technique (Reference 1).

Diffraction of radiant energy as it passes through an aperture is generally regarded as a manifestation of the wave-like nature of radiation. The theory then dictates that the diffraction pattern behind the aperture can only be obtained by simultaneously considering the total wave in the system, thus making it impossible to rigorously include diffraction effects by the Monte Carlo ray tracing approach.

A semi-empirical diffraction model is adopted in this program that assumes an angular probability density function of a ray as it passes through a small aperture (Reference 2). The model makes use of the prediction by the Uncertainty Principle (Reference 4) which allows the ray to be bent as a result of the interaction between the ray and the aperture edge. The model is successfully tested by comparing results of several simple systems with classical solutions.

To analyze radiant energy transfer in a system, the user first represents the system with a set of surfaces, expressible in terms of simple equations. A series of basic surfaces that can be used for such purpose are presented in Section 2. Although it is sometimes necessary to supplement by inputting surfaces in terms of general equations, these basic surfaces are sufficient for most systems commonly encountered. We then proceed to present the procedure of simulating the systems.

In Section 3, details are given for various radiation models. These include emission, absorption, reflection, transmission, refraction and diffraction. The total energy of a ray interacting with a surface is represented by an angular distribution function for each model.

The importance sampling technique is briefly described in Section 4. For the usage of the technique, the user is referred to the procedure of assigning important surfaces given in Section 2 as well as Section 4.

For users who wish to gain better understanding of the program, Section 5 presents a brief description of the program structure and the purpose of each subroutine. Flow charts are given for the main program and the commanding subroutines.

The complete set of input parameters is listed in Section 6. Each parameter is followed by a brief definition and the page number for reference. An experienced user of the program can complete a set of input data with the help of this section alone.

Most of the output listing and the error messages are self-explanatory. However, the user can refer to Sections 7 and 8 for more detailed explanations lacking in the output listing.

Finally, a series of examples are presented in Section 9. Experiences on the part of this writer indicate that, in learning the usage of a new program, it is sometimes easier to follow the lead of examples. For this reason, the examples are presented for problems with different degrees of complexity. As many features as deemed necessary to demonstrate the common usage of the program are included in the examples.

Section 2

SYSTEM CONFIGURATION

The basis of the Monte Carlo method is in tracing the probable paths of an energy bundle as it interacts with the optical system. The present program is concerned primarily with radiant energy transfer through non-participating media. Thus, interactions occur only when a ray is intercepted by an optical surface of the system.

In order to detect such interceptions, it is necessary to represent the surfaces by some mathematical model, preferably in the form of analytical equations that define the surfaces and their boundaries. A series of simple surfaces have been developed as the basis of a general optical system. While these surfaces are sufficient for the simulation of the systems encountered during the development of the program, some additional basic surfaces will undoubtedly be added as needs arise.

The basic surfaces with their standard boundaries (the boundaries defined by the basic parameters) will be first described. The boundaries, which we refer to as constraints, are represented by a set of constraint equations. Frequently, a surface requires a set of constraints other than the standard set. Thus, attention will be given to the method of prescribing these special constraints.

When a surface cannot be represented by any of the basic surfaces, the coefficients of the surface equation:

$$C_1 X^2 + C_2 Y^2 + C_3 Z^2 + C_4 XY + C_5 XZ + C_6 YZ + C_7 X + C_8 Y + C_9 Z = C_{10}$$

$$(2-1)$$

can be read in through the array

$$COEF(J,I) = C_J \qquad J = 1, 2, \ldots, 10$$

where I is the surface number. The degree of the equation is specified by the array IDGREE in input data set NAME2. Namely, IDGREE(I) is set at 1 if the first six coefficients in the surface equation are zero. Otherwise, it is set equal to 2. The set of constraints for the surface is specified as special constraints (see Subsection 2.2).

2.1 BASIC CONFIGURATION

2.1.1 Plane

A plane bounded by two concentric circles as shown in Figure 2-1 is used as the basic plane configuration. It is described by the coordinates of the center point (X_c, Y_c, Z_c), the unit normal vector (α, β, γ) and the radii of constraints R_1 and R_2. When it is possible, the unit normal should point into the region. The parameters in this sequence are stored as PTLCTR of the surface.

In subroutine PLANE coefficients of the surface and the constraint equations in terms of the system coordinates X-Y-Z* are calculated. The two inverse transformation matrixes between the two coordinate systems are calculated and stored. The unit normal $\hat{n}$ is used as the z-axis. The orientation of the x and y axes is immaterial.

There are two standard constraints. The first is the cylinder of radius R_1 around the unit normal $\hat{n}$ while the second is one of radius R_2 also around $\hat{n}$. $R_1 = 0$ indicates that there is no inner constraint.

2.1.2 Cone

A cone bounded by two planes perpendicular to the axis, see Figure 2-2, is used as the basic cone configuration. It is described by the coordinates of the two center points (X_1, Y_1, Z_1), (X_2, Y_2, Z_2) and the radii R_1 and R_2. The parameters in this sequence are stored as PTLCTR of the surface.

In subroutine CONE coefficients of the surface and the constraint equations in terms of the system coordinates X-Y-Z are calculated. Two transformation matrixes between the system and the local coordinates are calculated and stored. Note that the local coordinate origin is at the first center point (X_1, Y_1, Z_1) and the z-axis points toward the second center point (X_2, Y_2, Z_2).

There are two standard constraints. The first is the perpendicular plane through (X_1, Y_1, Z_1) while the second is the one through (X_2, Y_2, Z_2).

---

* X-Y-Z are the system coordinates while x-y-z are the local coordinates except as otherwise noted.

1072-347A

REPRESENTED BY A
LINEAR EQUATION

R_2 R_1

$\dot{n} = (a, \beta \gamma)$

(X_C, Y_C, Z_C)

TWO STANDARD CONSTRAINTS
REPRESENTED BY TWO
QUADRATIC EQUATIONS
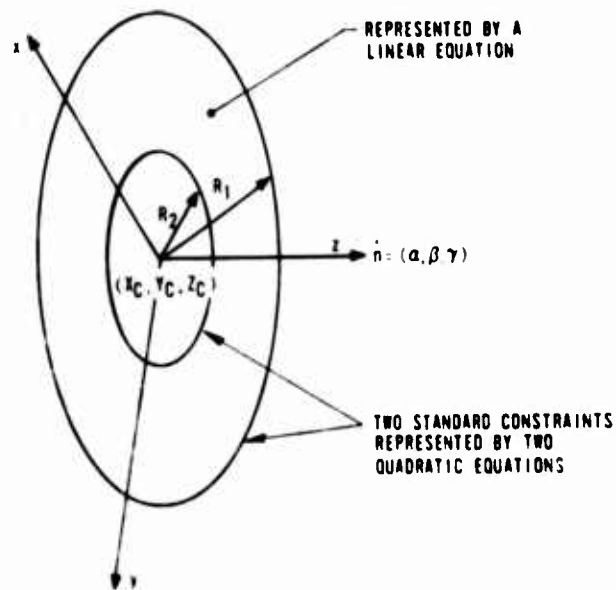
FIGURE 2-1. PLANE CONFIGURATION

1072-348

R_2

R_1

(X_2, Y_2, Z_2)

(X_1, Y_1, Z_1)

REPRESENTED BY A
QUADRATIC EQUATION

TWO STANDARD CONSTRAINTS
REPRESENTED BY TWO LINEAR EQUATIONS
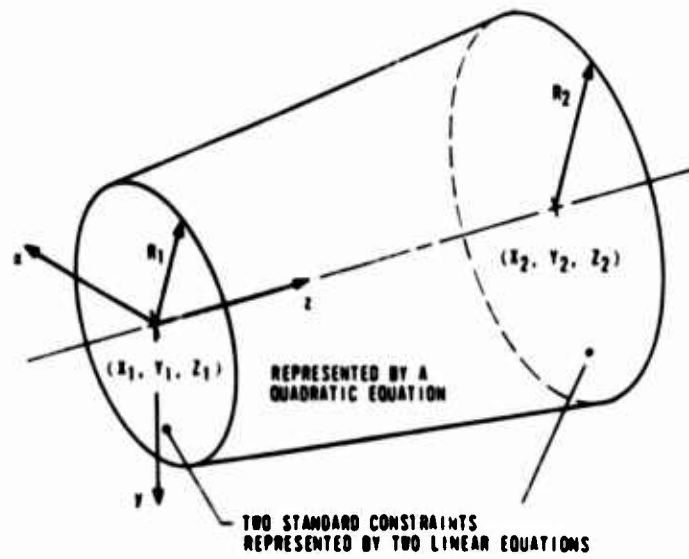
FIGURE 2-2. CONE CONFIGURATION

2.1.3 Sphere

A sphere is best described by the center (X_1, Y_1, Z_1) and a point on the surface (X_2, Y_2, Z_2), see Figure 2-3. Similar to a plane, a sphere is bounded by two cylinders of radii R_1 and R_2. The parameters in this sequence are stored as PTLCTR of the surface.

In subroutine SPHERE coefficients of the surface and the constraint equations in terms of the system coordinates are calculated. As before two transformation matrixes are obtained. The origin of the local coordinates is at (X_1, Y_1, Z_1) and the z-axis points toward (X_2, Y_2, Z_2).

There are two standard constraints: (1) the outer cylinder of radius R_1 and (2) the inner one of radius R_2. Again $R_2 = 0$ indicates that there is no inner constraint.

2.1.4 Paraboloid

A paraboloid is described by two points on the axis of revolution, see Figure 2-4. The first point is the vertex (X_1, Y_1, Z_1) while the second is the focal point (X_2, Y_2, Z_2). Similar to the plane and the sphere configurations, two standard cylindrical constraints are obtained from two radii R_1 and R_2. The parameters are stored in this sequence as PTLCTR of the surface.

In subroutine PARABL coefficients are obtained for the surface and the constraint equations. Two transformation matrixes between the system and the local coordinates are calculated. The origin of the local coordinates falls on the vertex (X_1, Y_1, Z_1) and the z-axis points toward the focal point (X_2, Y_2, Z_2).

There are two standard constraints given by the cylinders of radii R_1 and R_2. Again $R_2 = 0$ indicates that there is no inner constraint.

2.1.5 Plane Baffle

A thin plate with sharp edged circular aperture can be represented by four surfaces as shown in Figure 2-5. The first surface is a hyperboloid of half width δ. Besides the radius of the aperture R, the surface equation can be chosen to satisfy the edge radius. This is important because it is the sharpness of the edge that determines the amount of reflection off a knife edge aperture.
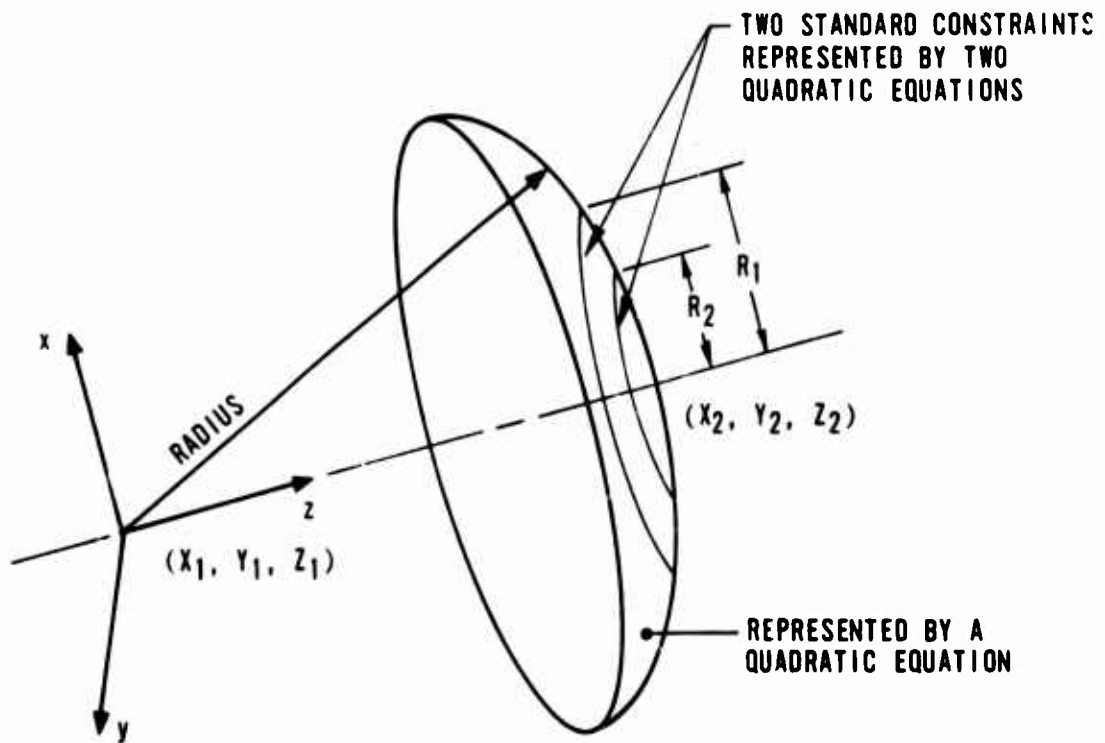
FIGURE 2-3. SPHERE CONFIGURATION

1072-350A

TWO STANDARD CYLINDRICAL
CONSTRAINTS REPRESENTED
BY TWO QUADRATIC EQUATIONS

R_1

R_2

z

AXIS OF REVOLUTION

FOCAL POINT
(X_2, Y_2, Z_2)

VERTEX
(X_1, Y_1, Z_1)

REPRESENTED BY A QUADRATIC EQUATION
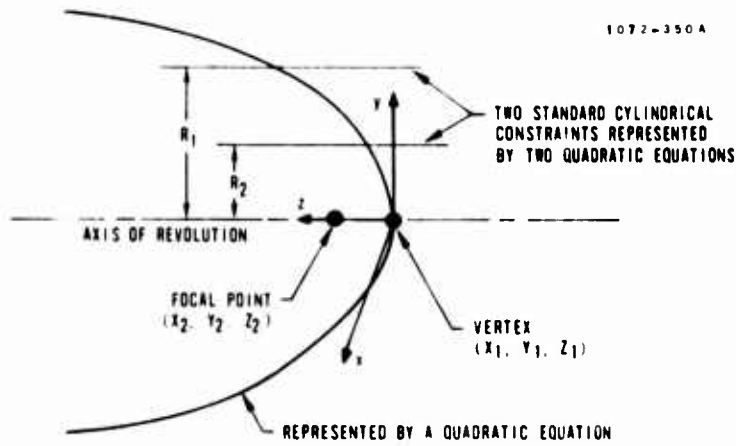
FIGURE 2-4. PARABOLOID CONFIGURATION

1072-351A

3 (PLANE)

4 (PLANE)

t

δ δ

α

2 (CONE)

1 (HYPERBOLOID)

r_e

r

r_e = EDGE RADIUS
t = THICKNESS
δ = HYPERBOLOID HALFWIDTH
α = BLADE ANGLE
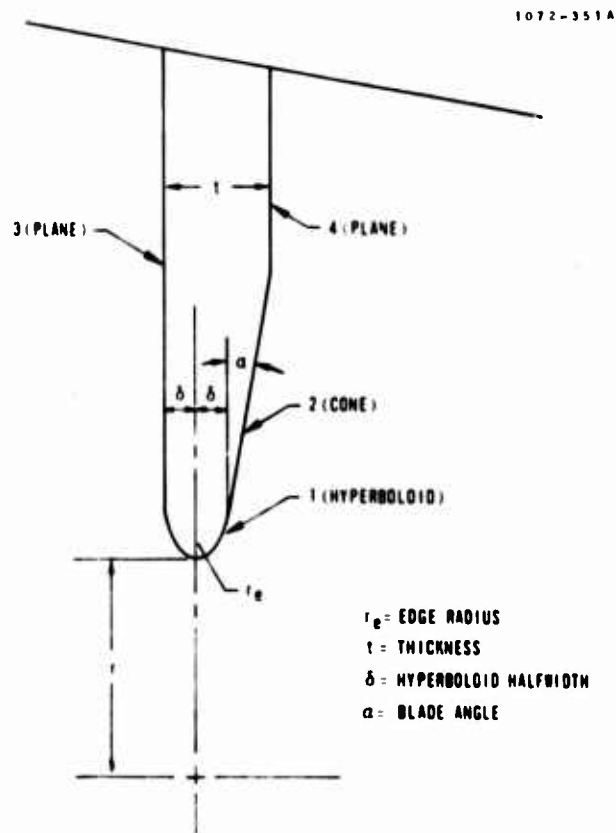
FIGURE 2-5. PLANE BAFFLE

The second surface is a cone representing the blade of the knife edge. The remaining two plane surfaces are two side faces of the baffle. The values of the edge radius R_e, the hyperboloid half-width δ, the blade angle and the baffle thickness are read in as a set of constants.

In addition to the above constants, the parameters necessary to describe a baffle are similar to those of a plane. The first three values of PTLCTR refer to the center of the aperture (X_c, Y_c, Z_c), and the second refer to the unit normal of the aperture (α, β, γ) (see Figure 2-5). Note that the unit normal is on the opposite side of the blade surface 2. The radius of the aperture R and the angle of inclination, β in Figure 2-6, which is zero for a plane baffle, are the last two parameters stored as PTLCTR of the baffle. Since there are four surfaces referred to by a set of PTLCTR, it is necessary to read in the parameter for the first surface only.

In subroutine BAFFLE, coefficients are calculated for the surface and the constraint equations. There are two standard constraints for each of the first two surfaces. Each of the remaining surfaces has only one. It is sometimes necessary to describe an outer constraint for each of them in terms of special constraints.

2.1.6 Conical Baffle

The parameters of a conical baffle are arranged in exactly the same way as that of a plane baffle. A non-zero value is given for the angle of inclination, β (see Figure 2-6).

Instead of hyperboloid, the first surface is now represented by a toroid. This gives a better representation of the knife edge quality, although it results in slower execution due to its more complicated equation. The second is again a cone representing the blade. The last two surfaces are cones instead of planes.

Again there are two standard constraints for each of the first two surfaces, but only one for each of the remaining two. If necessary, additional outer constraints are specified as special constraints for surfaces 3 and 4.

2.2 CONSTRAINTS

The boundary of a surface is defined by a set of constraints. Figure 2-7 shows a surface with one of its constraint surfaces. In order to test whether an intercepting point $P(X_1, Y_1, Z_1)$ is within the boundary, we substitute (X_1, Y_1, Z_1) in the equation that defines the constraint surface,

1072-352A
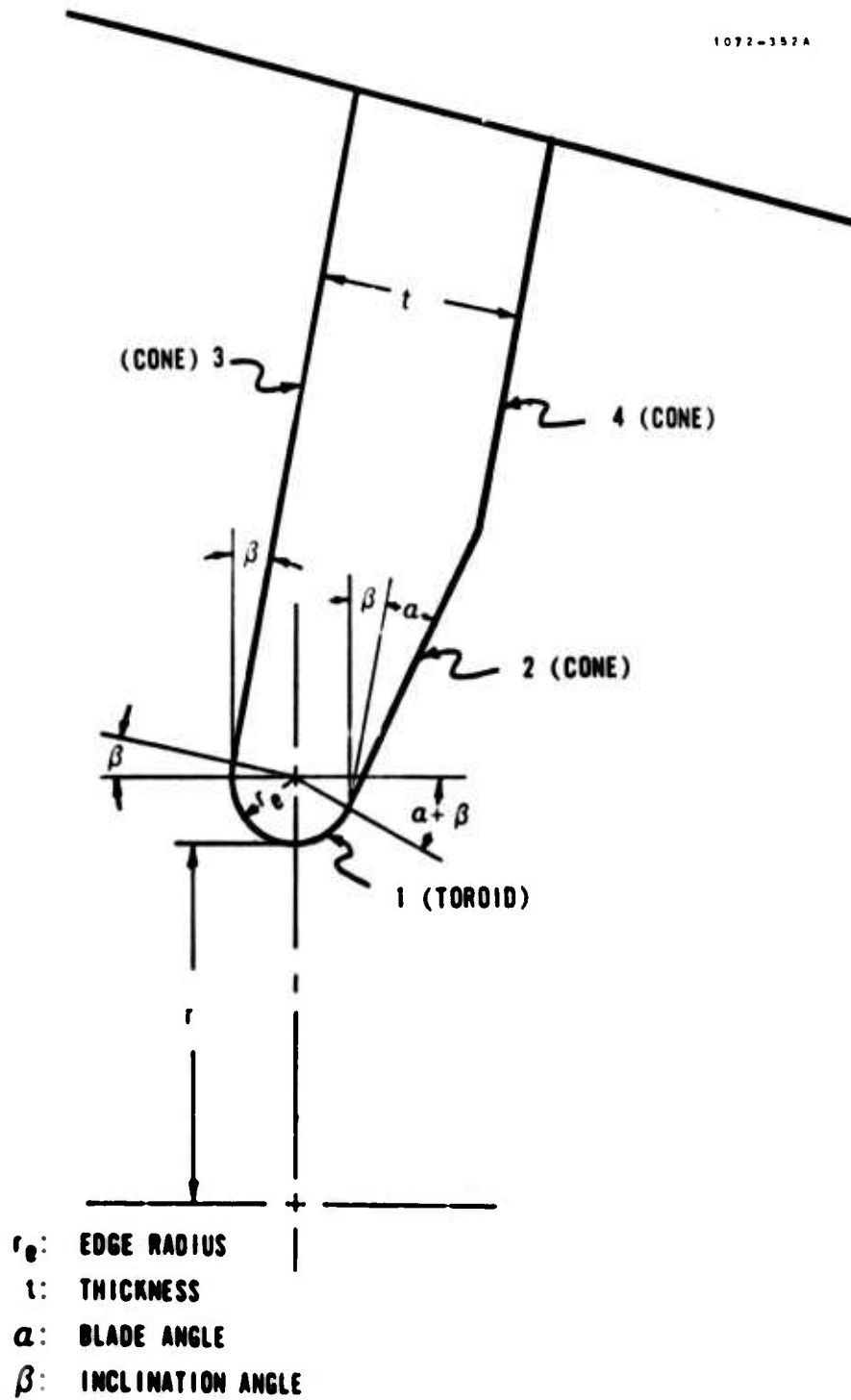
FIGURE 2-6. CONICAL BAFFLE

r_e: EDGE RADIUS

t: THICKNESS

a: BLADE ANGLE

β: INCLINATION ANGLE

1072-353A
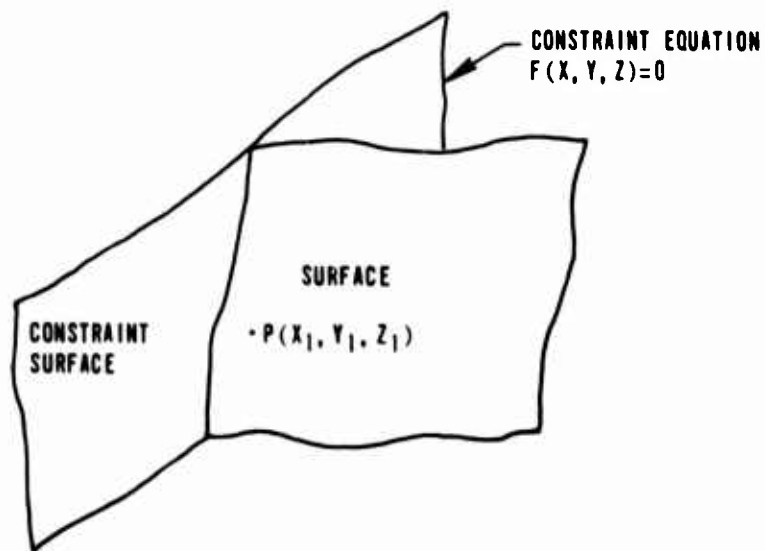
FIGURE 2-7. CONSTRAINT

$F(X, Y, Z)$. The sign of this value indicates on which side of the constraint surface the point P is. It is necessary to predetermine and store the sign of P in the region. A region is the side of a constraint where the system surface exists.

There are three types of constraints as follows:

Linear   - Plane

Quadratic   - Cone, sphere, paraboloid, hyperboloid, etc.

Angular   - Toroid

The angular constraint is specified in subroutine BAFFLE and used in subroutine GEOM. Since no input data is required, we will bypass its discussion. The other two types of constraints are presented below followed by a detailed discussion of special constraints.

The type of a constraint surface and the sign of the constraint function value in the region, for the Ith constraint of surface J, are designated by the parameter KSTRT(I, J) as follows:

KSTRT	Type of Constraint and Sign
1	Linear constraint with $F < 0$ in the region
2	Linear constraint with $F > 0$ in the region
3	Quadratic constraint with $F < 0$ in the region
4	Quadratic constraint with $F > 0$ in the region

2.2.1 Linear Constraint - Plane

Referring to the Subsection 2.1.1, we know that a plane is described by a point on the surface and a unit normal. In subroutine PLANE the coefficients of the plane are chosen such that $F > 0$ on the side where the unit normal is pointing. Thus, in using an existing plane as a constraint, assign

KSTRT = 1 when the unit normal of the plane is pointing away from the region

2 when it is pointing into the region.

2.2.2 Quadratic Constraints

A general quadratic constraint is represented in the system coordinates by the equation:

$$F(X, Y, Z) = C_1 X^2 + C_2 Y^2 + C_3 Z^2 + C_4 XY + C_5 XZ + C_6 YZ + C_7 X$$
$$+ C_8 Y + C_9 Z + C_{10} = 0 \tag{2-2}$$

which is obtained from transforming the equation in the local coordinates,

$$f(x, y, z) = c_1 x^2 + c_2 y^2 + c_3 z^2 + c_4 xy + c_5 xz + c_6 yz + c_7 x + c_8 y + c_9 z + c_{10} = 0$$

Because of the second degree terms in the equations, the sign of the function value is invariant to transformation. In other words, for any point in space $P(X_1, Y_1, Z_1) = p(x_1, y_1, z_1)$ we have

Sign of $F(X_1, Y_1, Z_1)$ = Sign of $f(x_1, y_1, z_1)$.

This makes it very easy to identify the orientation of a quadratic surface by the following arrangement.

a. <u>Cone.</u> In subroutine CONE, we use the z-axis as the axis of the cone (see Figure 2-2). Thus both c_1 and c_2 are positive, and if we substitute the coordinates of any point on the z-axis $(0, 0, z)$ in the equation, we will obtain

$$f(0, 0, z) < 0.$$

Therefore, we have

$f < 0$ and $F < 0$ for any point inside the cone

and

$f > 0$ and $F > 0$ for any point outside the cone.

b. <u>Sphere.</u> In subroutine SPHERE, we start with the equation

$$f(x, y, z) = x^2 + y^2 + z^2 - R^2 = 0$$

Thus we have

$f < 0$ and $F < 0$ for any point inside the sphere.

$f > 0$ and $F > 0$ for any point outside the sphere.

c. <u>Paraboloid.</u> The paraboloid equation is written as

$$f(x, y, z) = x^2 + y^2 + c_9 z = 0$$

in subroutine PARABL (see Figure 2-4). By keeping a constant z and decreasing the magnitude of x and y, we obtain

$f < 0$ and $F < 0$ for any point "inside" the paraboloid (see Figure 2-8)

and consequently.

$f > 0$ and $F > 0$ for any point "outside" the paraboloid.

2-11

1072-354A
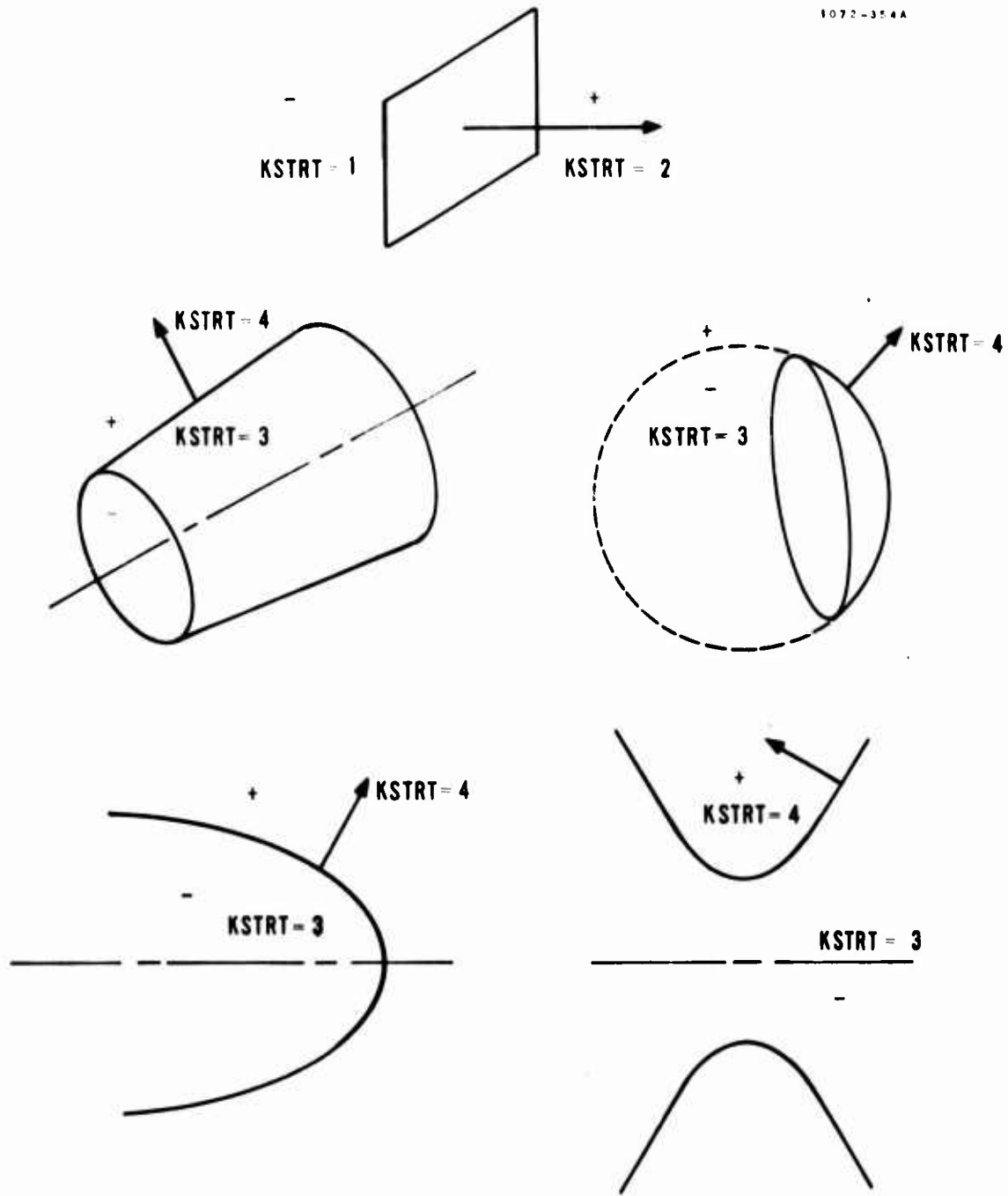
FIGURE 2-8. TYPES OF CONSTRAINTS

d. <u>Hyperboloid.</u> Referring to Figure 2-5, we see that the hyperboloid surface is in the form

$$f(x, y, z) = c_1 x^2 + c_2 y^2 + c_3 z^2 + c_{10} = 0$$

where

$$c_1 = c_2 > 0$$

and

$$c_3 < 0$$

By holding z constant and decreasing the magnitude of x and y, we obtain

$f < 0$ and $F < 0$ for any point in the region including the center (see Figure 2-8).

and

$f > 0$ and $F > 0$ for any point in the opposite region.

The above observation is summed up, together with that of a plane, in Figure 2-8. The unit normals are included to assist in memorizing the orientation of the surfaces. They always point toward the positive sides of the surfaces.

Modification of the set of standard constraints given by the basic configurations (see Subsection 2.1) is accomplished by specifying the arrays NSTRT, KSIDSP, KSTRT, PTLCSP and CSTRT in Namelist NAME3.

NSTRT(I) is the number of constraints for surface I. The default value is given by the basic parameters of the surface PTLCTR (see Subsection 2.1).

KSIDSP(J, I) specifies the Jth constraint of surface I in the following manner:

KSIDSP	Constraint Surface
-1	Given by array PTLSCP
0	Standard
Positive	Surface number given by KSIDSP

When the standard constraint is to be left intact, the parameter KSIDSP assumes the value zero as given by default. When the constraint is to be replaced by an existing surface, the number of the surface to be used as the new constraint is specified by KSIDSP. When no existing surface is available for the constraint, KSIDSP is set at -1.

KSTRT(J, I) is the type of the Jth constraint of surface I. When the type of a constraint is different from the standard type (see Subsection 2.1), the parameter KSTRT is specified as follows:

Existing Surface:

  KSTRT = 1 for plane with normal pointing away from the region

  2 for plane with normal pointing into the region

  3 for quadratic with normal pointing away from the region

  4 for quadratic with normal pointing into the region

New Surface:

  KSTRT = 1 or 2 for plane

  3 for quadratic with normal pointing away from the region

  4 for quadratic with normal pointing into the region

The parameters of a new surface as the Jth constraint of surface I are specified by

  PTLCSP(K, J, I)   K = 1, 2, ..., 6 or 8

The parameters have the same meaning as those of PTLCTR for basic configurations described in Subsection 2.1. However, there are only six parameters instead of eight for a plane, a sphere or a paraboloid because no radii are required for the constraints.

The above can be best demonstrated by the following example. In Figure 2-9 we have surface 17 to be bounded by the following four constraints-- existing cone of surface number 34, existing paraboloid of surface number 26, existing plane of surface number 43, and a new surface.

Referring to Figure 2-8, we obtain the directions of the unit normals for the three existing surfaces. The types of constraints are determined as 3, 4 and 1, respectively, for these surfaces.

1072-3554
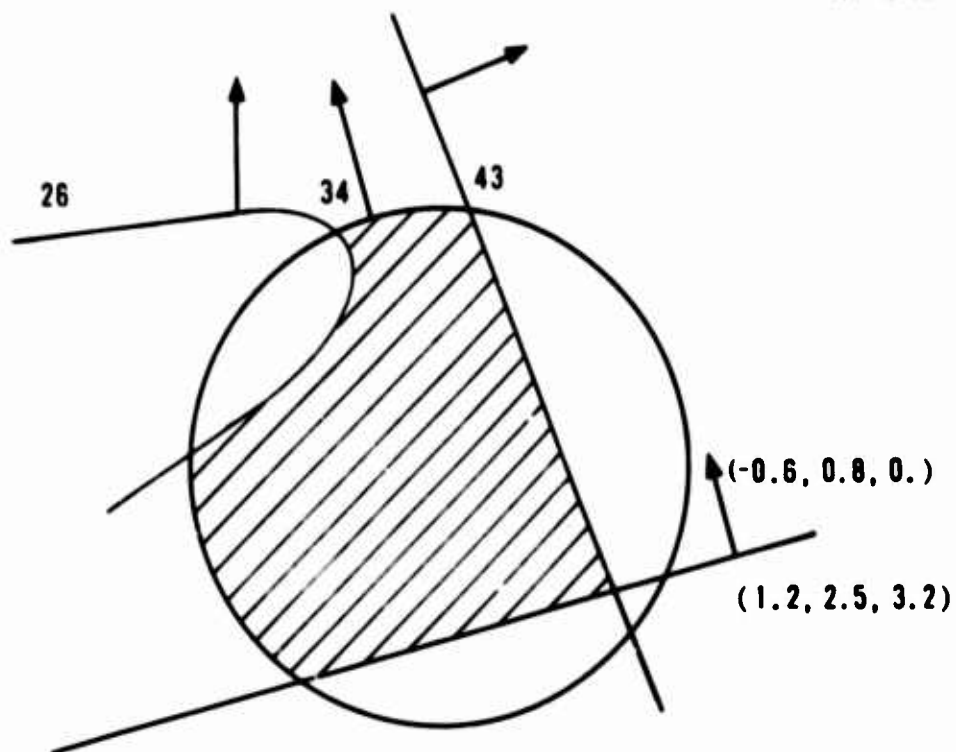
(-0.6, 0.8, 0.)

(1.2, 2.5, 3.2)

CONSTRAINT NUMBER	EXISTING SURFACE NUMBER	TYPE OF CONSTRAINT
1	34	3
2	26	4
3	43	1
4	-1	1

FIGURE 2-9. SPECIAL CONSTRAINT EXAMPLE

The new surface is determined by a point on the surface (1.2, 2.5, 3.2) and the unit normal pointing into the region (-0.6, 0.8, 0). The input data thus appears as follows:

NSTRT (17) = 4

KSIDSP (1, 17) = 34, 26, 43, -1

KSTRT (1, 17) = 3, 4, 1, 1

PTLCSP (1, 4, 17) = 1.2, 2.5, 3.2, -0.6, 0.8, 0

When a constraint surface is required for which there is no available basic surface, the coefficients of the constraint equation, Equation 2-2, can be read in through the array

$$CSTRT(K, J, I) = C_K \qquad K = 1, 2, \ldots, 10$$

for the Jth constraint of surface I.

In the development of the program, the last term of the equation was placed on the right hand side. The user should change the sign of C_{10} when he inputs the coefficients of Equation 2-2.

2.3 SYSTEM MODELING

A tremendous gain in efficiency of the program is achieved by dividing an optical system into sections. Whether they are separated by real surfaces such as apertures and lenses or by artificial surfaces, reduced numbers of surfaces in each of the sections result in fewer calculations in search of an intercept.

Thus, in describing a system, we first divide it into a convenient number of sections. In each of the sections, the surface numbers are assigned that relate them to the basic surfaces generated.

In addition to the surface number, several pertinent parameters are assigned to each surface. These are described in full detail in the sequel.

2.3.1 Surface Number - ISFACE

The surface number refers to the basic surface that has been specified in namelist NMGEOM. The information related to the surface number includes:

    a.   The degree of polynomial of the surface equation - IDGREE.

b. The coefficients of the surface equations - COEF.

c. Number of constraints - NSTRT.

d. Type of each of the constraints - KSTRT.

e. Coefficients of the constraint equations - CSTRT.

f. The surface radiation coefficients - COAT.

When a standard basic surface is used, the first five parameters are automatically computed by the related subroutine. When a set of constraints other than the standard constraints is required, the parameters "c" through "e" are obtained by prescribing special constraints according to the steps given in Subsection 2.2. However, the first five parameters can be read in as part of the input data.

When the standard basic surface is a baffle, four consecutive ISFACE numbers are required for the four surfaces defining the baffle geometry. The user inputs only the first number and one PTLCTR (see Subsections 2.1.5 and 2.1.6). The remaining three numbers are then automatically associated with the baffle and cannot be used with other surfaces.

The first parameter IDGREE is used to describe the type of equation representing the surface. The following three types of equations have been developed in this program.

IDGREE	Equation
1	$C_7 X + C_8 Y + C_9 Z = C_{10}$
2	$C_1 X^2 + C_2 Y^2 + C_3 Z^2 + C_4 XY + C_5 XZ + C_6 YZ + C_7 X$ $+ C_8 Y + C_9 Z = C_{10}$
4	Toroid equation

An IDGREE of value 4 is restricted to use with a toroid surface rather than the general bi-quadratic equation.

The surface radiation coefficients are input in accordance with the model description given in Subsection 3.3.

2.3.2 Surface Type - ISFTP

When a ray is intercepted by a surface in the section, it has to be determined first whether the ray is to be reflected back into the same section or transmitted into an adjacent one. In some cases, e. g., lens surfaces, the ray can be split in both directions. The parameter surface type carries such informations in the following manner:

ISFTP

1	Transmitting surface, e. g., aperture, toward entrance, i. e., to the next lower numbered section
2	Transmitting surface toward exit, i. e., to the next higher numbered section
3	Transmitting and reflecting surface, e. g., lens, toward entrance
4	Transmitting and reflecting surface toward exit
5	Reflecting surface, i. e., non-transmitting

The section numbers are assigned in the ascending sequence from the entrance to the exit. In other words, the first section always has the entrance aperture as one of its surfaces. Its adjacent section is Section 2 and so on until the last section where the exit aperture or a detector is located.

When the intercepting surface has a surface type 1 or 3 and the ray is to be transmitted, the ray is directed into the next section toward the entrance. Likewise, the ray is directed into the next section toward the exit when the surface type is 2 or 4.

2.3.3 K Coefficient - KCOEF

An intercept between a ray and a surface is obtained by solving the simultaneous equations of the ray and the surface. Theoretically, the point of interception thus obtained is on the surface. Unfortunately, the set of numbers available to a computer is only a finite subset of the entire set of real numbers and precise solution is exception rather than rule.

Frequently the calculated point of interception falls a short distant in front of or behind the surface. No particular problem is caused by the first situation. However when the point is behind the surface, the ray can be forced to reflect off the surface twice instead of once.

This is best illustrated by Figure 2-10. A ray at point P is pointing in the direction $\hat{p}$. Looking for interception of this ray by the surface S, we solve the pertinent simultaneous equations. Due to round-off errors in the calculation, the intercepting point fall a short distance behind S.

The command then goes on to obtain the direction $\hat{q}$ of the reflected ray and searches for the subsequent interception. As is clearly seen in the figure, the ray is intercepted immediately by the same surface at point R. After another reflection at this point, the ray in effect penetrates the surface even though S is a non-transmitting surface.

This is only one of many examples that a ray is forced into a wrong path due to round off error in the calculations. However, we will refrain from exhausting all the other possibilities and be content with describing a practical remedy which has been mechanized.

In the Cartessian coordinates, we represent a surface by the general equation:

$$F\ (X,\ Y,\ Z) = 0$$

If we substitute the coordinates of a point $P_1\,(X_1,\ Y_1,\ Z_1)$ into the equation and obtain

$$F\ (X_1,\ Y_1,\ Z_1) \ne 0$$

we know that P_1 is not on the surface.

Furthermore, we can show mathematically that in the vicinity of the segment of surface S, F has a constant sign on each side of the surface. In other words, if $F\ (X_1,\ Y_1,\ Z_1) < 0$, $F < 0$ for all points on this side of the surface S and $F > 0$ for all points on the opposite side.

This is where the K coefficient comes into play. The coefficient is defined as follows:

KCOEF

0	Function value of the surface equation is negative in the region.
1	Function value of the surface equation is positive in the region

1072-356A
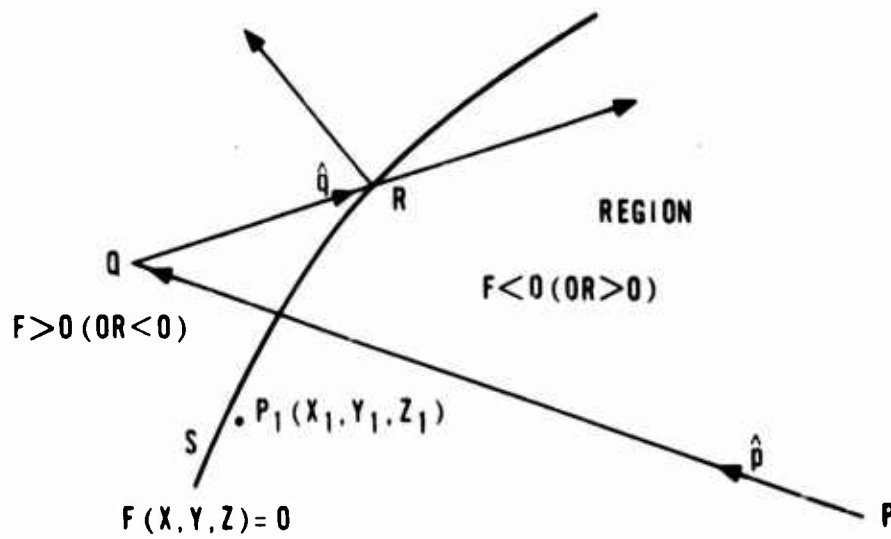
FIGURE 2-10. DOUBLE REFLECTION DUE TO ROUND-OFF ERROR

A region is used here to represent the spatial domain that is inside the section.

In the above example, we have

$$F(X_1, Y_1, Z_1) < 0$$

where P_1 is inside the region; therefore,

KCOEF = 0.

When the program finds that point R is the next intercept and that it is at a rather short distance from point Q, it tests the validity of this interception. The coordinates of point Q are substituted into the function F. The sign of this value compared with KCOEF will immediately tell whether point Q is inside the region or not. In this particular example, Q is outside the region, and the interception at point R is ignored.

2.3.4 Importance Sampling Surface - IMPSF

While the importance sampling technique will be discussed in full detail in Section 4, the procedure of assigning importance sampling surfaces, which we will simply call important surfaces, will be briefly described here.

In each section, there can be up to three important surfaces. The parameter IMPSF given for each surface indicates whether the rays from the surface will be split such that one or more rays will be directed towards the important surfaces. Such a decision is specified in the following manner.

IMPSF

0	No importance sampling
1	Importance sampling toward important surface 1
2	Importance sampling toward important surface 2
3	Importance sampling toward important surface 3
4	Importance sampling toward important surfaces 1 or 2
5	Importance sampling toward important surfaces 1 or 3
6	Importance sampling toward important surfaces 2 or 3
7	Importance sampling toward important surfaces 1, 2, or 3

Although more detailed discussion will be presented later, it should be pointed out here that the above splittings are in addition to those that cover specular components of the radiation coefficients.

When IMPSF = 0 for the surface, the ray will not be split. When
IMPSF = 1, 2 or 3, the ray is split toward the particular important surface
named. When IMPSF = 4, 5, 6 or 7, a uniform random number is used to
decide which of the important surfaces the splitted important ray is aimed
at.

Section 3

STATISTICAL MODELING OF RADIATION

Probability density functions giving the probable paths of the radiant energy are the heart of the Monte Carlo ray tracing method. Whether it be a collimated laser beam, slightly divergent solar energy, a reflected beam off a surface, or an emission off a black body, a well-defined distribution function has to be determined before we can proceed to obtain the probable path of the rays.

We present here a number of radiation models that have been used in a variety of optical systems. However, it should be emphasized that additional models will be needed for certain new problems. The computer program is arranged in such a way that it is fairly easy to include additional models.

Available radiation models up to this point include a collimated or divergent beam coming into a system through a circular aperture, emission, absorption (by a surface), specular, near specular, and diffuse reflection, refracted specular, and diffuse transmission, and diffraction through a circular aperture.

3.1 EXTERNAL RADIATION

We consider here collimated or divergent radiant energy entering the system uniformly through a circular aperture. Since a collimated beam can be obtained by specifying a zero divergence angle to a divergent beam, we will limit our discussion to the latter.

A typical divergent beam is shown in Figure 3-1, passing through a circular entrance aperture. The aperture is placed on the x-y plane of the local coordinates x-y-z, with the z-axis passing through the center. The local coordinates can be in any orientation with respect to the system coordinates X-Y-Z.

The direction of the beam as a whole, which we shall call the center beam, is defined by the elevation and the azimuthal angles. The beam is uniformly spread over the solid angle around the center beam within the divergence angle.
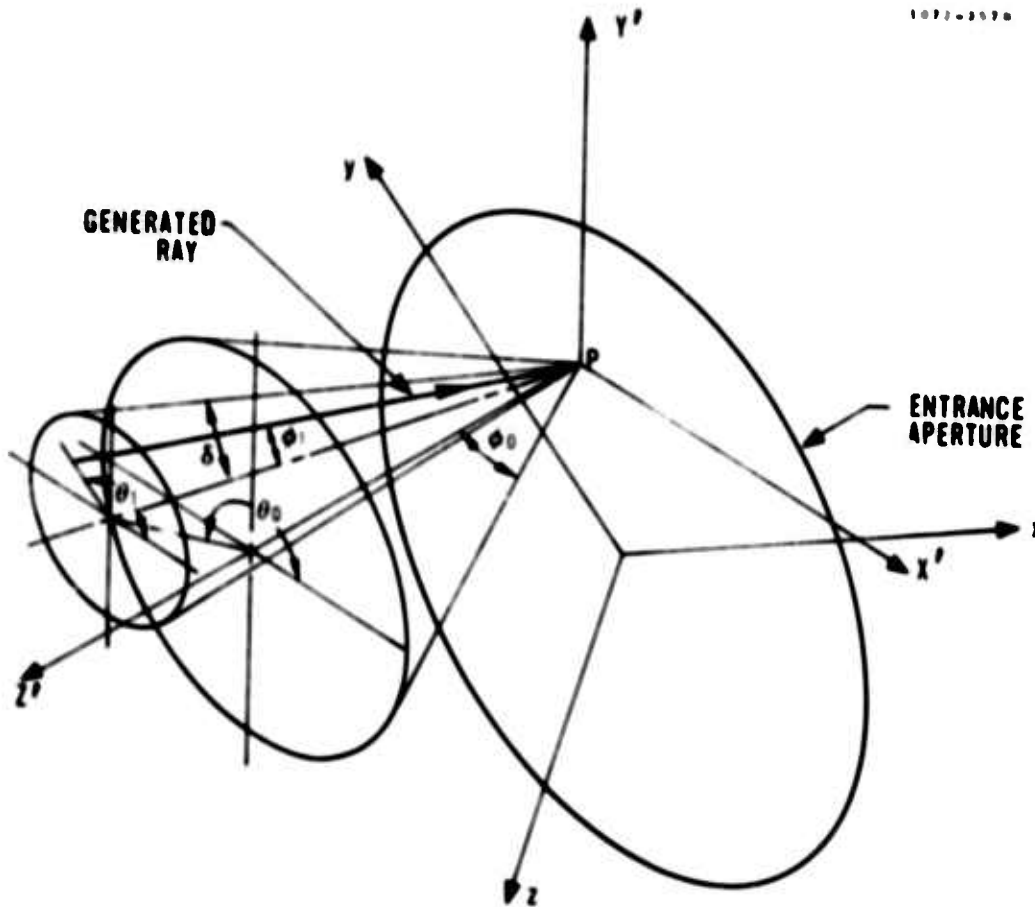
ϕ_0 ELEVATION ANGLE

θ_0 AZIMUTHAL ANGLE

$\hat{\delta}$ DIVERGENCE ANGLE

FIGURE 3-1. EXTERNAL RADIATION MODEL

it is important to realize that the elevation angle, ϕ_0, and the azimuthal angle, θ_0, are defined with respect to the system coordinates. This is clearly shown in Figure 3-1 where the coordinate system X'-Y'-Z' is a translation of the system coordinates to point P, the point of interception between the entering beam and the aperture. ϕ_0 is the angle between the center beam and the Z'-axis. θ_0 is the angle between the projection of the center beam on the X'-Y' plane and the X'-axis.

To generate a ray statistically, we first locate point P on the aperture with two uniform random numbers. The deviation angles ϕ_1 and θ_1 are obtained with two additional random numbers. With these angles and the direction of the center beam, calculation of the ray direction is straightforward.

3.2 EMISSION

The emissive power of a surface is given by

$$e = \epsilon \, \sigma \, T^4 \, A$$

where ϵ is the emittance, σ the Stefan-Boltzmann constant, T the temperature and A the area. If the emittance and the temperature of a surface are known, the emission can be simulated by generating a series of rays coming off the surface. The starting points of the rays should be uniformly distributed over the area and the angular distributions are governed by certain emission models. We shall first concentrate on the method of picking the starting points uniformly over an area.

The location of a point on a surface is generally defined by two coordinates, say ξ and η. In most cases, the coordinates can be orthogonal and the area bounded by infinitesimal lengths of the coordinates are simply the product of the sides, namely $\Delta A = \Delta \xi \, \Delta \eta$. Under this condition the point of uniform probability is obtained by uniform selection of the coordinates. Planes and spheres are typical surfaces of this type. Unfortunately a general surface does not always satisfy this condition.

In addition to the above difficulty, excessive calculations are required when emission is to be considered for a large number of surfaces. First, a surface will have to be selected among all the surfaces in accordance with their area ratios. The chore of calculating areas for all surface elements becomes extremely complicated for a general program. These difficulties lead to the idea of selecting the points by following a statistical procedure and compensating the probability with equivalent areas. The method is described in detail as follows.

Consider an enclosure of arbitrary shape shown in Figure 3-2.

1072-358A
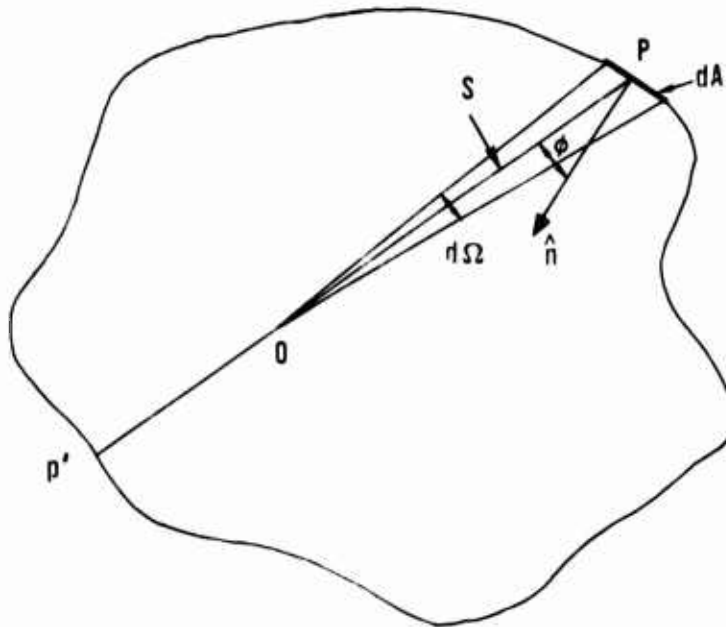
FIGURE 3-2.   EMITTING ENCLOSURE

P is a point on the enclosure surface, while O is anywhere in the space.
If an infinitesimal enclosure surface dA is encompassed by an infinitesimal
solid angle $d\Omega$ as shown in the figure, the area is given by

$$dA = \frac{S^2 \, d\Omega}{|\cos\phi|}$$

where S is the length of OP and ϕ is the angle between OP and the surface
normal at P.

We can directly apply the above relation to obtain the emitting point and
the equivalent area of an emitted ray. First, we place a point O, which we
shall designate as a pole, anywhere in the system and generate a series
of pilot rays out of it uniformly over all directions. For each of these
rays, we search for interceptions by the system surfaces.

Each of these intercepts is an emitting point with the equivalent emitting area proportional to the factor $S^2/|\cos \phi|$. If n pilot rays are initiated and intercepts are sought in both directions of the pilot rays, the equivalent area of an emitting ray is

$$A_e = \frac{2\pi S^2}{n|\cos \phi|}$$

Thus, the emissive power associated with the emitted ray is

$$e = \frac{2\pi S^2 \epsilon \sigma T^4}{n|\cos \phi|}$$

Clearly, the above expressions are valid regardless of the shape of the system surfaces. Furthermore, there can be many or no intercepts for each of the pilot rays.

An interesting consideration arises in the selection of a pole location. It is clear from the above discussion that the probability of a surface intercepting a pilot ray is proportional to the factor $|\cos \phi|/S^2$. More often than not, we are particularly interested in the emission of certain surfaces and would like to have more rays simulating the emission off these surfaces. This is easily achieved by placing the pole at short distances from these surfaces.

In some systems, the emitting surfaces are so far apart that it is desirable to initiate pilot rays from different locations. Under these circumstances, as many poles as necessary are placed at optimum locations and the system surfaces are divided into groups, each corresponding to a pole.

The emissive power of a surface is assumed diffusely distributed over the hemisphere. The direction of a ray is selected in the same way as that of a diffuse reflection. Also the splitting of rays for importance sampling can be treated in the same manner as in diffuse reflection. Discussion of this matter is included in Subsection 3.3.

3.3 ABSORPTION-REFLECTION-TRANSMISSION

The tracing of a ray on its interception by a surface is best treated by dividing the probability into components; namely that of absorption, reflection, and transmission. Absorption can be easily accounted for by reducing the energy of the ray. A random number is then used to choose between reflection and transmission.

The direction of the reflected or transmitted ray is governed by certain probability density functions. Calculations will be greatly simplified if we can express these functions in analytical forms.

For most reflecting surfaces, the distribution of energy can be approximated by specular and diffuse components (Reference 3). The specular component is a collimated beam leaving the surface in the specular direction. The energy of the diffuse component is uniformly distributed over the entire hemisphere and its probability density is given by Lambert's cosine law.

$$e = e_n \cos \phi$$

where e_n is the probability density in the normal direction and ϕ the angle between the normal and the emerging ray.

These two components cover the extreme cases of perfect mirrors and gray bodies. In most real surfaces, however, there is a concentration of energy within a finite solid angle around the specular beam with the energy dropping exponentially from its peak at the specular direction. The probability density of this near-specular component is

$$\text{const} \cdot e^{-K\alpha}$$

where K is an angular decay constant and α is the angle between the emerging ray and the specular direction.

While one near-specular component, together with the specular and the diffuse components, is sufficient to approximate most probability density functions, it is sometimes necessary to include two such components with different angular decay constants. This will be demonstrated by an example later in this section.

Transmitted energy through a surface is usually well approximated by a specular ray and diffuse scattering. The specular ray is refracted according to Snell's law, which we will discuss in more detail in the next section. The diffuse scattering follows Lambert's cosine law on the back side of the surface.

Adding up all the components, we have

$$\sum_{i=1}^{7} C_i = 1$$

where

C_1 = absorption coefficient

C_2 = specular reflection coefficient

C_3 = diffuse reflection coefficient

C_4 = first near specular reflection coefficient

C_5 = second near specular reflection coefficient

C_6 = specular transmission coefficient

C_7 = diffuse transmission coefficient

The probability density distribution functions for the diffuse and the near-specular components are given by

$$f_r = A \cos \phi + B e^{-K_1 \alpha} + C e^{-K_2 \alpha} \qquad (3-1)$$

and

$$f_t = D \cos \phi' \qquad (3-2)$$

where f_r and f_t are, respectively, the reflection and the transmission distribution functions, ϕ is the angle between the reflected ray and the normal, ϕ' is the equivalent of ϕ for transmission, α is the angle between the reflected ray and the specular ray, and K_1 and K_2 are two angular decay constants. A, B, C and D are constants determined from the coefficients C_i in the following manner:

3-7

The total energy of a diffuse reflection is obtained by integrating the density function over the hemisphere. Hence, we have

$$C_3 = \int_0^{2\pi} \int_0^{\pi/2} (A \cos \phi) \sin \phi \, d\phi \, d\theta$$

where θ is the azimuthal angle. Integration gives

$$C_3 = \pi \cdot A \tag{3-3}$$

Similarly, we have

$$C_4 \cong \int_0^{2\pi} \int_0^{\pi/2} (B e^{-K_1 a}) \sin a \, da \, d\theta,$$

a good approximation as long as $e^{-K_1 a}$ is negligible when a is replaced by the minimum angle between the specular ray and the surface tangent.

Integration gives

$$C_4 = \frac{2\pi B(1 - K_1 e^{-K_1 \pi/2})}{1 + K_1^2}$$

For $K_1 \gg 5$, this can be approximated by

$$C_4 = \frac{2\pi B}{1 + K_1^2} \tag{3-4}$$

Similarly for the second near-specular scattering, we have

$$C_5 = \frac{2\pi C}{1 + K_2^2} \tag{3-5}$$

A slight modification is introduced here for the near-specular component. In the model presented above, the radiant density drops down exponentially from its peak at the specular direction. In most cases, the angular decay constant is so large that the density is negligible outside a fairly small α angle. However, when the angular decay constant is small and the incident ray is close to the surface tangent, a significant amount of energy would go into the surface according to the density function. To prevent this situation from occurring, the probability distribution function is normalized by one of two methods selected by the user through the parameter IEXP.

Referring to Figure 3-3, we have a ray incident on a surface at point O. OP is the specular direction and plane π is perpendicular to it at point P. OQ is the direction under consideration and α is, as defined previously, the angle between OP and OQ. The plane formed by OPQ is intersected by the tangent plane at OR. The angle $<$ POR is the maximum value of the angle α in that direction before the ray will enter the surface.

If IEXP $=$ O, the probability distribution function for α is normalized by

$$P(\alpha) = \int_0^\alpha C_{\alpha max} \quad Be^{-K_1\alpha} + Ce^{-K_2\alpha} \quad \sin \alpha \, d\alpha$$

where $C_{\alpha max} = \dfrac{1}{\int^{\alpha max} (Be^{-K_1\alpha} + Ce^{-K_2\alpha}) \sin \alpha \, d\alpha}$

and Equation (3-1) becomes

$$f_r = A \cos \phi + C_{\alpha max} \quad Be^{-K_1\alpha} + Ce^{-K_2\alpha} \tag{3-6}$$

Since the exponential factor is independent of the direction of PQ, this is referred to as "symmetric" near-specular scatter.

If IEXP $=$ 1, a new variable given by

$$\xi = \frac{\pi \alpha}{2\alpha_{max}}$$

is substituted for α in Equation 3-1 to give

$$f_r = A \cos \phi + B e^{-K_1\xi} + C e^{-K_2\xi} \tag{3-7}$$

1072-359A
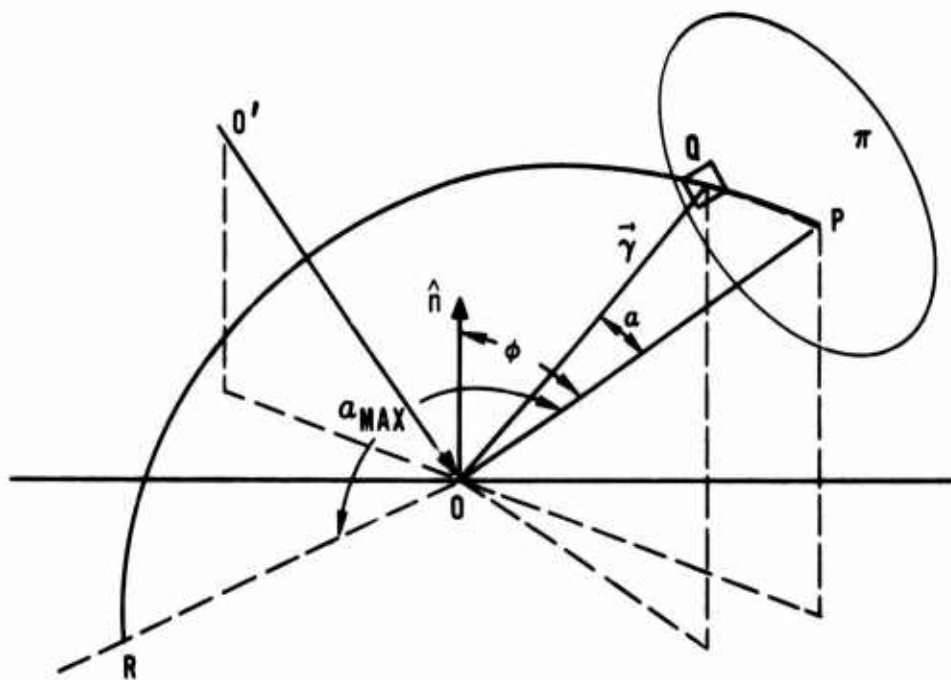
FIGURE 3-3. MODIFIED NEAR-SPECULAR REFLECTION MODEL

The factor $\pi/2$ is included here so that $\xi = \alpha$ for normal incidence. Since the exponential factor is dependent on the direction PQ through the variable ξ, this is referred to as "skewed" near-specular scatter.

The input parameters for a surface are summarized in Table 3-1.

The following example of a typical high quality mirror is presented to demonstrate the usage of the various components.

Example: Instead of attempting to match a measured angular radiant energy distribution by trial and error, we shall assume a set of parameters and plot the resultant distribution of a typical high quality mirror. Using the symmetric near-specular model, we assume the following:

$$C_3 = \pi \times 10^{-6}$$

$$C_4 = 10^{-6} \qquad\qquad K_1 = 500$$

$$C_5 = 5 \times 10^{-7} \qquad\qquad K_2 = 250$$

TABLE 3-1. SURFACE RADIANT DISTRIBUTION PARAMETERS

Input Data	Parameters and Choice of Models	
COAT (I, J)*	C_I	* J is the surface number.
	$I = 1, 2, \ldots, 7$	
COAT (14, J)	K_1	
COAT (15, J)	K_2	
IEXP = 0	Symmetric near-specular model given by Equation 3-6.	
IEXP = 1	Skewed near-specular model given by Equation 3-7.	

Substituting these parameters in Equations 3-3, 3-4, 3-5, and 3-6, we obtain the individual and the combined angular radiant density distributions plotted in Figure 3-4.
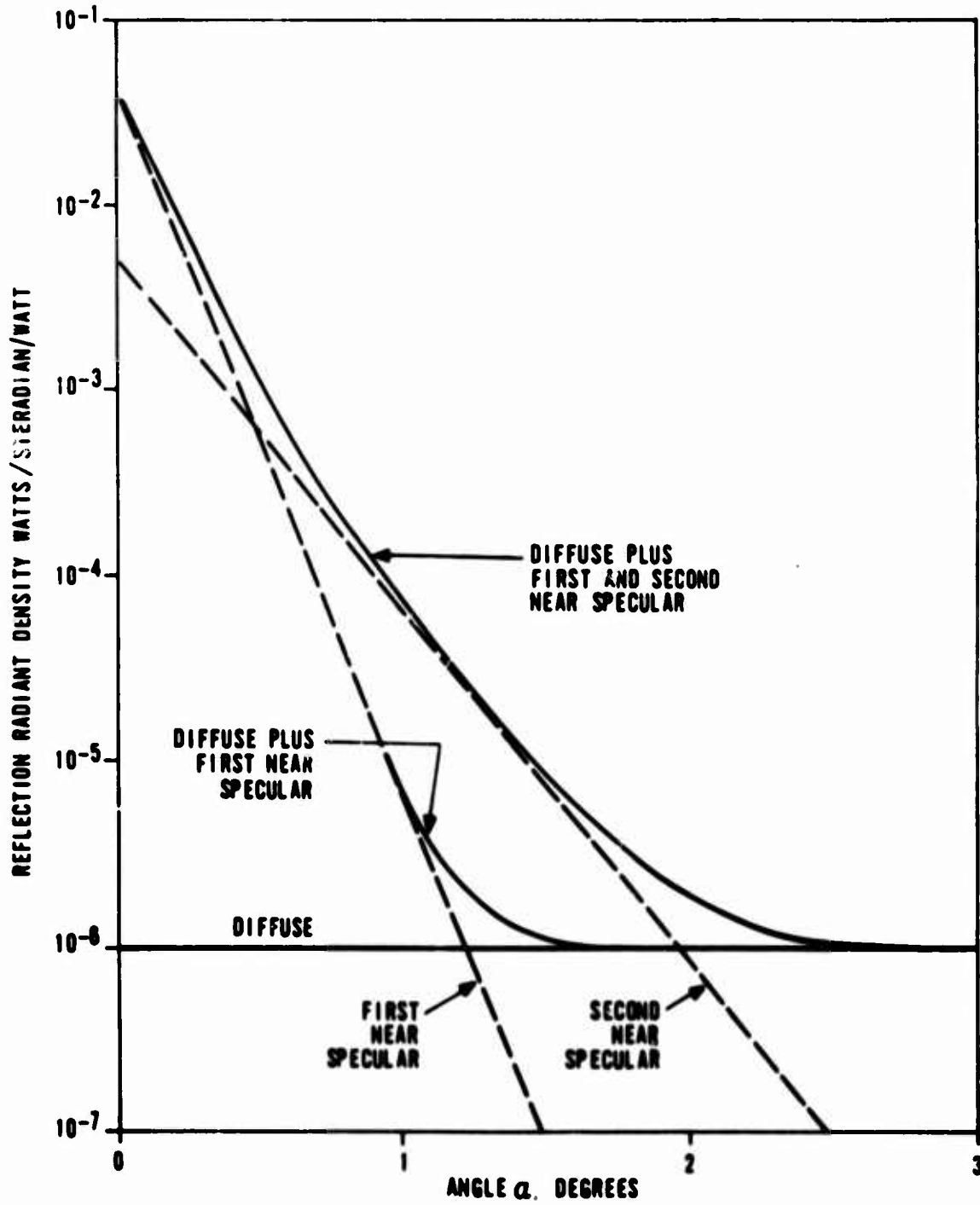
FIGURE 3-4. RADIANT DENSITY DISTRIBUTION OF DIFFUSE AND
NEAR-SPECULAR REFLECTION

In the simulation of a mirror with a measured biangular radiant energy distribution, a different set of component coefficients is assumed and substituted in the equations until the combined density distribution will represent the measured distribution curve.

3.4 REFRACTION

Given the indices of refraction for both sides of a surface, the direction of the refracted ray is determined by Snell's law, which states, "the refracted ray lies in the plane of incidence, and the sine of the angle of refraction bears a constant ratio to the sine of the angle of incidence" (Reference 4). In the refraction at a boundary between two substances having indices of refraction n and n', it may be written in the form

$$n \, Sin \, \phi = n' \, Sin \, \phi'$$

where ϕ is the angle between the incident ray and the inward normal and ϕ' the angle between the refracted ray and the outward normal.

Tracing of a refracted ray accordingly is straightforward, except in the case of total internal reflection, where

$$\frac{n}{n'} \, Sin \, \phi' \geq 1$$

and the refracted ray is reflected instead. Lacking a reliable prediction of the probable path of the ray, we assume that the totally reflected ray is distributed according to the reflection components.

3.5 DIFFRACTION

Diffraction of a bundle of radiant energy through a plane aperture of arbitrary shape has been successfully modeled (Reference 2). Besides those given in the reference, additional tests of the model have been made, which we will present as examples in Section 9.

The procedure to be followed in determining the direction of a diffracted ray is summarized below:

a. Follow the ray until it strikes the aperture plane. Shown in Figure 3-5 is such an aperture and P is the point of interception.

b. σ_1 is the shortest distance from P to the aperture edge.

c. Using P as the center and σ_1 as the mirror radius, fit the biggest ellipse possible inside the aperture. σ_2 is the major radius. ξ - η are coordinate axes in the directions as shown.

d. Two angle constants are calculated from

$$\theta_1^* = \tan^{-1} \frac{1}{2k\sigma_1}$$

and

$$\theta_2^* = \tan^{-1} \frac{1}{2k\sigma_2}$$

where k is the wave number.
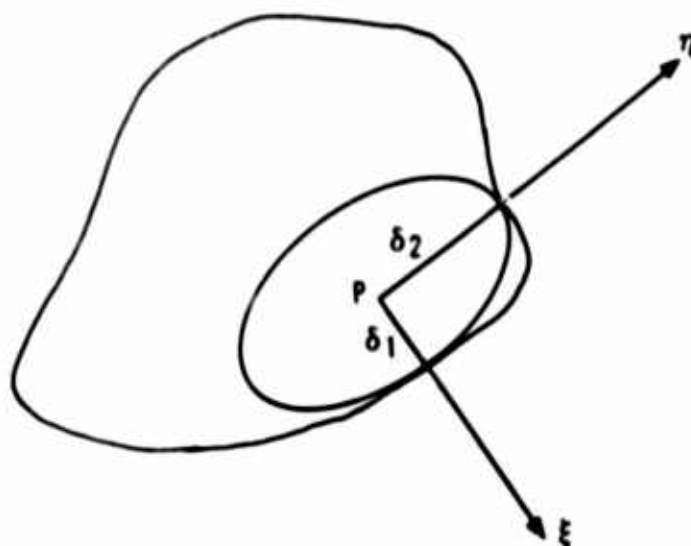
FIGURE 3-5. TYPICAL APERTURE PLANE

e. Illustrated in Figure 3-6, θ_1 is the deviation angle of the ray on
the plane given by the incident ray and the axis $P\xi$.

Similarly, θ_2 is the deviation angle in the $P\eta$ direction.

f. The direction of the diffracted ray is determined by the following
probability density functions.

$$P_1(\theta_1) = \frac{1}{\sqrt{2\pi}\,\theta_1^*} \quad \exp\left[-\frac{1}{2}\left(\frac{\theta_1}{\theta_1^*}\right)^2\right] \qquad (3-8)$$

$$P_2(\theta_2) = \frac{1}{\sqrt{2\pi}\,\theta_2^*} \quad \exp\left[-\frac{1}{2}\left(\frac{\theta_2}{\theta_2^*}\right)^2\right] \qquad (3-9)$$
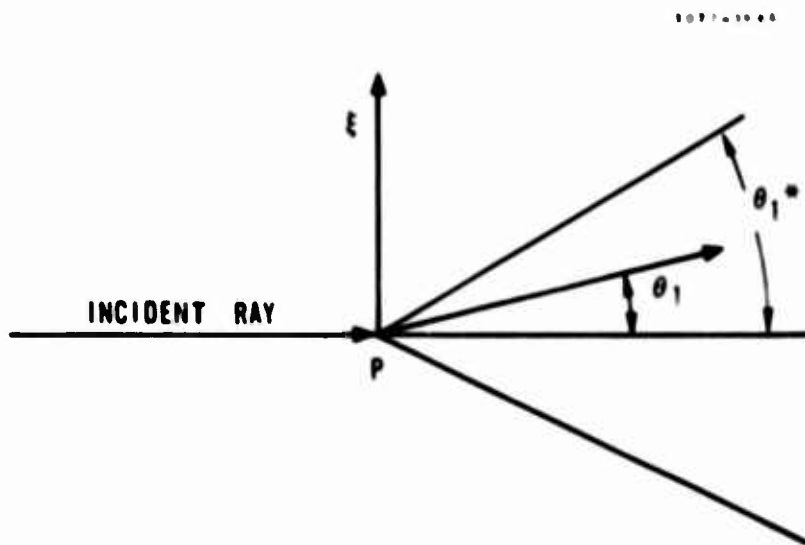
FIGURE 3-6. DEVIATION ANGLE OF RAY

Bending of rays according to the above procedure is available at circular
apertures. In order to include diffraction for certain of those apertures,
the users simply specify

$$KDIF \ (I) = 1 \quad for \ I = surface \ numbers.$$

From the above equations, we see that the angle constant θ^* is significant
only when the distance from point P to the aperture edge, σ, is in the order
of the wave length and only in this situation that diffraction needs to be
considered. When a ray strikes an aperture plane where diffraction is
called for, the shortest distance to the edge σ_1 is compared with the wave
length. If the ratio of σ_1 to the wave length is bigger than a constant
DEDGE, specified by the users, the diffraction of the ray is neglected.

Since the probability density is distributed over a finite solid angle, a
diffracted ray can be split for importance sampling. The procedure of pre-
scribing such splitting is in the general discussion on importance sampling
in the next section.

Section 4

IMPORTANCE SAMPLING

The Monte Carlo method, which is the basis of the GUERAP simulation
program, is a statistically accurate, but time-consuming approach to
system analysis. Fortunately, the execution time can be reduced several
orders of magnitude using the importance sampling technique (Reference 1).

When a ray strikes a surface where the energy is to be distributed among
several components, as described in Subsection 3.3, one of the compo-
nents is statistically chosen. If the energy of this component is scattered
over a finite solid angle, the direction of the scattered ray is randomly
selected according to the appropriate probability density function.

In certain surface radiation models, some components have such pre-
dominant probability that an extremely large number of rays will have to
be generated before any rays will select any of the other components.
As the first step in importance sampling, a ray is split into several
rays, each corresponding to one component. To keep the number of rays
under control, this splitting is done after the energy is reduced by absorp-
tion and the decision has been made between reflection and transmission.
The splitting is automatically performed by the program.

Further importance sampling, which requires specification by the user,
is explained in more detail in the following.

4.1 IMPORTANCE SAMPLING AND SCATTERING

Within a particular component where the energy is scattered over a
finite solid angle, the direction of the scattered ray is randomly selected
according to the probability density function. In most analyses, however,
we are most interested in the amount of radiant energy reaching certain
surfaces. If the rays are allowed to select their paths randomly, a
great portion of the execution time will be wasted in tracing rays
through areas of little interest to the user.

The situation can be dramatically improved by the use of importance sampling.
Similar to the component splitting given above, a non-specular component is
further split into multiple rays, each containing a portion of the scattered

4-1

energy. The directions of all but one of the rays, which we shall
designate as important rays, are chosen by the user to aim toward the
areas of interest, and the fractions of the energy to be assigned to each
ray are calculated from their appropriate probability density functions.
The remaining rays follow the direction statistically selected to complement
the entire probability density function. Its energy is equal to the total
energy less that assigned to the important rays but it is restricted to
directions outside the solid angle defined for the important rays.

The importance sampling technique as applied to scattering of energy is
summarized as follows.

Referring to Figure 4-1, we have energy radiating from a surface
element at 0. If I_0 is the total energy and $E(\Omega)$ is the angular distribution
function of the energy, we have

$$I_0 = \iint_\Omega E(\Omega) \, d\Omega$$

It will become clear later that it is not necessary to obtain the function
$E(\Omega)$ in the process of importance sampling.

The total energy which is simulated by a single ray in the basic Monte
Carlo method is to split into two rays at 0. One of the rays, the important
ray, is aimed at the surface A_1, the important surface, specified by the
user. Although A_1 appears as part of a plane, it could be any type of
surface as far as the importance sampling technique is concerned.

If A_1 is defined by the orthogonal coordinates $\xi - \eta$ and a point P in A_1
is randomly chosen with respect to the coordinates, OP can be used as
the important ray with energy given by

$$I_1 = \iint_{A_1} E(\xi, \eta) \, d\xi \, d\eta$$

or

$$I_1 = \bar{E}_1(\xi, \eta) A_1$$

where $\bar{E}_1(\xi, \eta)$ is the average energy per unit area of A_1. If a large
number of rays are traced, the average energy can be replaced by the
energy at point P and we have statistically
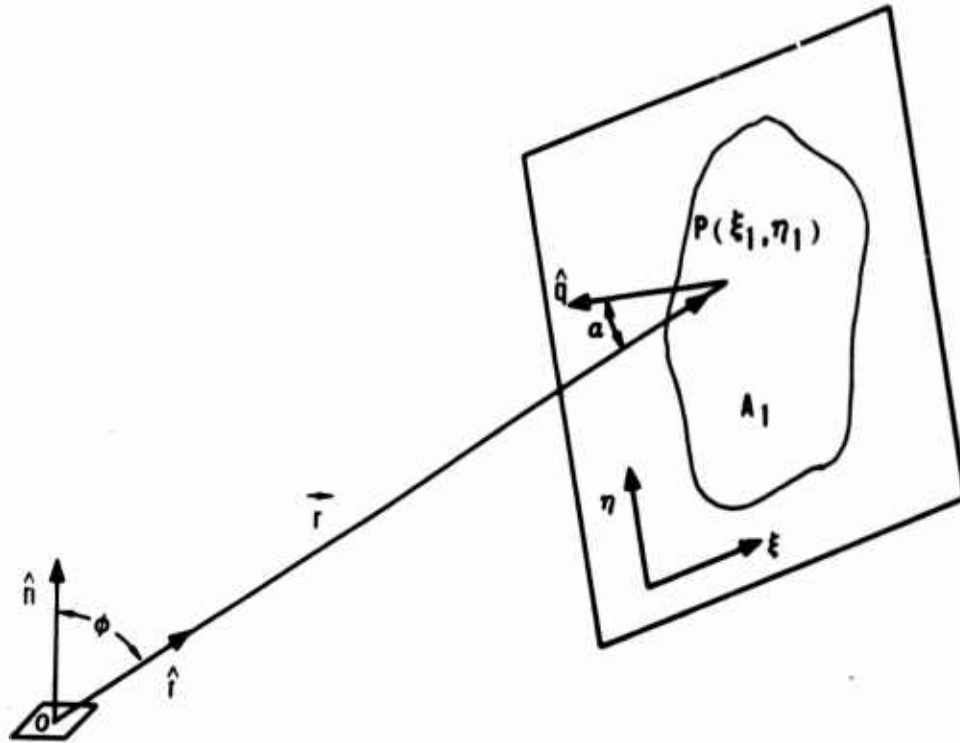
$$I_1 = E(\xi, \eta) A_1.$$

FIGURE 4-1. IMPORTANCE SAMPLING

The complementary ray which is required to miss surface A_1 will have the energy

$$I_2 = I_0 - I_1.$$

4.2 IMPORTANCE SAMPLING AND DIFFRACTION

Importance sampling of rays toward specified areas can be employed as soon as a probability density function exists over a finite solid angle. This can be reflection or transmission off a physical surface or diffraction through an aperture.

As described in Subsection 3.5, the direction of a ray in passing through an aperture is governed by the probability density functions given by Equations 3-8 and 3-9. As soon as a test shows that the intersection point is within DEDGE wavelengths of the aperture edge, the ray can be split as in surface scattering.

The same procedure is followed in selecting the directions of the important rays. The fractions of the energy assigned to these rays are determined by the probability functions. A ray is statistically selected to account for the remaining probability. Again, its energy is equal to the total energy less that assigned to the important rays and it is restricted to the directions outside the solid angle defined for the important rays.

A special importance sampling technique has been implemented at the entrance aperture. As we see from above, appreciable bending of rays due to diffraction occurs only when the ray is within a short distance of the aperture edge. In most optical systems, the entrance apertures are so large that most of the rays generated according to the model given in Subsection 3.1 will be in the center region.

In order to concentrate on the diffraction effect of the entrance aperture, it is divided into a narrow outer ring and the center circle. The width of this ring is given by the constant DRENT. When a positive value is specified for this constant, the number of rays generated at the entrance aperture are evenly divided between the two areas.

The rays in the ring are subsequently split into important and complementary rays if important surfaces are specified for the entrance aperture.

4.3 IMPORTANT SURFACE DEFINITION

For each of the important surfaces corresponding to a surface where a ray is to be split, a point is randomly selected on the important surface. The important ray is obtained by proceeding toward this point and the corresponding fraction of energy is calculated from the probability density function.

The number of important surfaces in each section, with 3 as the upper limit, is given by the array NIMPS(I), where I is the section number. Each important surface can be further partitioned as described in Sub-section 4.4.

An important surface must be defined as a plane bounded by an outer and probably an inner constraint. Since it is in exactly the same form as a basic plane described in Subsection 2.1, the important surfaces are simply read in as basic planes. These planes that are generated for the system configuration or additional planes generated solely as important surfaces.

After sufficient planes have been generated and their equation coefficients calculated, it is necessary only to specify the surface numbers of those surfaces to be used as important surfaces. These surface numbers are given as array IMPORT with the first subscript referring to the sequential number of important surfaces in the section, and the second subscript the section number. For example, IMPORT (J, I) = K means that the basic plane identified as surface K is the Jth important surface of section I. In addition, the number of important surfaces in each section must be specified in the array NIMPS with the subscript referring to the section number.

Assignment of the important surfaces to the system surfaces is specified by the array IMPSF. Users are referred to Paragraph 2.3.4 for its usage.

4.4 IMPORTANT SURFACE PARTITIONING

In the brief description of the importance sampling technique given in Subsection 4.1, we substitute the energy density at P for the average value, i.e.,

$$\int\limits_{A_1} \int E (\xi , \eta) \, d \xi \, d \eta = E (\xi_1, \eta_1) A_1$$

This is statistically correct and will provide accurate results if a large number of rays are traced through the system.

4-5

In order to keep in check the number of rays required it is advisable to reduce the error attributable to the above approximation. If we divide the surface A_1 into n area elements and generate an important ray for each of them the approximation will be in the form

$$\int\int_{A_1} E\ (\xi,\ \eta)\ d\ \xi\ d\ \eta = \sum_{i\ =\ 1}^{n} E\ (\xi_i,\ \eta_\xi)\ A_i$$

and clearly the individual error will be drastically reduced.

Applying the above improvement to the program, we divide each important surface into equal areas of rings and segments, as illustrated in Figure 4-2. This is specified by the user through the arrays NRING and NSEG. Similar to IMPORT, there are two subscripts for each of the arrays. The first subscript refers to the sequential number of important surface in a section while the second subscript refers to the section number. The choice between rings and/or segments is optional: rings should be emphasized if the probability density distribution is approximately axi-symmetric over the important surface and segments should be emphasized if it is not.

How much an important surface should be partitioned depends very much on the probability density distribution. A rule of thumb is that the density should vary no more than a factor of 5 over each area element and the energy given to any important ray should be at least a factor of 3 smaller than the total energy.

In cases where the density distribution is fairly uniform, e.g. diffuse emission, the above criteria is ascertained if we keep the area ratio, i.e., the ratio of the partioned area to the square of the average length of an important ray to the area element, within the factor 0.2. In other cases, e.g., diffraction, the above area ratio should be kept very small. The user should inspect the energy levels to ensure that the above criteria are met.

4.5 IMPORTANT SURFACE DEFINITION GUIDE

The key to efficient use of GUERAP is a judicious use of importance sampling. Much of the judgment must be obtained by experience; the purpose of this section is to provide a basis for avoiding the more obvious difficulties that the user may encounter.
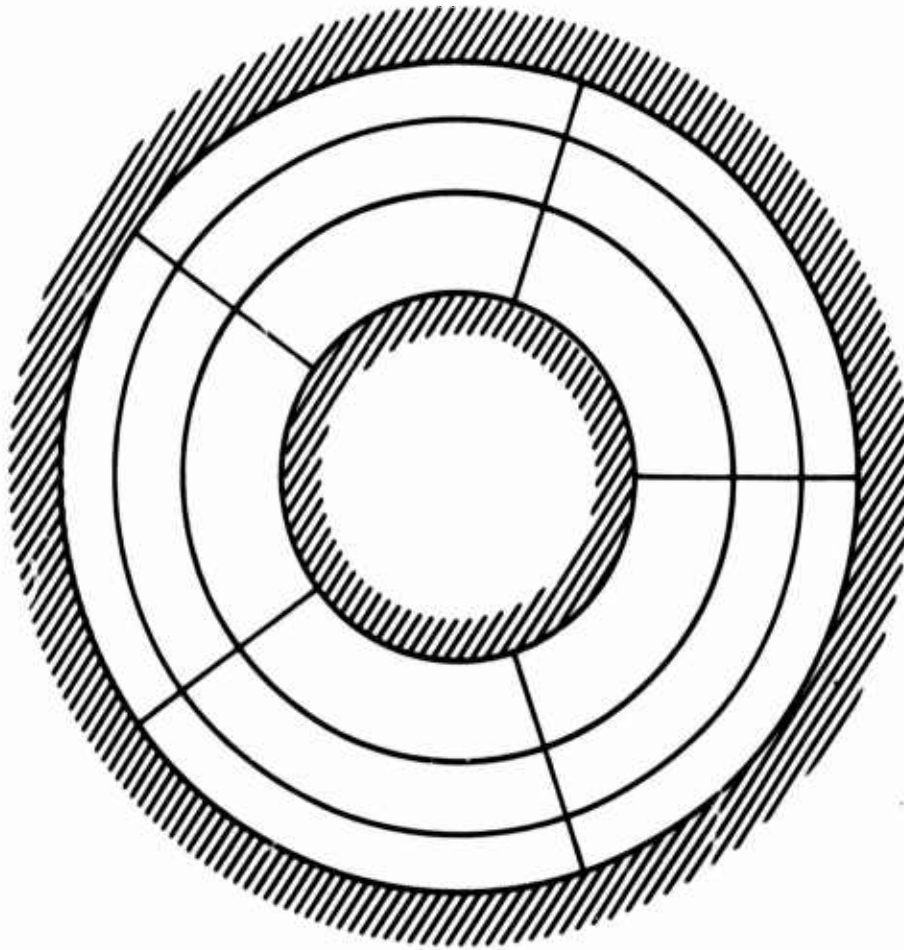
1072-485A

FIGURE 4-2. PARTITIONED ANNULAR IMPORTANT SURFACE
(NRING=3, NSEG=5)

4.5.1 Importance Surface Selection

Locating an important surface for the direct scattered energy from each real surface is relatively simple. In addition, the user must investigate the possibility that indirect scattered energy (e.g. multiple reflection energy) will be as significant as the direct scattered energy. In this case the user should define a set of additional importance surfaces to "guide" the indirect scattered energy to the principal importance surface.

Figure 4-3 illustrates this technique. The single section in Figure 4-3 consists of two planes, surfaces 2 and 4, defining a circular entrance aperture (surface 1) and a circular exit aperture (surface 3) respectively. The planes are bounded by a concentric cylinder, surface 5.

Energy striking surface 4 cannot be scattered directly into the exit aperture, the principal important surface. However, a significant fraction of the energy leaving surface 4 will strike surface 2 and then be rescattered from surface 2 through the exit aperture. Surface 2 should therefore be defined as an importance surface for surface 4.

4.5.2 Important Surfaces for Diffracted Energy

In many cases, as energy is diffracted at an aperture, what is significant is not the energy that subsequently strikes a real surface or exit aperture, but is the energy that is diffracted into the field of view at the aperture. In this case the user should define an imaginary important surface which subtends a solid angle representing the system field of view at the diffraction zone.

Figure 4-4 illustrates this situation. Only the energy which is diffracted into the field of view will be focused by the lens into the exit aperture. The exit aperture cannot be used as the importance surface; the lens will focus the resulting important rays in front of the exit aperture. The lens surfaces cannot be used; very few of the resulting rays will be in the field of view.

The user must define the imaginary surface which essentially defines the field of view at the diffraction ring. This is illustrated in Figure 4-5. Two cones defining the field of view are extended from opposite sides of the diffraction zone, parallel to the system optical axis. The cones are extended past their point of intersection A, and the important surface is located at B, with an outer radial constraint equal to the overlap radius BC. This surface subtends a solid angle equal to a fraction of the field of view, which

is defined by the outside limits of the cones, radius BD. As AB is made larger and larger, the fraction approaches unity. If AB is made too large however, the simulation will suffer due to computer round-off errors. A practical choice is to make AB just large enough that the fraction is 0.90 to 0.95.

1072-470-A
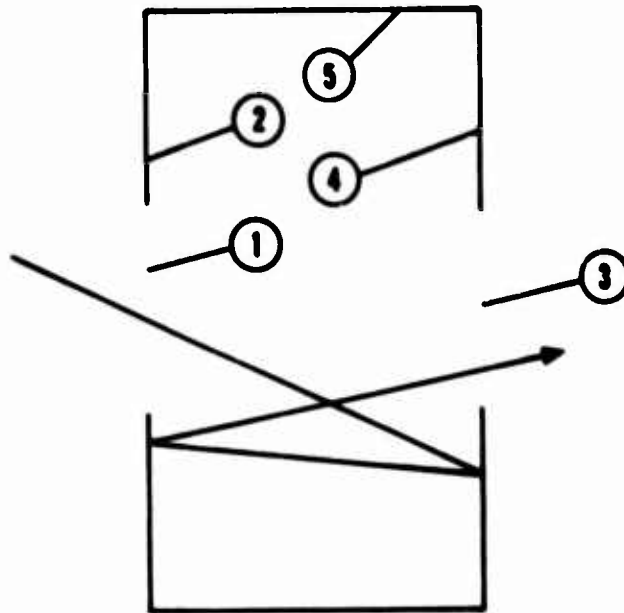
FIGURE 4-3. SECONDARY IMPORTANT SURFACES

1072-471-A
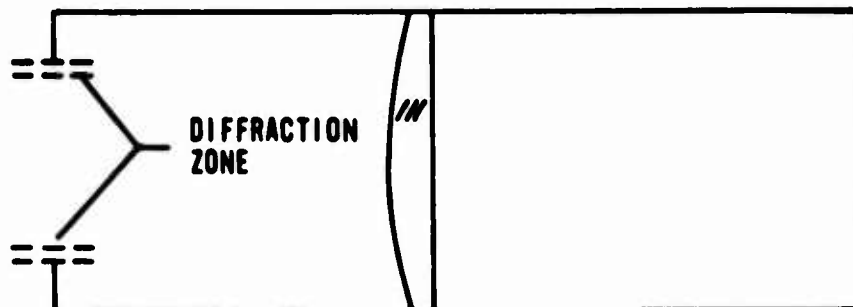
FIGURE 4-4. DIFFRACTION-SENSITIVE SYSTEM
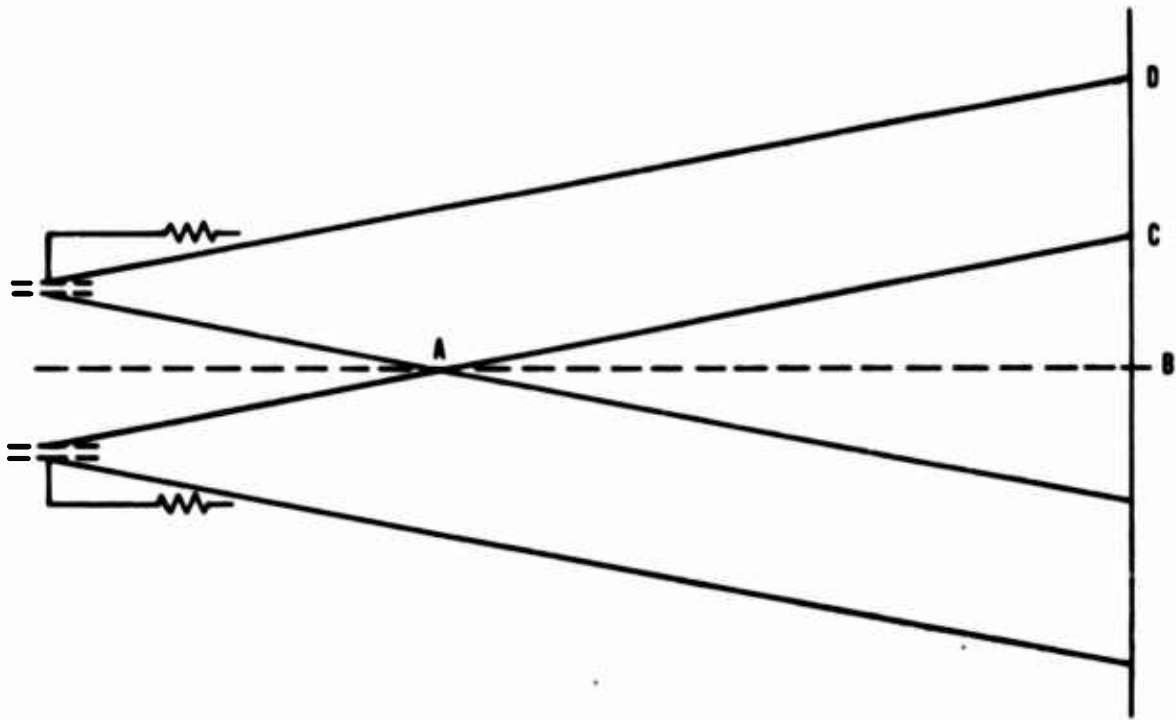
FIGURE 4-5. IMAGINARY IMPORTANT SURFACE FOR DIFFRACTION -
4-11

Section 5

PROGRAM DESCRIPTION

To assist the user in his understanding of the GUERAP computer program and in his effort to modify it when necessary, we present a concise description in this section.

The program can be divided into seven major portions, each consisting of several closely related subroutines. After a brief description of its main task, we list the subroutines and their corresponding functions.

At the end of this section, skeleton flow charts are given for the main program and its major subroutines. Together with the embedded comments throughout the program deck, these should greatly facilitate any desired user modifications.

5.1 MAIN PROGRAM GUERAP

a. Sets the values of constants and non-zero default values of variables.

b. Reads in surface parameters.

c. Calls subroutines PLANE, CONE, SPHERE, PARABL and BAFFLE to generate the basic surfaces and their standard constraints.

d. Reads in the parameters of and calculates the special constraints.

e. Reads in and prepares surface radiation coefficients.

f. Reads in parameters describing the system.

g. Reads in parameters describing the set of important surfaces.

h. Reads in the parameters of and performs ray tracing of external radiation.

i. Prints out results thereof.

j. Reads in the parameters of and performs ray tracing of internal emission.

k. Prints out results thereof.

5.2 BASIC SURFACE SUBROUTINES

These subroutines generate basic surfaces and handle transformation of their equations between system and local coordinates.

a. Subroutine PLANE

1. Calculates coefficients for the equations of planes and their standard constraints.

2. Calculates coefficients for the equations of plane special constraints.

3. Calls subroutine EQUATN to transform the equations into the system coordinates.

b. Subroutine CONE

1. Calculates coefficients for the equations of cones and their standard constraints. Note that circular cylinders are treated as cones.

2. Calculates coefficients for the equations of conical special constraints.

3. Calls subroutine EQUATN to transform the equations into system coordinates.

c. Subroutine SPHERE

1. Calculates coefficients for the equations of spheres and their standard constraints.

2. Calculates coefficients for the equations of spherical special constraints.

3. Calls subroutine EQUATN to transform the equations into the system coordinates.

d. Subroutine PARABL

1. Calculates coefficients for the equations of paraboloids and their standard constraints.

2. Calculates coefficients for the equations of parabolic special constraints.

3. Calls subroutine EQUATN to transform the equations into the system coordinates.

e. Subroutine BAFFLE

1. Calculates coefficients for the equations of surfaces representing baffles and their standard constraints.

2. Calls subroutine EQUATN to transform the equations except those of toroids into the system coordinates.

f. Subroutine EQUATN

1. Transforms the above equations into system coordinates.

2. Generates and stores the transformation matrixes.

g. Subroutine TRNSFM

Transforms the location and orientation of a ray between local and system coordinates.

5.3 SUBROUTINES ON EXTERNAL RADIATION

a. Subroutine EXTRADN

1. Calls subroutine EXT to generate rays at entrance aperture.

2. Calls subroutine TRACING and traces the rays.

3. Prints out results on external radiation.

b. Subroutine EXT

Generates rays at entrance aperture.

5.4 SUBROUTINES ON INTERNAL EMISSION

a. Subroutine EMISSN

1. Generates pilot rays at poles.

2.   Obtains emitting points through interceptions between pilot rays and related surfaces.

3.   Calls subroutine BBRFN to calculate black body radiation function.

4.   Generates emitted rays.

5.   Calls subroutine TRACING to trace the rays.

6.   Prints out results on internal thermal emission.

b.   Subroutine BBRFN

Calculates black body radiation function in terms of wave bands.

5.5 SUBROUTINES ON RAY TRACING

This group handles Monte Carlo ray tracing through system in detail.

a.   Subroutine TRACING

1.   Traces rays through the system.

2.   Recalls important rays from storage and traces them through the system.

b.   Subroutine GEOM

1.   Calculates points of interception between rays and surfaces.

2.   Tests the points in terms of constraints.

3.   Selects the closest interception.

c.   Subroutine NORM

Calculates direction cosines of surface unit normals at points of interception.

d.   Subroutine TRANS

Transforms orientation of rays from local coordinates at points of interception to system coordinates.

e. Subroutine REFLIN

    1. According to surface radiation model, obtains directions of rays after its interactions with surfaces.

    2. Calls subroutine REFRN for refracted rays.

    3. Calls subroutine EXPECT to generate and store important rays.

f. Subroutine REFRN

    1. Calculates directions of refracted rays according to Snell's Law.

    2. Tests total internal reflection.

g. Subroutine ANGSSD

    Calculates directions of rays for specular reflection, diffuse reflection, near specular reflection and diffuse transmission.

h. Subroutine SCATTR

    Calculates off-specular angle for near-specular reflected rays.

i. Subroutine DIFRN

    1. According to diffraction model, obtains directions of rays after they pass through circular apertures.

    2. Calls subroutine DIFEXP to generate and store important rays.

j. Subroutine DISTB

    Records and prints ray count and energy maps on exit apertures.

5.6 SUBROUTINES ON IMPORTANCE SAMPLING

a. Subroutine EXPECT

    1. Calls subroutine ISELECT to select important surfaces.

    2. Generates important rays according to surface radiation models.

    3. Calls subroutine RAYSAV to store important rays.

4. Generates random rays according to surface radiation models.

5. Calls subroutine TESTSS to test interceptions of complementary rays by important surfaces.

b. Subroutine DIFEXP

    1. Calls subroutine ISELECT to select important surfaces.

    2. Generates important rays according to diffraction model.

    3. Calls subroutine RAYSAV to store important rays.

    4. Generates random rays according to diffraction model.

    5. Calls subroutine TESTSS to test interceptions of complementary rays by important surfaces.

c. Subroutine ISELECT

Selects important surfaces.

d. Subroutine TESTSS

Tests interceptions of complementary rays by important surfaces.

e. Subroutine RAYSAV

Stores important rays.

5.7 MISCELLANEOUS SUBROUTINES

a. Subroutine PLOT

Plots radial energy density distribution on the exit aperture.

b. Subroutine BIQUA

Solves the bi-quadratic equation,

$$C_1 X^4 + C_2 X^3 + C_3 X^2 + C_4 X + C_5 = 0.$$

c. Subroutine CUBIC

Solves the cubic equation,

$$C_1 X^3 + C_2 X^2 + C_3 X + C_4 = 0.$$

d. Function ACOS

Obtain $y = \cos^{-1} X$.

5.8 MAIN PROGRAM AND SUBROUTINE FLOW CHARTS

Flow charts are given for the main program and selected subroutines in Figures 5-1 through 5-7.
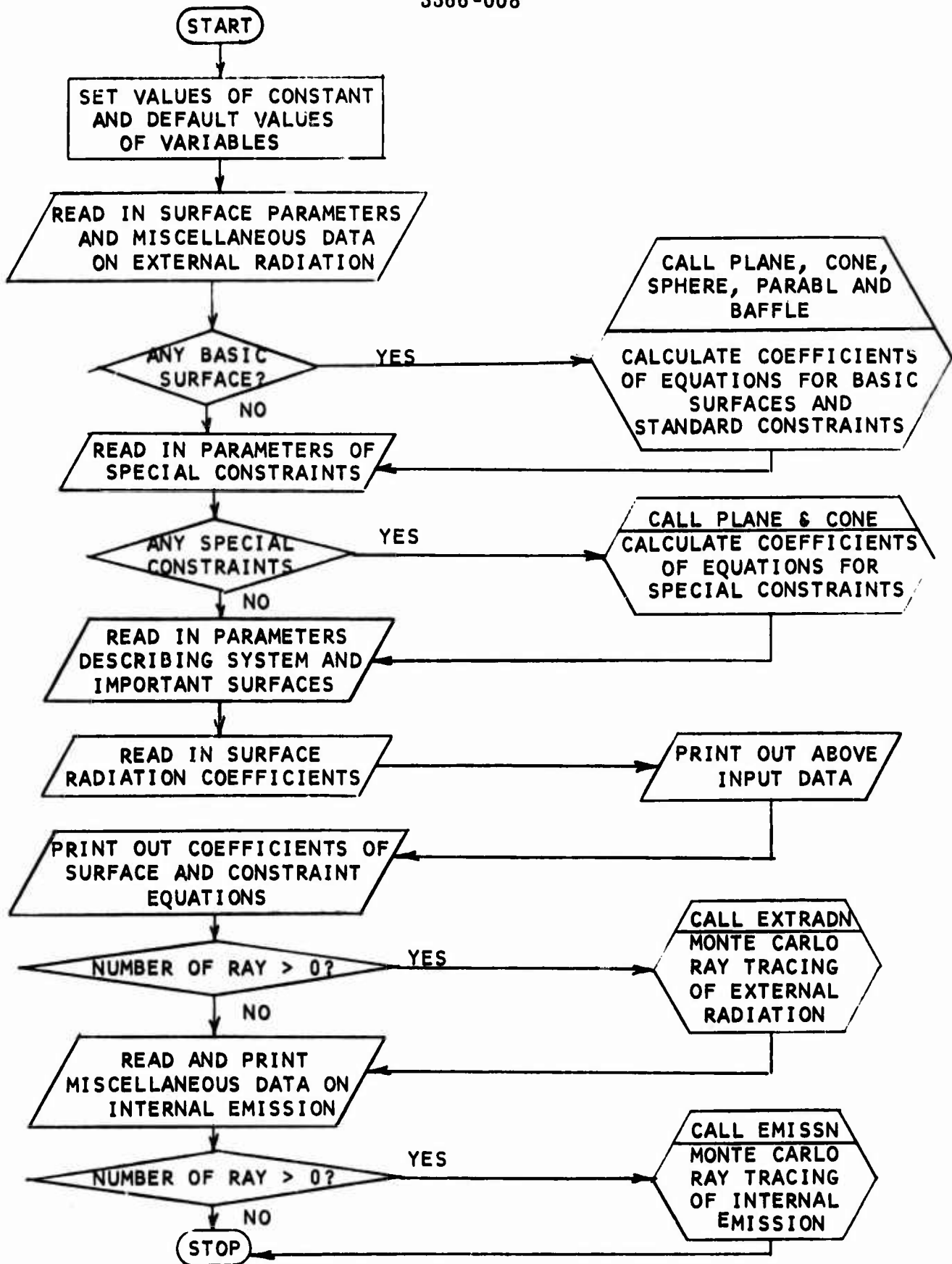
FIGURE 5-1. MAIN PROGRAM FLOW CHART
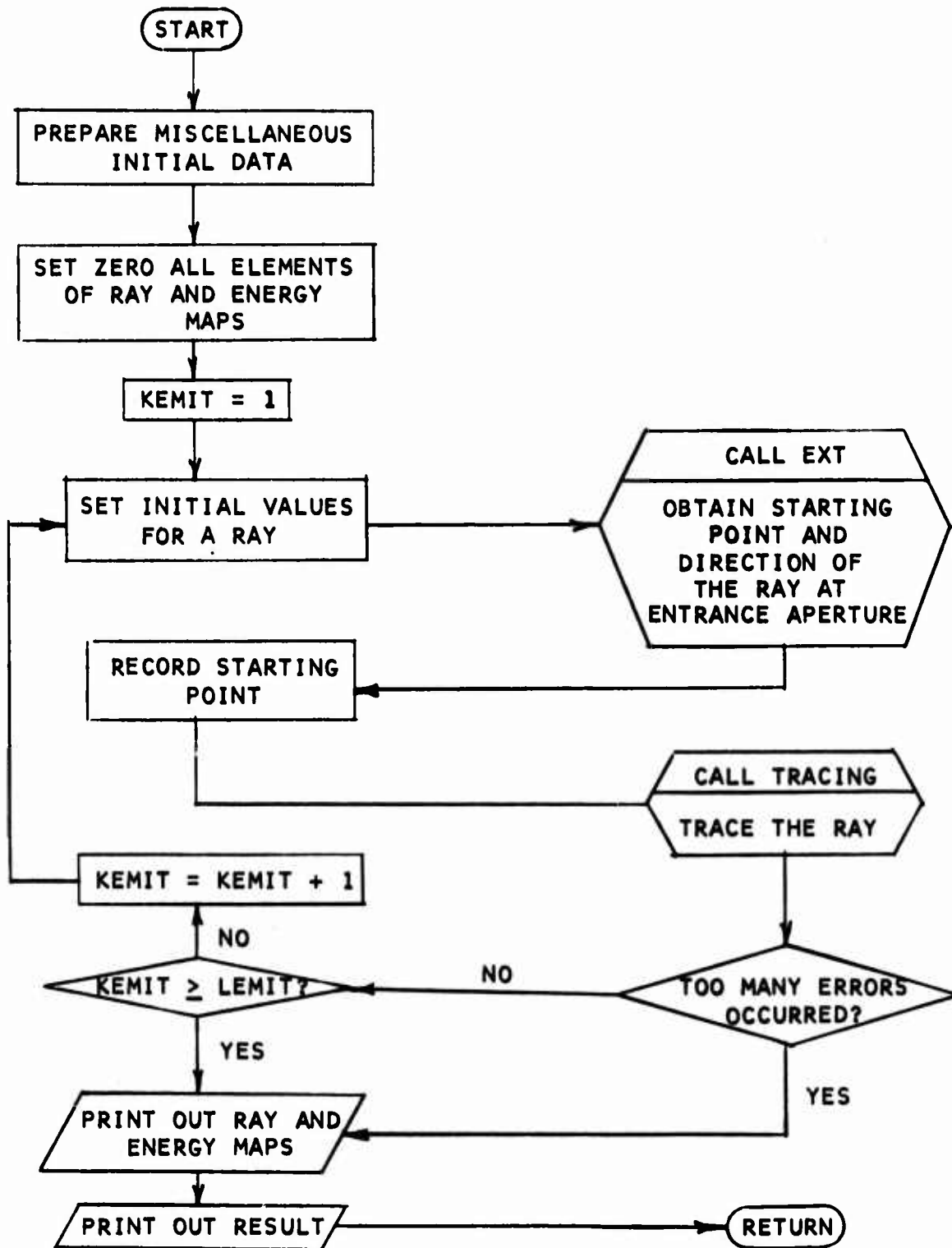
FIGURE 5-2. SUBROUTINE EXTRADN FLOW CHART

FIGURE 5-3. SUBROUTINE EMISSN FLOW CHART (1 of 2)

FIGURE 5-3. SUBROUTINE EMISSN FLOW CHART (2 of 2)
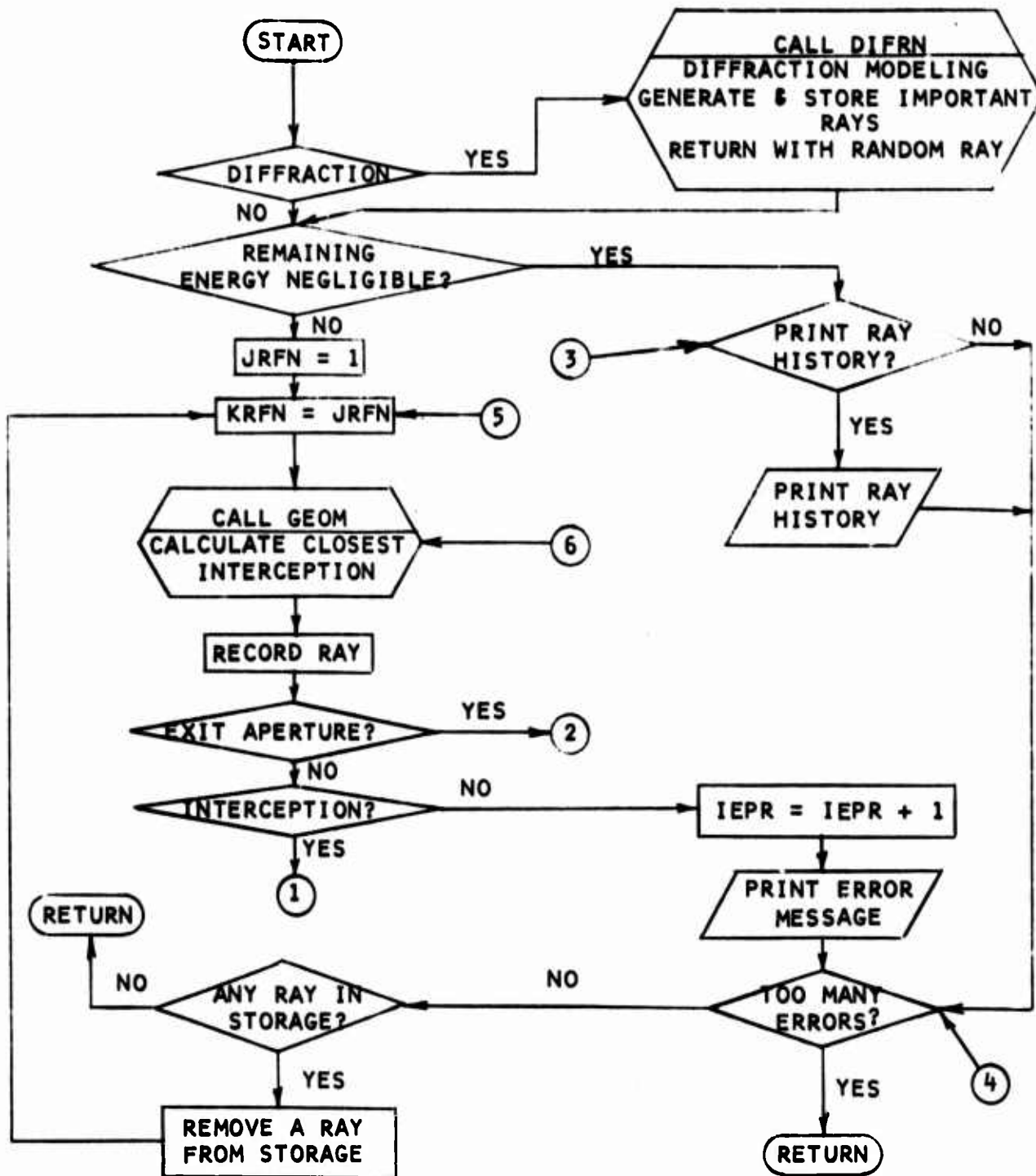
FIGURE 5-4. SUBROUTINE TRACING FLOW CHART (1 of 3)
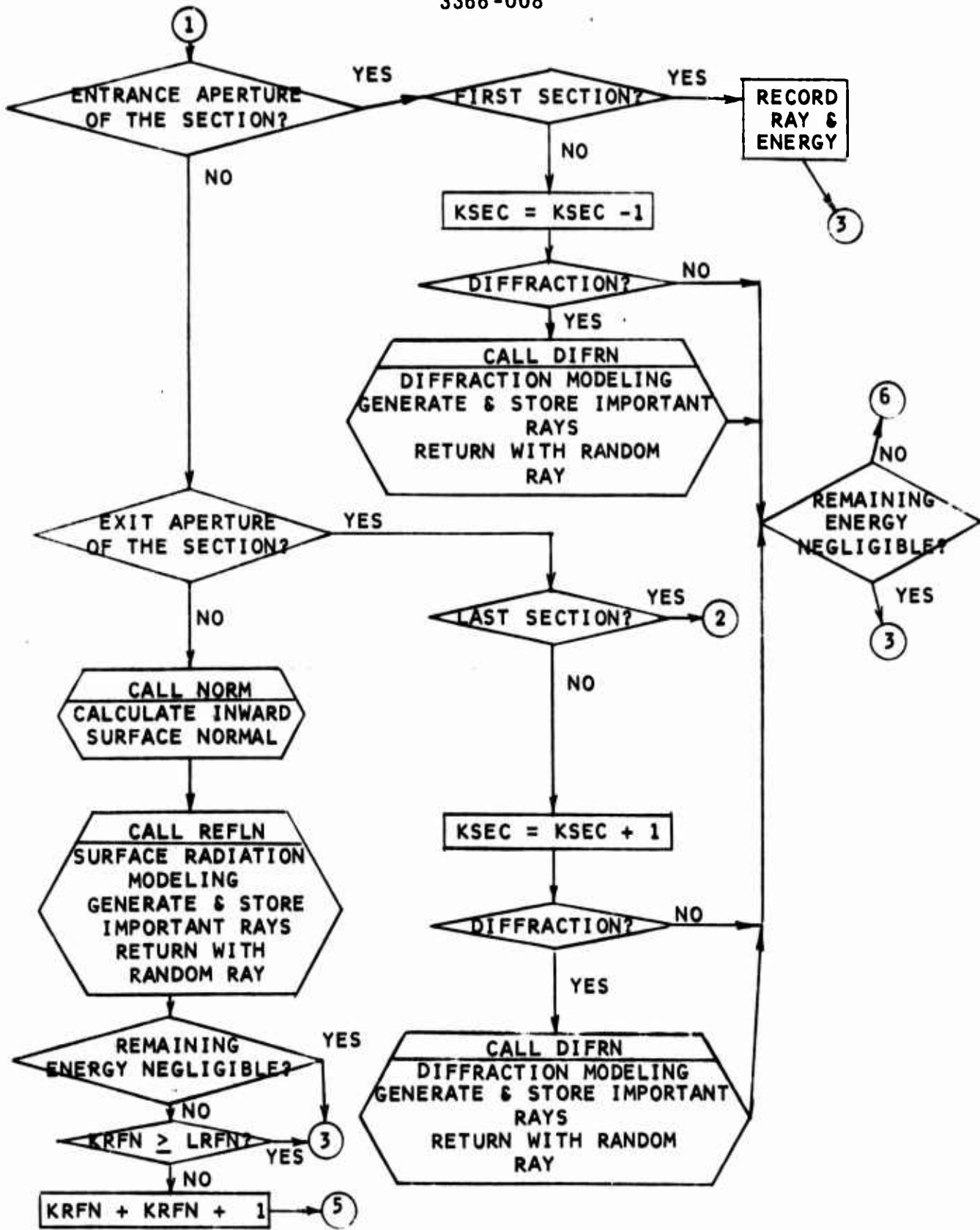
FIGURE 5-4. SUBROUTINE TRACING FLOW CHART (2 of 3)
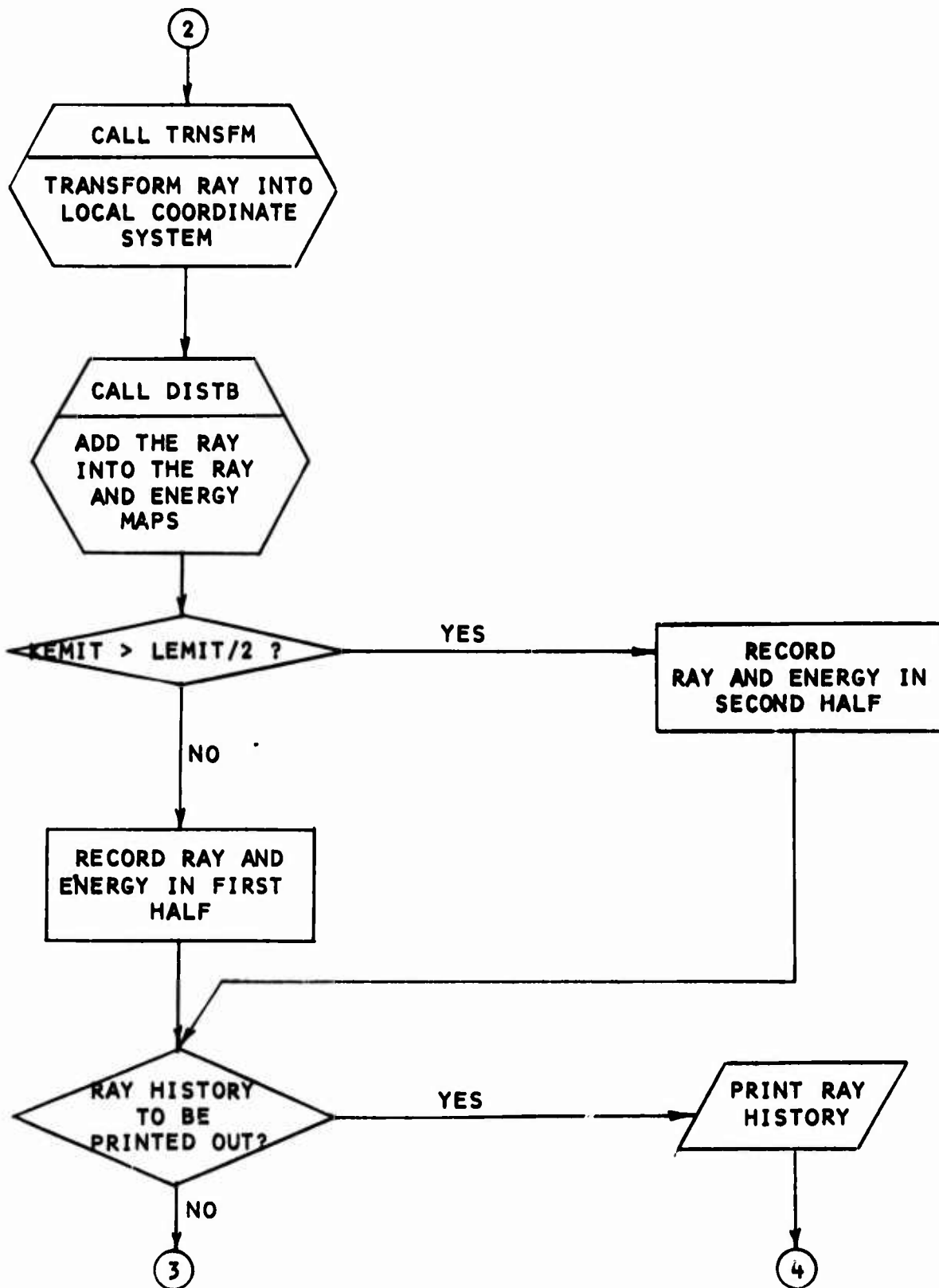
FIGURE 5-4. SUBROUTINE TRACING FLOW CHART (3 of 3)
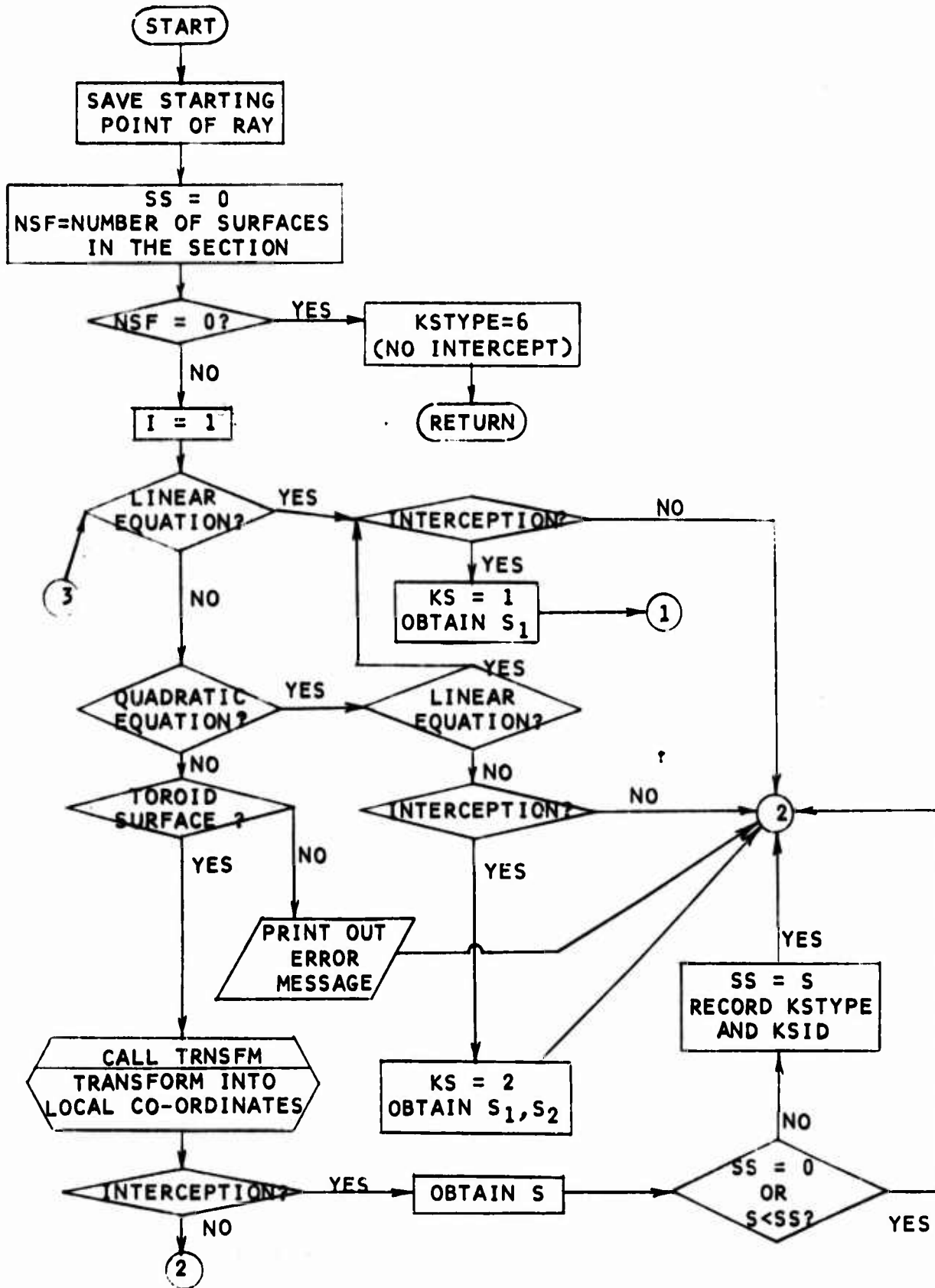
FIGURE 5-5. SUBROUTINE GEOM FLOW CHART (1 of 2)
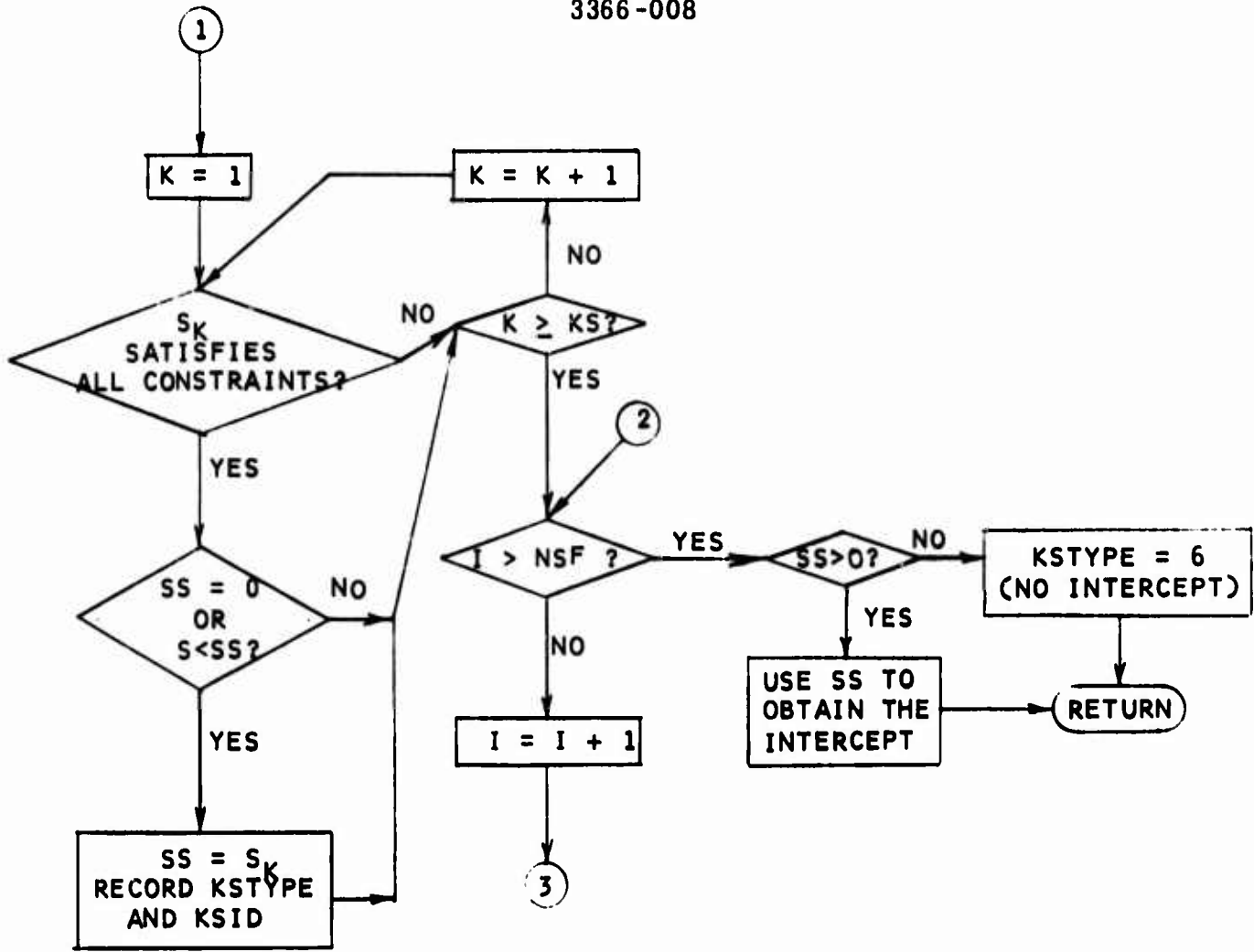
FIGURE 5-5.   SUBROUTINE GEOM FLOW CHART (2 of 2)
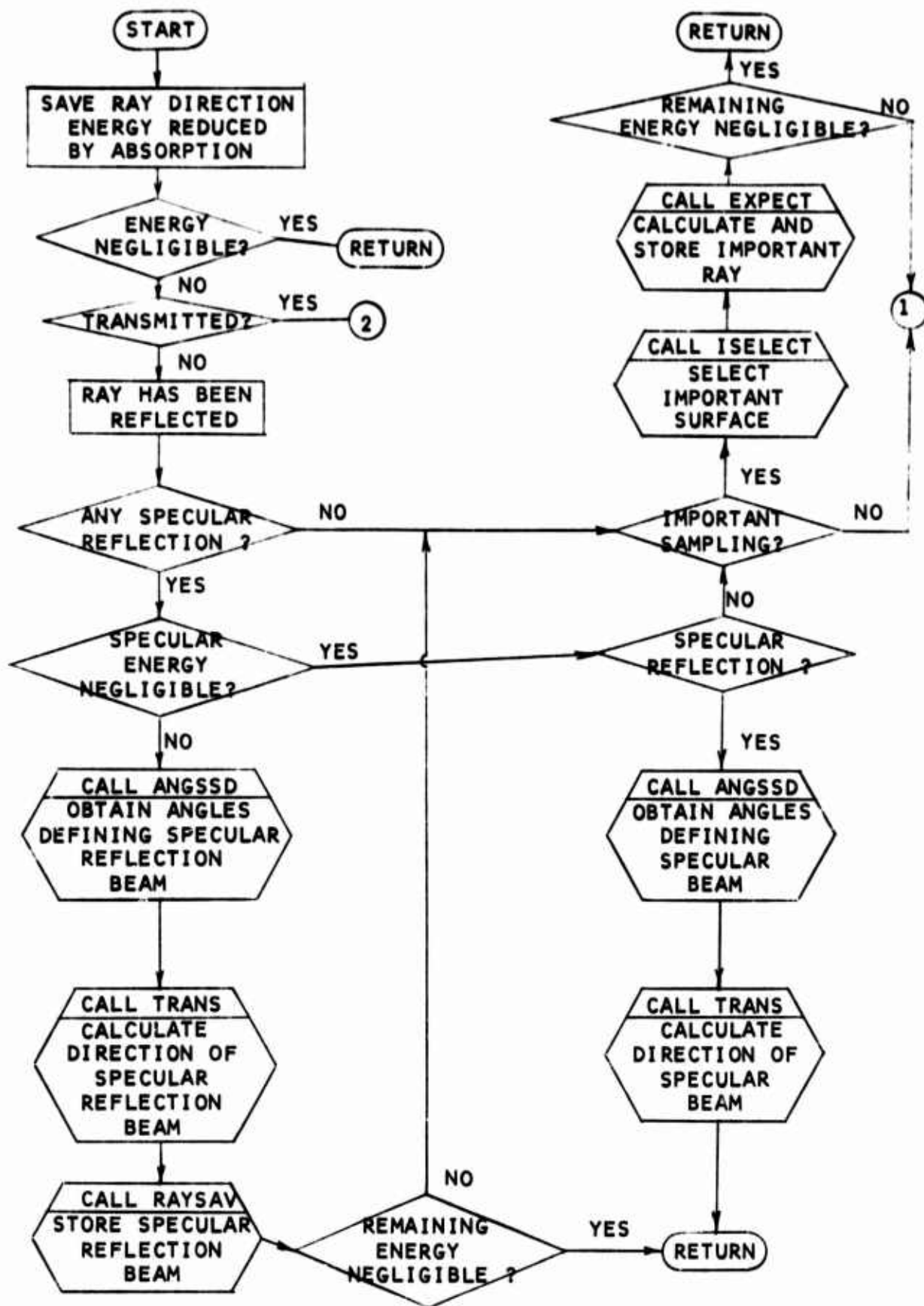
FIGURE 5-6. SUBROUTINE REFLN FLOW CHART (1 of 4)

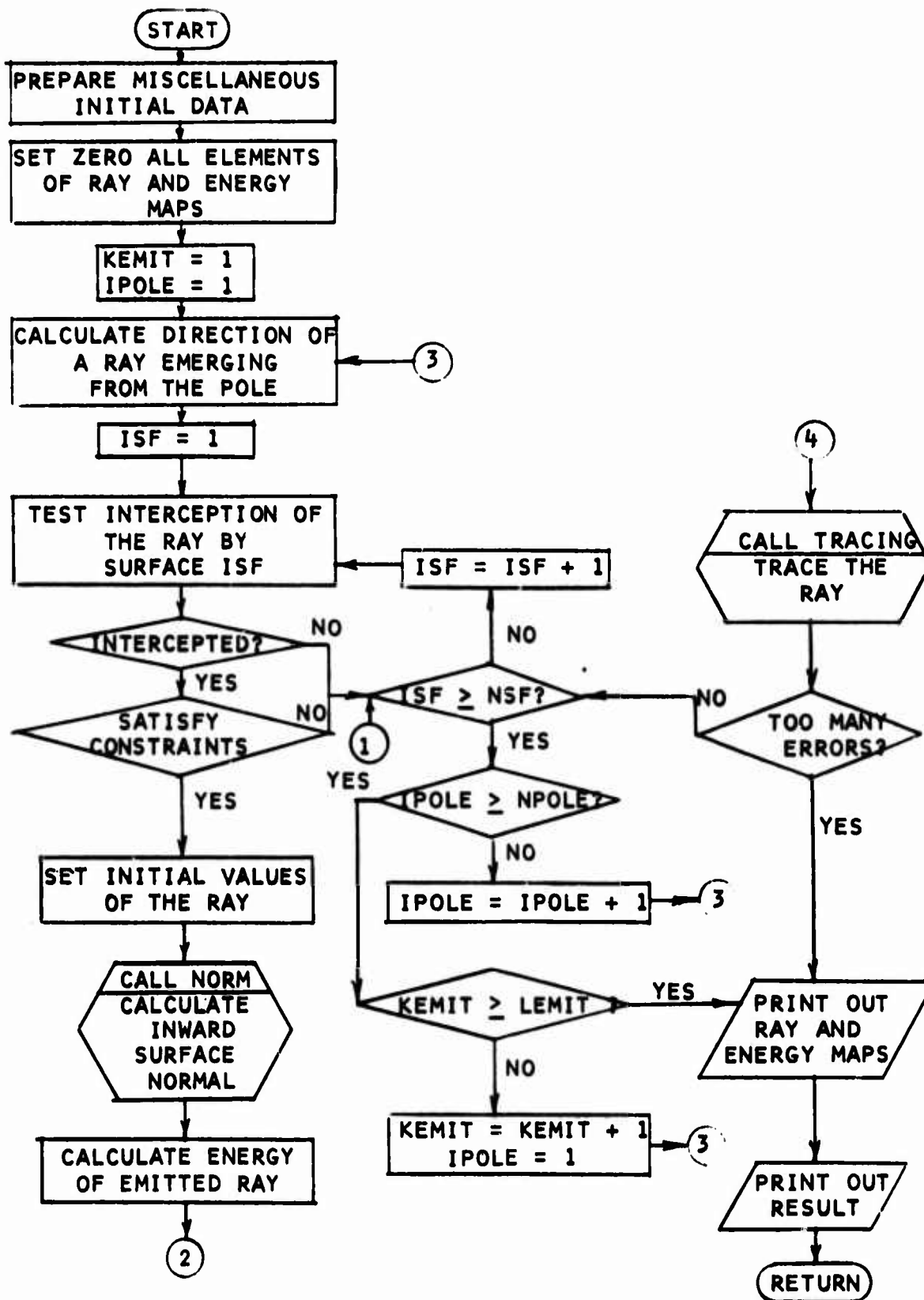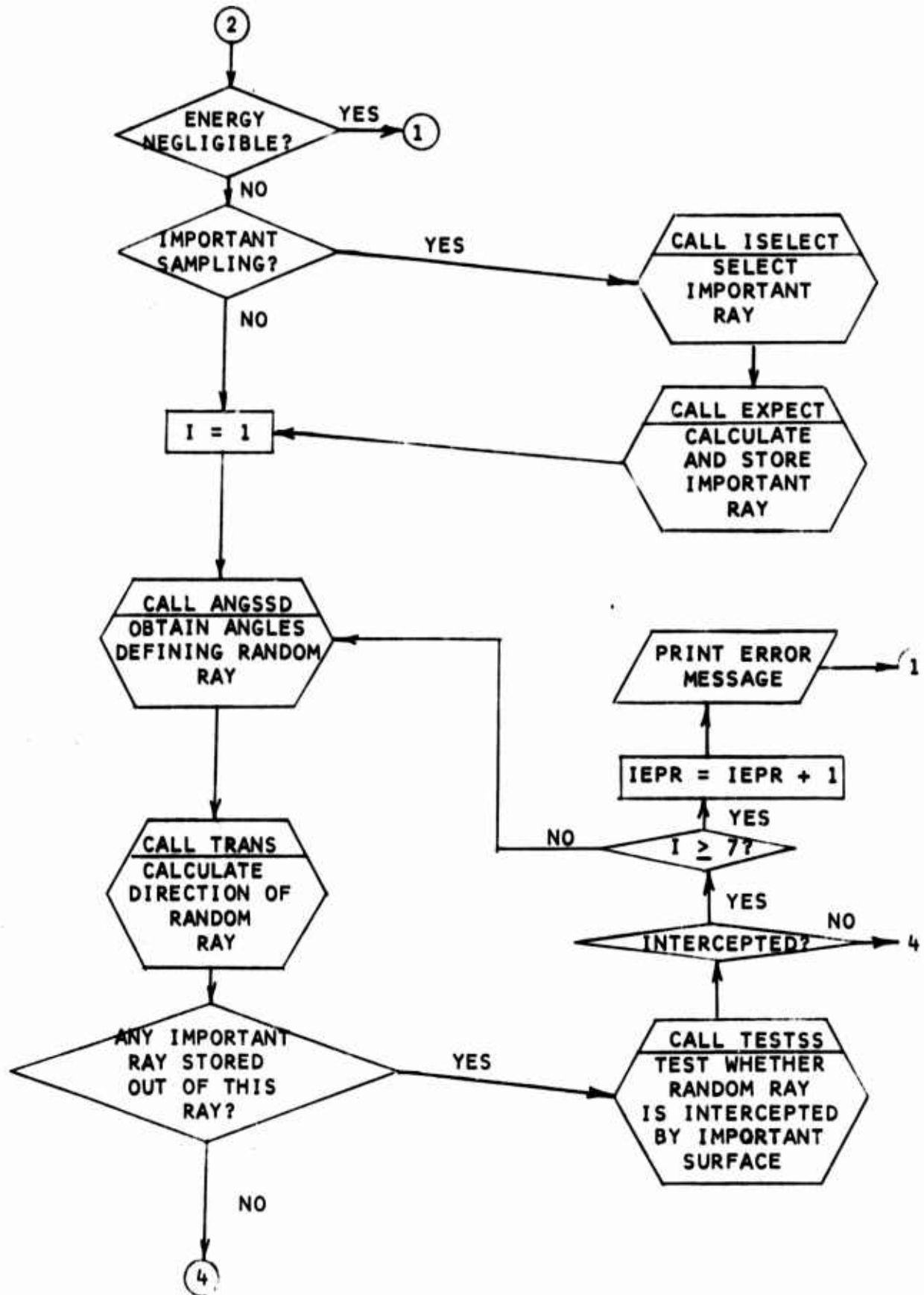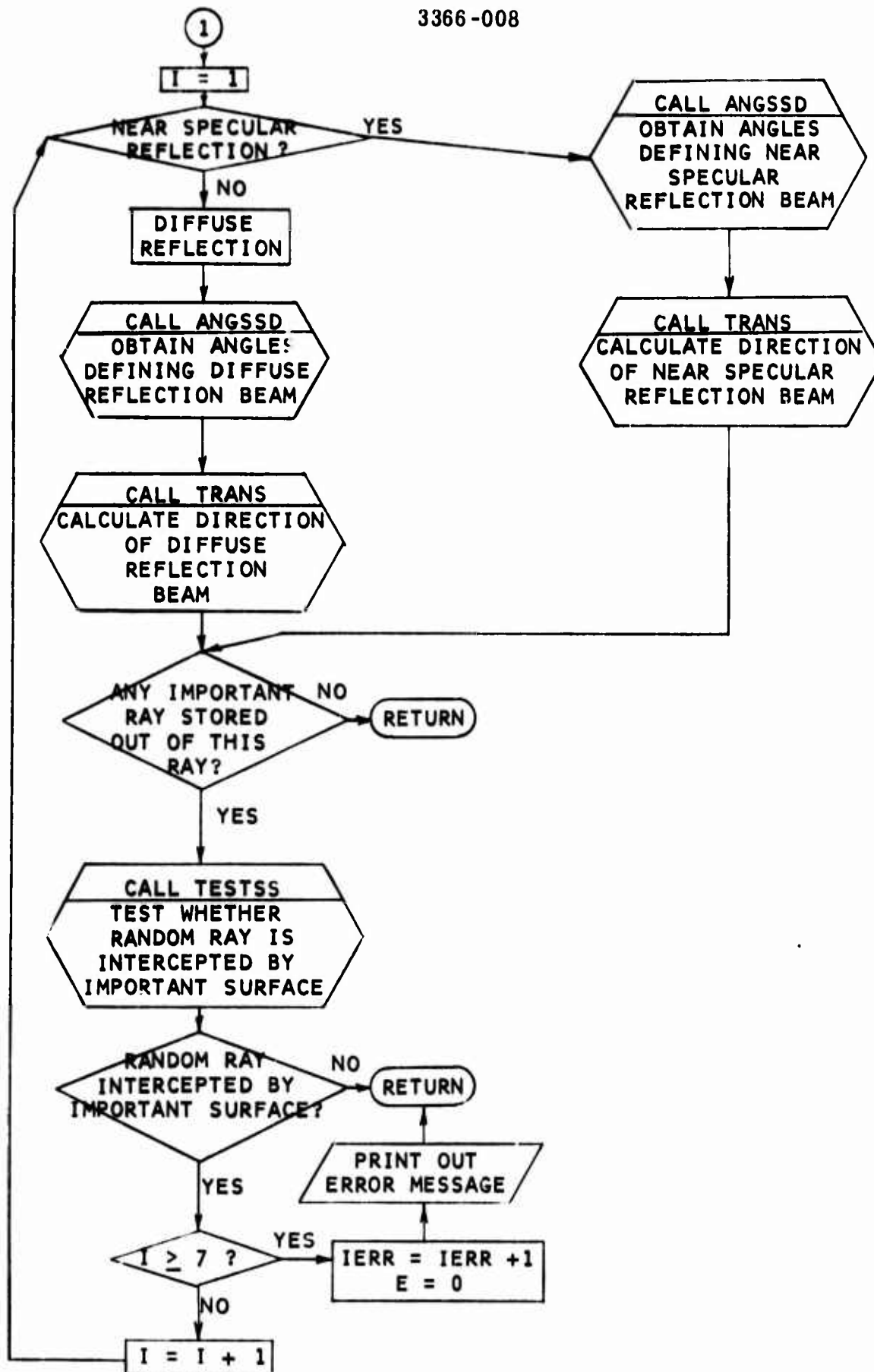FIGURE 5-6. SUBROUTINE REFLN FLOW CHART (2 of 4)
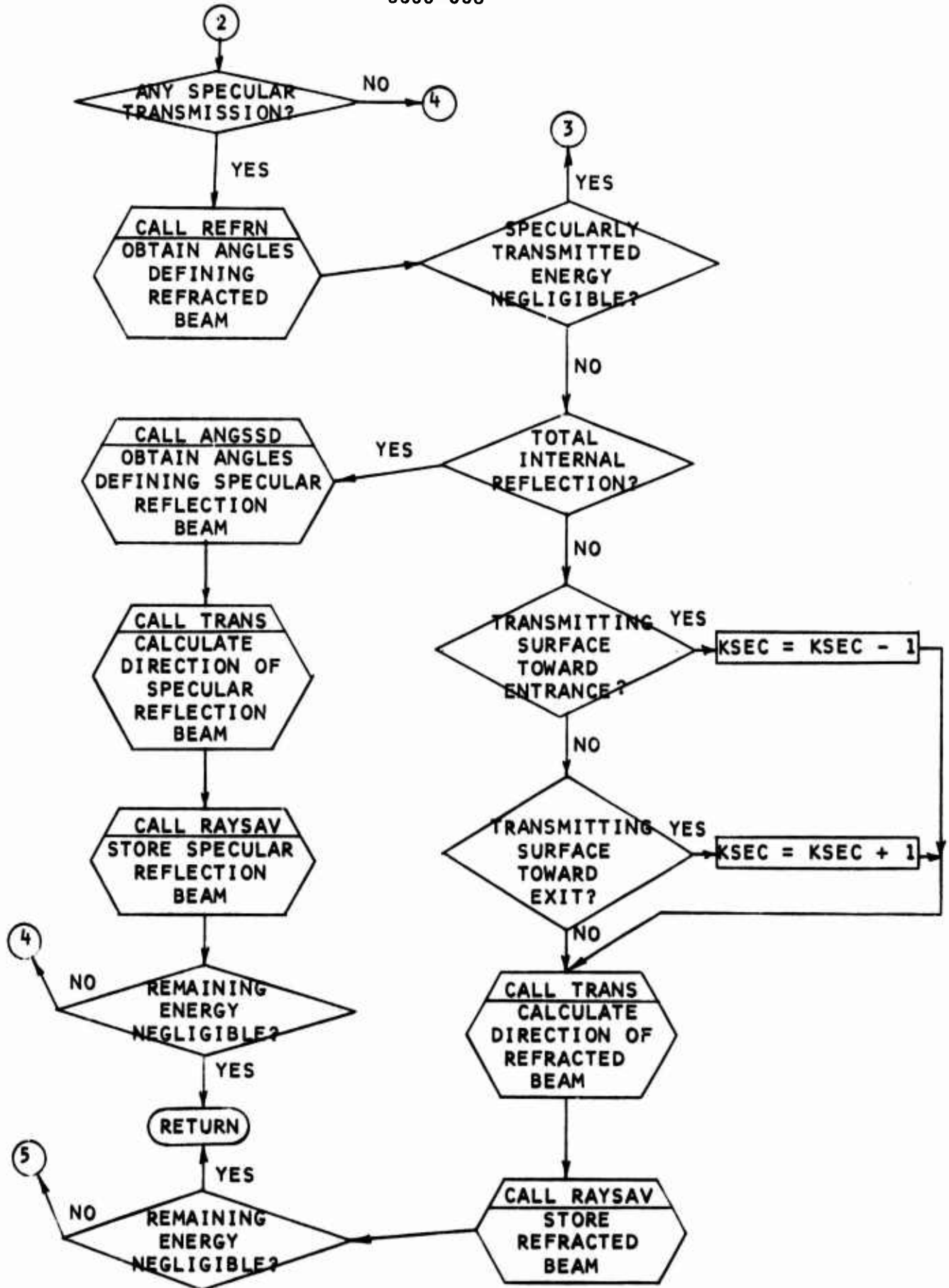
FIGURE 5-6. SUBROUTINE REFLN FLOW CHART (3 of 4)
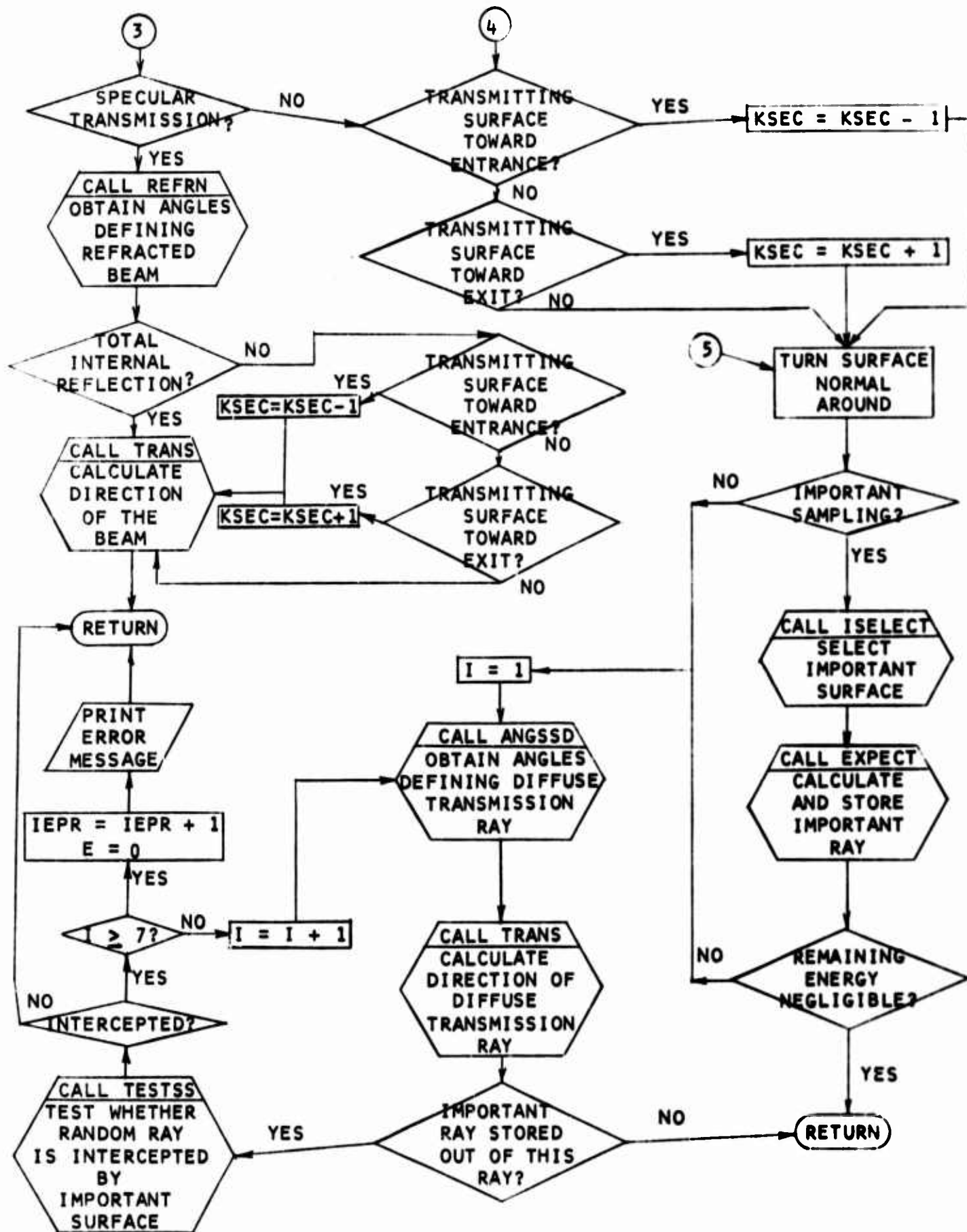
FIGURE 5-6. SUBROUTINE REFLN FLOW CHART (4 of 4)
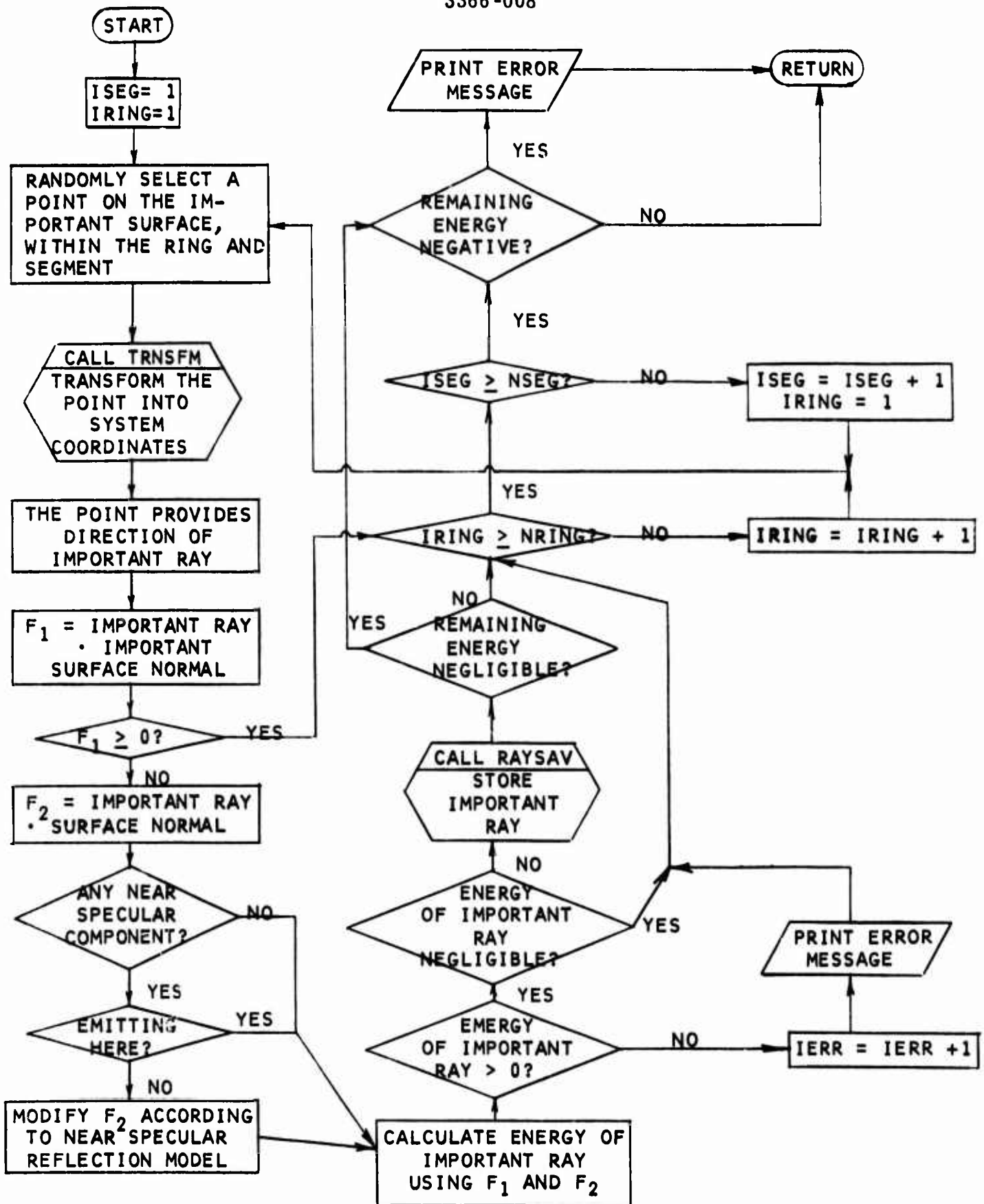
FIGURE 5-7. SUBROUTINE EXPECT FLOW CHART

Section 6

INPUT DATA

The complete input data variables of the GUERAP computer program are listed in this section. The data are divided into eight groups arranged in the sequence given in the listing.

A variable can be either a scalar or an array. A scalar variable is designated simply by the variable name, while an array is indicated by the name followed by the suitable number of subscripts in a pair of parentheses.

Each variable is accompanied by a brief definition, the default value and the page number where the related description may be found. While the non-zero default values are given in the program, the user has to set the entire field length to zero before execution.

Except for the first group, the data are input via namelist statements, a standard feature in FORTRAN V. The user is referred to any modern FORTRAN manual for description of the usage.

Although the number of elements in each array is limited by the assigned dimension, the user can readily extend such limits. For the current limits and the alteration procedure, the user is referred to the section "INSTRUC-TION FOR CHANGING DIMENSIONS" in the listing of main program GUERAP.

6.1 HEADING AND RANDOM NUMBER PILOT SEED

Any number of cards with alphanumeric characters and blanks can be used as the problem header. It is terminated by a card with ENDTITLE starting in the first column. This header will appear in the beginning of the output.

Variable	Definition	Default Value	Reference Page
ISEED (in $\emptyset$20 format)	Pilot number for the random number routine. Any odd positive integer less than 2^{57}.	Must be input.	

6.2 NAMELIST NAME1

Miscellaneous data for the system and external radiation is presented below.

Variable	Definition	Default Value	Reference Page
SUNAGD	Elevation angle of incident beam. *	0	3-2
SUNAZD	Azimuthal angle of incident beam.	0	3-2
SUNDVD	Divergence angle of incident beam.	0	3-2
DELTAE	Relative energy level of a ray, with respect to its energy at the entrance aperture, below which it will be abandoned.	10^{-12}	
DEPRT	Minimum relative energy level of a ray for which the trace history will be printed in arriving at the exit aperture. Normally it is larger than DELTAE to avoid listing of too many rays with low energy.	10^{-12}	7-2
LEMIT	Number of rays to start at entrance aperture for external radiation calculation.	100	
LREN	Limit on number of reflections and transmissions of a ray.	20	
ISEEDP	After every ISEEDP rays are finished, the value of ISEED is printed out. These ISEED values can be used to continue the computation.	100	

* All angles are in degrees except when otherwise noted.

Variable	Definition	Default Value	Reference Page
NPRINT	Limit on number of rays for which the tracing will be printed in arriving at exit aperture.	200	
NERR	Number of error occurrences which will terminate program execution. The accumulated energy distribution on the exit aperture will be printed out.	20	
NSEC	Number of sections.	0	2-16
RMAP	Radius of the energy distribution maps at exit aperture.	0	7-3
KPRINT	Signal for printing ray history of rays that didn't reach the exit aperture. Set any positive integer and ray history will be printed out after first KPRINT rays. Set 0 if no such printout is desired.	0	7-2
WAVEL	Wave length in microns.	0	
DEDGE	Number of wave lengths from the edge of an aperture beyond which diffraction will be ignored.	100	3-15
DRENT	Width of the outer annular ring on the entrance aperture where, in the case of diffraction, 50% of the rays will be concentrated. Set zero if no such importance sampling is desired at entrance aperture.	0	4-4

Variable	Definition	Default Value	Reference Page
ISENT	Surface number of the entrance aperture.	0	
ISEXT	Surface number of the exit aperture.	0	
AREAEN	Area of the entrance aperture.	The area of a circle of radius PTLCTR (7, ISENT)	
AREAEX	Area of the exit aperture.	The area of a circle of radius PTLCTR (7, ISEXT).	

6.3 NAMELIST NAME2

Diffraction command, degrees of surface equations, and indices of refraction are listed below.

Variable	Definition	Default Value	Reference Page
KDIF (I)	Signal of diffraction at apertures. Set KDIF (I) = 1 for I = Surface number of all the apertures where diffraction is considered.	0	3-15
IDGREE(I)	Degree of equation for surface I.	Given by basic surfaces.	2-1
RINDEX (I)	Index of refraction for section I.	1	3-11

6.4 NAMELIST NMGEOM

Basic surfaces are shown below.

Variable	Definition	Default Value	Reference Page
IPLANE (I)	Surface number of the Ith plane.	0	2-2

Variable	Definition	Default Value	Reference Page
ICONE (I)	Surface number of the Ith cone.	0	2-2
ISPHER (I)	Surface number of the Ith sphere.	0	2-4
IPARAB (I)	Surface number of the Ith paraboloid.	0	2-4
IBAFF (I)	Surface number of the knife edges of the Ith baffle. Note that there are four surfaces for each baffle.	0	2-4
PTLCTR (K, J)	Parameters describing surface J: The kind of basic surface is given by the parameters IPLANE, ICONE, ISPHER, IPARAB and IBAFF. Meaning of PTLCTR is fully described in Section 2.	0	2-2 through 2-7
PKNIFE	Radius of the cross section of knife edges.	0	2-4, 2-6, 2-8
TBAFF	Thickness of baffles.	0	2-4, 2-6, 2-8
DBAFF	Halfwidth of hyperboloids on plane baffles.	0	2-4, 2-6
ABAFFD	Blade angle of baffle knife edges.	0	2-4, 2-6, 2-8
COEF (J, I)	Coefficients of the surface equation, Eq (2-1), for surface I.	0	2-1

6.5 NAMELIST NAME3

Special constraints are listed in this subsection.

Variable	Definition	Default Value	Reference Page
NSTRT (I)	Number of constraints of surface I.	Number of standard constraints.	2-13
KSIDSP (J, I)	Surface number of the surface to be used as the Jth constraint of surface I. Set -1 if no surface is available and a new surface is to be read in as the constraint. Set 0 if the standard constraint is used.	0	2-13
KSTRT (J, I)	Type of constraint - the Jth constraint of surface I.	Type of the standard constraint if coefficients of the surface has been generated otherwise 0.	2-14
PTLCSP (K, J, I)	Parameters of the new surface to be used as the Jth constraint of surface I.	0	2-14
CSTRT (K, J, I)	Coefficients of the constraint surface equation, Eq. (2-2), for the Jth constraint of surface I.	0	2-10

6.6 NAMELIST NAME4

System Configuration is listed below.

Variable	Definition	Default Value	Reference Page
NSFACE (I)	Number of surfaces of Section I.	0	2-16

Variable	Definition	Default Value	Reference Page
ISFACE (J, I)	Surface number of the Jth surface of Section I.	0	2-16
ISFTP (J, I)	Surface type of the Jth surface of Section I.	0	2-17
KCOEF (J, I)	Coefficient indicating which side of the Jth surface Section I is on	0	2-18
IMPSF (J, I)	Parameter relating important surfaces to the Jth surface of Section I.	0	2-21
NIMPS (I)	Number of important surfaces in Section I.	0	4-5
IMPORT (J, I)	Surfaces number of the Jth important surface of Section I.	0	4-5
NRING (J, I)	Number of rings of equal area in important surface IMPORT (J, I).	0	4-6
NSEG (J, I)	Number of angular segments, of equal area, for each ring of the important surface IMPORT (J, I).	0	4-6

6.7 NAMELIST NMCOAT

Coefficients of radiation properties are shown below.

Variable	Definition	Default Value	Reference Page
COAT (J, I)	Coefficients of radiation property of surface I.	0	3-7
IEXP (I)	Type of near specular reflection model of Surface I.	0	3-9

6.8 NAMELIST NMEMSN

Miscellaneous data for internal thermal emission are listed in this subsection.

Variable	Definition	Default Value	Reference Page
NPOLE	Number of poles where pilot rays are generated.	0	3-4
LEMIT	Number of pilot rays leaving each pole.	Value given in namelist NAME1.	
POLE (J, I)	Co-ordinates of the Ith pole.	0	3-4
NSFEM (I)	Number of emitting surfaces associated with the Ith pole.	0	3-5
KSECEM (J, I)	Section number of the Jth surface of the Ith pole.	0	3-5
KSIDEM (J, I)	Surface number of the Jth surface of the Ith pole.	0	3-5
TEMP (I)	Temperature of the Ith surface.	0	3-5
STBLTZ	Stefan-Boltzmann constant.	$3.657E-11$ watt/inch $2°K^4$	3-3
DELTAE	Energy level of a ray below which it will be abandoned.	Value given in Namelist NAME1.	
DEPRT	Minimum energy level of a ray of which the trace history will be printed in arriving at the exit aperture.	Value given in Namelist NAME1.	7-2
LRFN	Limit on number of reflections and transmissions of a ray.	Value given in Namelist NAME1.	

Variable	Definition	Default Value	Reference Page
ISEEDP	After every ISEEDP pilot rays are traced, the value of ISEED is printed out. These ISEED values can be used to continue the computation	Value given in Namelist NAME1.	
NPRINT	Limit on number of rays for which the tracing will be printed in arriving at the exit aperture.	Value given in Namelist NAME1.	
NERR	Number of errors having occurred when the computation will be terminated. The accumulated energy distribution on the exit aperture will be limited out.	Value given in Namelist NAME1.	
KPRINT	Signal for printing ray history of those that didn't reach the exit aperture. Set any positive integer and ray history will be printed out after first KPRINT pilot rays. Set 0 if no such print out is desired.	Value given in Namelist NAME1.	7-2
WVBDL WVBDH	Lower and upper limits, respectively, of the wave band in microns. When WVBDH is 0, the emission will cover the whole spectrum.	0	

Section 7

OUTPUT

The output listing of an execution is usually self-explanatory. For convenience to the user, however, we list below the complete contents of an output according to their proper sequence. The contents are divided into seven major groups, some of which may not appear in the result of a particular computation. Except for the error diagnosis, we briefly describe in this section the significance of the output.

7.1 INPUT DATA AND SYSTEM MODEL

The input data set is first listed exactly as it appears on the data deck. After subsequent listing of the parameters in namelists NAME1 and NAME2, tables are constructed for planes, cones, spheres, paraboloids and baffles. This is followed by the numbers of constraints and a table for special constraints.

The array ISFACE that defines the surfaces is given for each section. The corresponding parameters ISFTP, KCOEF, and IMPSF are listed in similar tables. The important surfaces, if any, are then given for each section, together with the numbers of rings and segments into which each important surface is to be partitioned.

In the table of radiation properties, a set of components is listed for each surface. For each of the surfaces with near specular components, the angular decay constants are given at the end of the table.

The ten coefficients in Equation 2-1 are listed for each of the surfaces except toroids. Immediately following these coefficients, the type of constraint and the coefficients of the constraint surface as expressed by Equation 2-2 are given for each of the constraints. In the present version of the program, C_{10} has the opposite sign that it would have according to Equation 2-2.

The coefficients given for toroids are expressed in local coordinates and are meaningless to the user since the equation has not been presented in the manual. There is no input data directly involved, however, and the user can disregard these coefficients.

7.2 EXTERNAL RADIATION RAY TRACING

When a ray reaches the exit aperture and the relative energy, with respect to its energy when it started at the entrance aperture, is greater than DEPRT, the trace of the ray will be printed out as in the following:

KEMIT	KPOLE	E_n
X_1	X_2	$X_3 \ldots X_n$
Y_1	Y_2	$Y_3 \ldots Y_n$
Z_1	Z_2	$Z_3 \ldots Z_n$
E_1	E_2	$E_3 \ldots E_n$

where KEMIT is the ray number, KPOLE the pole number, and E_n is the relative energy of ray when it reaches the exit aperture. Since poles are not used in external radiation, KPOLE will be zero in this part. (X_1, Y_1, Z_1) is the initial location of the ray at the entrance aperture, (X_2, Y_2, Z_2) is the first intercept, and so forth. (X_n, Y_n, Z_n) is the intercept at the exit aperture. E_1 is the relative energy of the ray at the initial point, E_2 the relative energy at the first intercept, and so forth.

When KPRINT is a positive integer, traces are printed out for all rays with KEMIT > KPRINT regardless of whether they reach the exit aperture or not.

After each group of ISEEDP rays has been initiated and finished, KEMIT and ISEED are listed. By using one of these ISEED values as the initial ISEED for the next computation, the user can continue calculation at some intermediate point or at the end. This is useful in troubleshooting in the moddle of a calculation.

Error messages appearing in this part will be discussed in Section 8.

7.3 RAY COUNT AND ENERGY DISTRIBUTIONS OF EXTERNAL RADIATION

a.   Spatial Ray Count Distribution

A square of sides 2· RMAP is divided into a grid of 30 by 30 square elements. The horizontal distance corresponds to the local x-axis at the exit aperture plane while the vertical distance the local y-axis.   The number at each element indicates the number of rays striking the element.

b.   Spatial Energy Distribution

Energy distribution is printed out in the same way as the ray count.   Due to limitation in space, it is divided into three portions.   The first lists the first 10 columns, the second lists the middle 10 columns and the rest appears on the third.   The values are based on a unit energy input at the entrance aperture.

c.   Radial Ray Count Distribution

The circle of radius RMAP at the exit aperture is divided into 100 rings of equal width.   Listed here are numbers of rays in each of the rings.

d.   Radial Energy Density Distribution

Similar to "c", the energy density distribution, energy per unit area per unit energy input, is listed for the 100 rings.   The energy density distribution is then plotted against the radial distance in the figure that follows.

e.   Spatial and Angular Ray Count Distribution

The square of side 2· RMAP on the exit aperture is divided into a grid of 3 by 3 area elements as follows:
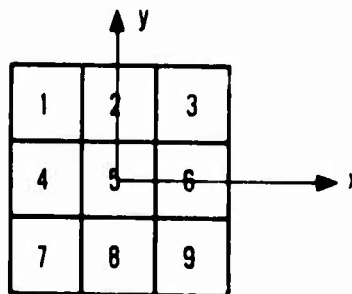
where x and y are the local coordinate axes. The numbers 1 through 9 refer to the elements. The rays are grouped by the elements they hit in arriving at the aperture plane. In addition, they are grouped by the angles between the ray and the exit aperture normal.

f. Spatial and Angular Energy Distribution

Similar to "e", energy distributions are listed according to the elements and the angles to the normal when they reach the exit aperture.

7.4 SUMMARIZED RESULTS OF EXTERNAL RADIATION

a. Number of Rays Entering

Number of rays actually started at entrance aperture. This will be the same as LEMIT except when computation is terminated due to excessive errors.

b. Rays and Energy Through Entrance Aperture

Number of rays and the total relative energy that leaves the system via the entrance aperture.

c. Rays Through Exit Aperture

Number of rays hitting the exit aperture. There are three numbers. The first covers all the rays in the first half, that is, KEMIT < LEMIT/2, the second cover those in the second half, and the last is the total number. The number is divided into two parts for an indication of the accuracy. Since a statistical analysis of the error is also given, the user could disregard this division.

d. Total Energy Through Exit Aperture

Energy reaching the exit aperture per unit energy entering the system. The first number is from the first half, the second from the second half, and the last from the whole. Again, the user could disregard the first two numbers.

e.   Attenuation

Ratio of energy intensity of the incident beam to the energy density at the exit aperture.   The latter includes energy bundles in all directions.   The first number is the attenuation obtained from the first half, the second from the second half, and the last from the whole.   Again the user disregard the first two numbers.

f.   Off-Axis Rejection

Ratio of energy entering the system to that reaching the exit aperture.

g.   Standard Deviation/$\sqrt{n}$ · Average

Relative error of total energy hitting the exit aperture with 90 percent confidence.

h.   Total Energy Reaching Target

Range of the total relative energy in "d" with 90 percent confidence.

i.   Attenuation

Range of attenuation in "e" with 90 percent confidence.

j.   Maximum Number of Rays Stored

The maximum number of rays stored due to splitting at any time of the entire external radiation computation.   The limit is 100, although it can readily be increased if necessary.   If at any time the number of rays stored exceeds the limit, the exceeding rays are abandoned.

7.5 INTERNAL EMISSION RAY TRACING

After a listing of the parameters in namelist NMEMSN, ray tracing is given for the internally emitted rays in the same manner as that given for the external rays described in Subsection 7.2.   The energy is in terms of the basic power unit, watts.

Error messages, if any, will appear in this part of the output.   The discussion will be given in Section 8.

7. 6 RAY COUNT AND ENERGY DISTRIBUTIONS OF INTERNAL EMISSION

The ray count and energy distributions are given for internal emission in the same way as those given for external radiation (see Subsection 7. 3). Again, the energy is in terms of the basic power unit.

7. 7 SUMMARIZED RESULTS OF INTERNAL EMISSION

a.   Number of Pilot Rays

Number of pilot rays generated at each pole.   It is given by LEMIT except when computation is terminated due to excessive errors.

b.   Rays and Energy Through Entrance Aperture

Number of rays and the total emitted energy that leave the system via the entrance aperture.

c.   Rays Through Exit Aperture

See "c" of Subsection 7. 4.

d.   Total Energy Through Exit Aperture

Emitted energy that reaches the exit aperture.

e.   Standard Deviation$/\sqrt{n} \cdot$ Average

Relative error of total emitted energy hitting the exit aperture with 90 percent confidence.

f.   Total Energy Reaching Target

Range of the total emitted energy in "d" with 90 percent confidence.

g.   Maximum Number of Rays Stored

The maximum number of rays stored due to splitting at any time of the entire internal emission computation.   This limit is 100, although it can readily be increased if necessary.   If at any time the number of rays stored exceeds the limit, the exceeding rays are abandoned.

Section 8

DIAGNOSTICS

Aside from minor errors in a Namelist data, for example, a mispunch of a character, most of the errors occur in the middle of the ray tracing. This section presents such error messages and the procedure to follow in tracking down the sources of errors. Each error message is accompanied by a set of informative parameters. Definitions are first given below for the frequently used parameters.

KEMIT   Ray number, from 1 to LEMIT

IPOLE   Pole number, from 1 to NPOLE

KSTYPE   Type of surface, given by ISFTP of the surface that intercepts the ray immediately before the error. When no interception of a ray appears after testing with all the surfaces in the section, KSTYPE is set equal to 6.

KSID   Surface number of the surface of latest interception.

E   Energy of the ray

        External Radiation   Per unit energy input at entrance aperture

        Internal Emission   In absolute power units

RAY   Location (X, Y, Z) and direction cosines (α, β, γ) of the ray

KSEC   Section number

ISF   Sequence number of the important surface in the section. Note that there can be up to three important surfaces in each section.

SURNOR   Direction cosines of the inward unit surface normal at the point of interception.

a. Error in Emission - KSID, IPOLE, T_1, T_0, RAY

Calculation of the interception between the pilot ray, location and direction given by RAY, and surface KSID results in the equation:

$$T_0 + T_1 S = 0$$

8-1

where S is the distance from the pole to the point of interception, and T_0 and T_1 are parameters obtained from substitution. The fact that the magnitude of T_1 approaches zero, less than 10^{-50}, renders the equation indeterminate. The user should examine whether the surface is parallel to the pilot ray. The problem can then be resolved by relocating the pole.

b. No Intercept - KEMIT, KSTYPE, KSEC, KSID, E, RAY

Each section is a complete enclosure. When no interception can be found for a ray, either some surface is missing or errors exist in the surface or the constraint parameters.

If a quick check fails to reveal the source of error, the user is advised to examine the ray location and direction in terms of the section configuration. If the ray is correctly situated in the section, he should then observe the section and find out the surface that should have intercepted the given ray. The coefficients of the surface and its constraint equation (see Subsection 7.1) will pinpoint the error source.

The user should also check the input values of NSFACE, ISFACE, ISFTP and KCOEF (see Subsection 6.6).

When the above error occurs, the ray is abandoned. However, when the number of errors exceeds NERR, the computation is terminated.

c. Error in GEOM - KSTYPE

The value of KSTYPE is limited 1 through 5. Examine ISFTP portion of the input data for possible error.

d. Error in GEOM, THIRD DEGREE, polynomial is not available - KSID, IDGREE.

The value of IDGREE is limited to 1, 2 and 4. Examine IDGREE portion of the input data for possible error.

e. Error in NORM. The Third Degree Polynomial not available.

Examine IDGREE input for possible error.

f. Secondary Ray Trapped by Important Surface in REFLN - KEMIT, IPOLE, KSEC, KSID, ISF, RAY, SURNOR

After an important ray is generated and stored, the direction of the random ray which carries the remaining energy is obtained according to the particular model of energy density distribution. According to the theory however, the random ray should not hit the important surface. If the ray so chosen happens to hit the important surface, a new direction is selected. This process is repeated until a ray is obtained that misses the important surface.

To avoid unnecessary waste of computation time, a ray is abandoned after it fails to miss the important surface seven times. The diagnostic is printed out to assist in deciding whether the important surface set should be modified.

g. Error in REFRN - KSID, KSEC, KSTYPE, IRTEST, COSPSN

The angle between the ray and the normal should be between 0 and $\pi/2$. If it is outside this range, the error message is printed out and the angle is defaulted to 0 or $\pi/2$ according to which side the value falls on.

The parameter IRTEST is 1 in case of total internal reflection.

COSPSN is the cosine of the angle between the ray and the inward surface normal.

h Error in ANGSSD - PSI (angle between the specular beam and the normal), ALPHA (the angle between the reflected ray and the specular reflected beam), BETA (the azimutnal angle of near specular scattering), ALPHAM (maximum angle of ALPHA) and PHI (the angle between the reflected ray and the normal).

Angle PHI should be between 0 and $\pi/2$. When it is outside this range, the message is printed out to warn of the error. The ray will be abandoned in the subsequent calculation in subroutine GEOM when no interception can be obtained.

i. Error in SCATTR, no solution found for X - last value equals X and difference DR equals DR.

Solution of the equation

$$X = f(a),$$

which is obtained from the near specular terms of Equation 3-1, by iteration, does not converge. X is the probability function and α is the off specular angle.

j. Error in DIFRN - KSEC, RAY and DELA (the distance from the inter-
   secting point to the aperture edge)

An interception of a ray by an aperture is determined before computation enters subroutine DIFRN. Thus the shortest distance from the intersecting point to the aperture should always be greater than zero. When it is zero or negative, the message is printed out to warn of possible error in the input data of the surfaces involved. The ray will be traced without being diffracted at this point.

k. Secondary Ray Trapped by Important Surface in DIFRN - KEMIT,
   IPOLE, KSEC, KSID, ISF, RAY, SURNOR, E.

See "f".

l. Negative Energy Ray - E, ESAVE (part of E that belongs to the
   important ray)

FAC1 (consine of the angle between the important ray and the unit normal of the important surface), FAC2 (factor of the energy going in the direction of the important ray), DENOM2 (quare of the length of the important ray), KEMIT, KSTYPE, KSEC, KSID, ISF, first half of RAY (initial point of the important ray), POINT (end point), OQ (vector of the important ray) and SURNOR.

When ESAVE is negative in subroutine EXPECT, the program by-passes splitting the ray. When FAC1 is positive, it is in most cases due to im-proper orientation of the important surface. The ray has come from the back side of the important surface. Sometimes, it may be necessary to arrange the important surfaces such that this does occur. In this case, the computation result is not affected.

m. Error in EXPECT - PHI (angle between the important ray and the
   surface normal), CBETA (cosine of the azimuthal angle of scattering),
   ALPHAM (maximum angle from the specular beam to the surface
   tangent for a particular BETA)

The important ray of near specular scattering is transmitted into the surface instead of being reflected. Subsequent calculation will show no interception and the ray will then be abandoned. See Figure 3-3.

n. Excessive Energy Given to Important Rays in EXPECT - KEMIT, IPOLE, KSEC, KSID, ISF, E, RAY (X, Y, Z)

The important surface is partitioned and NRING x NSEG important rays are generated. Ideally, the total amount of energy associated with these important rays is less than the total energy leaving the surface. However, since the energy of each important ray is approximated by using a randomly selected point in each partition, their sum might exceed the actual total energy leaving the surface.

When the energy is exhausted before NRING x NSEG important rays are generated, the remaining important rays and the complementary ray are abandoned. The user should examine the important surface. As we see from Section 4, the situation can be improved by reducing the size of the partitions, that is, increasing NRING and/or NSEG.

o. Negative Energy Ray in DIFEXP - FAC1 (cosine of the angle between the important ray and the unit normal of the important surface), DENOM2 (square of the length of the important ray), KEMIT, KSTYPE, KSEC, ISF, RAY, OQ (vector of the important ray) and POINT (end point)

When ESAVE is negative in subroutine DIFEXP, program by-passes splitting of ray. Very likely the error is due to incorrect orientation of the important surface. See "l".

p. Negative Energy Ray in DIFEXP-E, ESAVE, FAC1, DENOM2 (see "o"), A $(\frac{1}{2}[(\frac{\theta_1}{\theta_1^*})^2 + (\frac{\theta_2}{\theta_2^*})^2])$, TTHES (tan θ_1^*), TTHIS (tan θ_2^*), RRB (area of the important surface/π), KEMIT, KSTYPE, KSEC, ISF, RAY, OQ, POINT (see "o")

When ESAVE is negative in subroutine DIFEXP, program by-passes splitting of ray. The users should examine the parameters WAVEL, DEDGE and DRENT and the aperture surface through which the diffraction occurs.

q. Excessive Energy Given to Important Rays in DIFEXP - KEMIT, IPOLE, KSEC, KSID, ISF, E, RAY (X, Y, Z)

Similar to that of EXPECT given in "n".

r. Error in TESTSS - KEMIT, KSEC, KSID, ISF, IMPS (surface number of the important surface), T_1, T_0 (the two coefficients in the equation for the distance of the ray to the important surface) and RAY.

The splitting point is too close to the extended important surfaces. The testing of the secondary ray of being intercepted by the important surface is ignored. The user should check to see if the important surfaces need to be modified.

s. IRAY Exceeds NRAY - KEMIT, KSTYPE, KSEC, KSID, E, and RAY.

There is a limit of 100 rays that can be stored at any time. To raise this limit, the statement NRAY = 100 in main program GUERAP is changed to NRAY = any desired value.

t. Error in DISTB - K (group number with respect to angle), L (regions), KEMIT, KSTYPE, KSEC, KSID, RAY, and x, y, z (location in terms of the local coordinates).

When RMAP is smaller than the exit aperture radius, some of the rays that reach the exit aperture may miss the ray count and energy distribution maps. The rays are simply ignored.

u. Error in ACOS - X (argument) and KEMIT.

Absolute value of the argument of an arc-cosine is greater than unity.

Section 9

EXAMPLES

A series of examples are presented in this section to demonstrate the application of the GUERAP program in a wide variety of problems. The user is advised to follow through these examples before attempting the task of simulating complicated systems.

The first example is a brute force Monte Carlo solution of a simple diffraction problem. The radiant intensity distribution as a result of diffraction effects is obtained on a target screen. Comparison of the result with available solutions is presented in more detail in Diffraction Modeling (Reference 2).

When the radiant intensity is sought in only a small portion of the screen, the importance sampling technique is applied with great success. This is presented in the second example.

Examples 3 and 4 deal with internal thermal emission of simple cavities. The result of the third example is compared with an available independent solution.

In the last example, we compute the attenuation of a monochromatic collimated beam through a typical optical system. The example makes use of various features available in the program such as knife-edge baffles, lenses and mirrors. It also demonstrates the use of importance sampling in an optical system with high attenuation.

9.1 EXAMPLE 1

For the first example, we consider the simple system shown in Figure 9-1. A laser beam of 10.6 μ wave length enters a circular cylinder of 3 inches diameter through a small circular aperture of 0.1 inch diameter. The aperture has a perfect knife-edge so there will be no reflection off the aperture edge. The energy is collected on a screen 100 inches behind the entrance.

In the absence of diffraction, the energy will be uniformly distributed over a circle of the same size as that of the entrance aperture. When diffraction
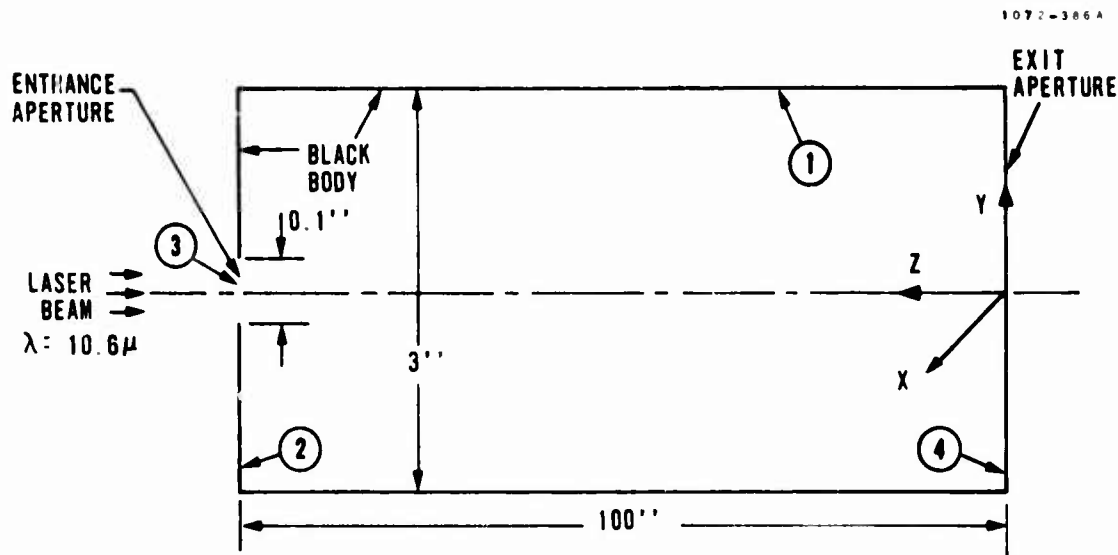
FIGURE 9-1. SCHEMATIC OF DIFFRACTION TEST

effects are included, however, the energy distribution on the screen should show an approximation of a Fraunhofer diffraction pattern (Reference 4, 5). This example was originally used to check the diffraction model of the program.

There are four surfaces, three planes and one cone, in the system when importance sampling is not utilized. The boundaries of all the surfaces can be completely described by standard constraints so no special constraint is needed. The complete set of input data is given in Table 9-1.

The title card is terminated by ENDTITLE starting at column 1. This is followed by ISEED = 1 in ∅20 format.

The laser beam enters the system parallel to the Z-axis and is assumed completely collimated, so SUNAGD, SUNAZD and SUNDVD are all zero, as given by default.

Energy levels of a ray for termination and listing of ray tracing, DELTAE and DEPRT, are both at 10^{-12} by default. This is immaterial because the rays will either reach the screen directly or be absorbed completely by the black body inner surfaces.

TABLE 9-1. INPUT DATA OF EXAMPLE 1

```
        DIFFRACTION TESTING
        NO IMPORTANT SAMPLING
        ENERGY DENSITY DISTRIBUTION SOUGHT FOR ENTIRE TARGET SCREEN
ENDTITLE
                        1
 $NAME1 LEMIT=20000,LRFN=1,ISEEDP=100,NSEC=1,RMAP=1.5,WAVEL=10.6,
 DRENT=0,ISENT=3,ISEXT=4,KPRINT=0,DEDGF=200$
 $NAME2 KDIF(3)=1$
 $NMGEOM IPLANE(1)=2,3,4,
 PTLCTR(1,2)=0,0,100,0,0,-1,1.5,.05,
 PTLCTR(1,3)=0,0,100,0,0,-1,.05,0,
 PTLCTR(1,4)=0,0,0,0,0,1,1.5,0,
 ICONE(1)=1,
 PTLCTR(1,1)=0,0,100,0,0,0,1.5,1.5$
 $NAME3 $
 $NAME4 NSFACE(1)=4,    ISFACE(1,1)=1,2,3,4,   KCOEF(1,1)=0,1,1,1,
 ISFTP(1,1)=5,5,1,2$
 $NMCOAT COAT(1,1)=1,   COAT(1,2)=1$
 $NMEMSN LEMIT=0$
```

A small number of rays are needed for a simple system when we are looking for the overall attenuation. However, a large number is required if we are interested in an accurate energy distribution over the screen. Thus 20000 rays are generated. The limit on the number of reflection LFRN is set at 1 because we are collecting only the energy that reaches the screen directly from the entrance aperture. ISEED is to be printed once every 100 rays.

By not specifying a value for either NPRINT or NERR, the number of rays to be printed out is 200 and the maximum number of errors permitted is 20 by default. There is only one section in the system, thus NSEC = 1.

The energy distribution is wanted over the entire target screen, thus we set RMAP at 1.5 inches. KPRINT is zero for the first trial when no additional diagnostics are needed. The wave length of the incident beam is 10.6μ. The example is mainly dealing with diffraction at the entrance aperture, so it is essential to include the entire aperture area in our consideration of diffraction. This is achieved by assigning 200 to the value of DEDGE, the number of wave lengths necessary to cover the entire diffraction zone. No importance sampling is needed at the entrance aperture so DRENT is zero. Surfaces 3 and 4 are, respectively, the entrance and the exit apertures.

Diffraction is sought for the entrance aperture with surface number 3, so we set KDIF(3) = 1.

The surface number of the planes are 2, 3 and 4, and that of the cone is 1. Referring to Figure 2-1, we see that surface 2 can be specified by the center of aperture (0, 0, 100) and the unit normal (0, 0, -1), which is to be preferred pointing into the system, although not mandatory. The surface is constrained by two circular cylinders around the prescribed center point and unit normal. The outer constraint has a radius of 1.5 while the inner one 0.05. These are the sequence of numbers specified by the array PTLCTR for the surface.

Surfaces 3 and 4 are similarly specified except that there are no inner constraints. The cone surface is described by the two center points (0, 0, 100) and (0, 0, 0), and the radii on both ends, 1.5 and 1.5; see Figure 2-2. These are given in the array PTLCTR for the surface.

The index of refraction is 1 for air. Referring again to Figure 9-1, we see that there are four surfaces in the section, namely 1, 2, 3 and 4. The parameters PTLCTR show that all the unit normals for the planes point into the region, so KCOEF is 1 for all the planes. It is 0 for the cylinder because the region, that is, the section, is inside the cylinder.

The first two surfaces in the section are non-transmitting, the third one is an aperture toward the entrance and the last surface is an aperture toward the exit. These are so specified by array ISFTP.

Surfaces 1 and 2 are black bodies with 100 percent absorptance, giving COAT(1, 1) = COAT(1, 2) = 1.

The resultant radiant energy density distribution on the target screen is plotted against the distance from the center in Figure 9-2. For comparison, the average densities at three small radial bands are listed in the second row of Table 9-3.

9.2 EXAMPLE 2

In this example, we shall demonstrate the use of importance sampling and the procedure of repeating calculations on the same system with minor modifications.

In Table 9-3, the energy densities at three narrow radius bands are listed from the previous example. We will show here how to obtain these densities with importance sampling.

Table 9-2 lists the complete input data for this example. There are three parts in the data set, each for one calculation. The first part is a variation of the input data of Example 1 given in Table 9-1.

In order to calculate the energy density in the center circle and rings given in Table 9-3, we generate these surfaces as surfaces 5, 6 and 7. Since all these surfaces are part of surface 4, the first six parameters are identical to those of surface 4.

Surface 5 is the center circle with 0.015 inch outer radius and no inner radius. Surface 6 is the ring with 0.375 inch outer radius and 0.36 inch inner radius. Similarly, surface 7 is the ring with 0.75 inch outer radius and 0.735 inch inner radius.

The important surfaces and their assignment are given in NAME4. There is one important surface, surface 5, in Section 1. The surface is not partitioned, so NRING and NSEG are both unity.

The splitting of rays toward the important surface given above is called for when rays pass the entrance aperture, surface 3. The corresponding number of IMPSF is given a value unity, assigning important surface number 1 to the surface, and it is zero for the rest of the surfaces.
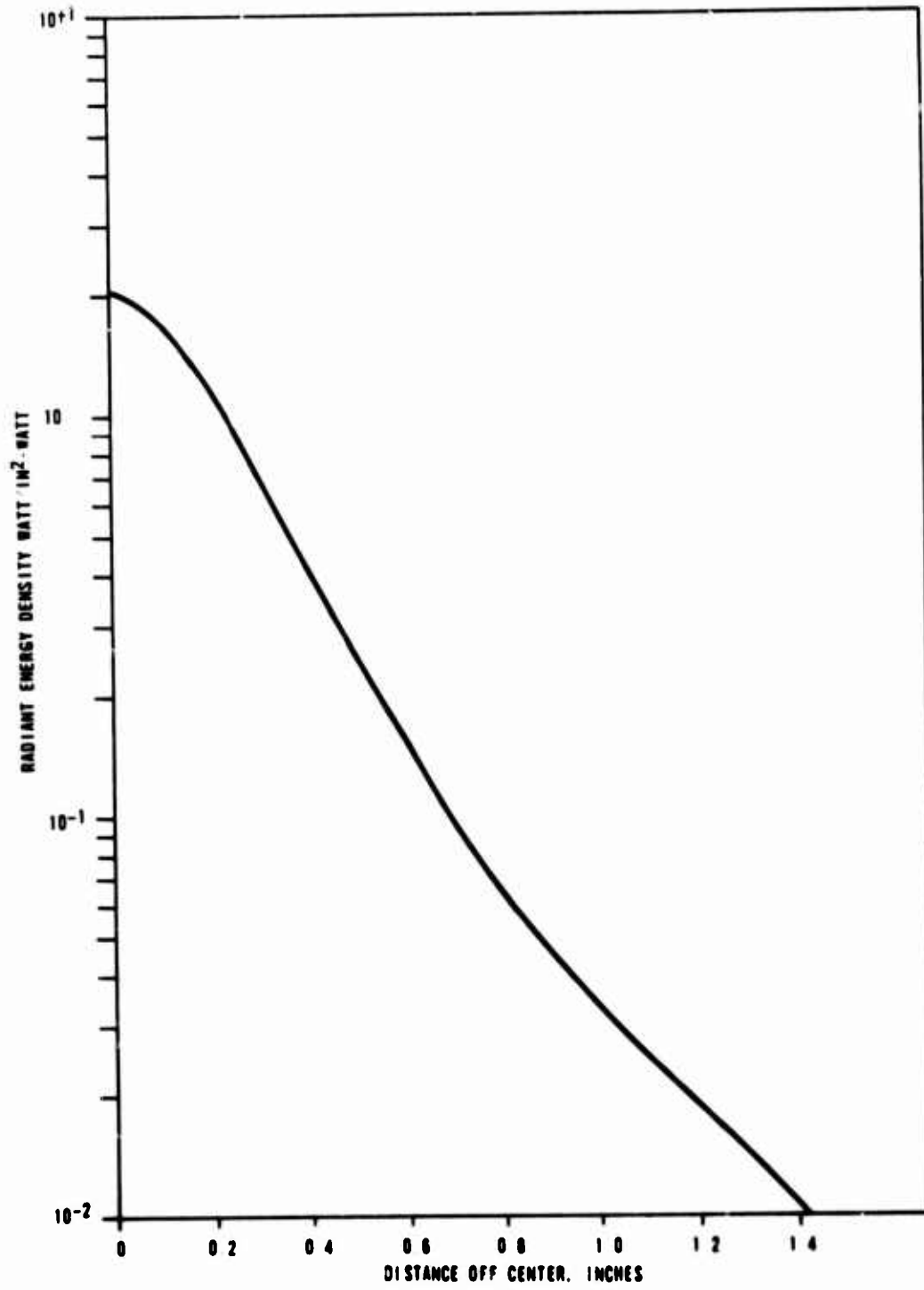
FIGURE 9-2. DIFFRACTION PATTERN BEHIND A CIRCULAR APERTURE

TABLE 9-2. INPUT DATA OF EXAMPLE 2

```
          DIFFRACTION TESTING
          CENTER CIRCLE IMPORTANT SAMPLING
ENDTITLE
                       1
 $NAME1 LEMIT=500, LRFN=1, ISEEDP=100, NPRINT=100, NSEC=1, RMAP=1.5,
 WAVEL=10.6, DRENT=0, ISENT=3, ISEXT=4, KPRINT=0, DEDGE=200$
 $NAME2 KDIF(3)=1$
 $NMGEOM IPLANE(1)=2,3,4,5,6,7,
 PTLCTR(1,2)=0.0,100.0,0.0,-1,1.5,.05,
 PTLCTR(1,3)=0.0,100.0,0.0,-1,.05,0,
 PTLCTR(1,4)=0.0,0.0,0.0,1,1.5,0,
 PTLCTR(1,5)=0.0,0.0,0.0,1,.015,0,
 PTLCTR(1,6)=0.0,0.0,0.0,1,.375,.36,
 PTLCTR(1,7)=0.0,0.0,0.0,1,.75,.735,
 ICONE(1)=1,
 PTLCTR(1,1)=0.0,100.0,0.0,0,1.5,1.5$
 $NAME3 $
 $NAME4 NSFACE(1)=4,   ISFACE(1,1)=1,2,3,4,            KCOEF(1,1)=0,1,1,1,
 IMPSF(1,1)=0,0,1,0, NIMPS(1)=1, IMPORT(1,1)=5, NRING(1,1)=1, NSEG(1,1)=1,
 ISFTP(1,1)=5,5,1,2$
 $NMCOAT COAT(1,1)=1,  COAT(1,2)=1$
 $NMEMSN LEMIT=0$
          DIFFRACTION TESTING
          SECOND RING IMPORTANT SAMPLING
ENDTITLE
                       1
 $NAME1 LEMIT=500$
 $NAME2 $
 $NMGEOM $
 $NAME3 $
 $NAME4 IMPORT(1,1)=6$
 $NMCOAT $
 $NMEMSN LEMIT=0$
          DIFFRACTION TESTING
          THIRD RING IMPORTANT SAMPLING
ENDTITLE
                       1
 $NAME1 LEMIT=500$
 $NAME2 $
 $NMGEOM $
 $NAME3 $
 $NAME4 IMPORT(1,1)=7$
 $NMCOAT $
 $NMEMSN LEMIT=0$
```

TABLE 9-3. COMPARISON OF ENERGY
DENSITIES AT SELECTED RING

R	Energy Densities (watts/in^2/watt)			CDC-6600 Execution Time
(inches)	0-0.015	0.360-0.375	0.735-0.750	(sec)
EXAMPLE 1 No Importance Sampling	1.981	0.507	0.083	63.2
EXAMPLE 2 Importance Sampling	2.033			11.4
Importance Sampling		0.543		9.1
Importance Sampling			0.082	9.4

Notice that the number of rays given for the external radiation in NAME1 is 500 instead of 20,000 in Example 1. In Example 1, the rays are allowed to select their directions randomly according to the probability density functions and the number of rays to strike a particular radial band such as the center circle is in the order of the total number of rays divided by the number of bands. In order to obtain a significant number of rays for each band, it was necessary to generate an extremely large number of rays at the entrance aperture.

In the first part of Example 2, each of the rays generated is split into two rays, one of which, the important ray, is aimed at the center circle. Thus, a substantially smaller number of rays are required to get good statistical accuracy.

After the calculation of energy density at the center circle, we now proceed to calculate the density at the two rings, namely surfaces 6 and 7. In the second and the last parts of the data set, we direct the calculations with the given modifications. The second part is for surface 6, while the last is for surface 7. Note that it is necessary to respecify LEMIT in NAME1 because the same variable is set equal to zero in NMEMSN in the preceding part.

The energy densities obtained from this example are compared with those of Example 1 in Table 9-3.

9.3 EXAMPLE 3

We now consider the conical cavity illustrated in Figure 9-3. This simple configuration is chosen because of an available independent solution. The cavity has a depth of 10 inches and a circular opening of 2 inches radius.

The interior surface is a gray body, diffuse emitting and reflecting, with 0.7 emittance and at a uniform temperature of 300° K. We shall calculate the total radiant flux out of the cavity.

The input data for this calculation is listed in Table 9-4. This is a calculation of internal thermal emission rather than external radiation so LEMIT is zero, as given by default, in NAME1. No input is needed in NAME2 because neither diffraction nor refraction occurs in the problem.

The conical surface is divided into two parts for importance sampling. The surface definition given in NMGEOM is clear from the discussion in Example 1. No special constraint needs to be specified in NAME3.

TABLE 9-4. INPUT DATA OF EXAMPLE 3

```
CONE CAVITY TO VERIFY EMISSION
ENDTITLE
                    1
 $NAME1 NSEC=1.  RMAP=2..   ISEXT=3$
 $NAME2 $
 $NMGEOM IPLANE(1)=3.   ICONE(1)=1,2.
PTLCTR(1,1)=0.0.10.0.0.2.0.1.6.
PTLCTR(1,2)=0.0.2.0.0.0.1.6.2.
PTLCTR(1,3)=0.0.0.0.0.1.2.0$
 $NAME3 $
 $NAME4 NSFACE(1)=3.   ISFACF(1,1)=1,2,3.
KCOEF(1,1)=0.0.1.  ISFTP(1,1)=5,5,2.   IMPSF(1,1)=1,0,0.
NIMPS(1)=1.   IMPORT(1,1)=3.   NRING(1,1)=1.   NSEG(1,1)=5$
 $NMCOAT COAT(1,1)=.7,0..3.   COAT(1,2)=.7,0.,3$
 $NMEMSN NPOLE=2, LEMIT=200, POLE(1,1)=0,0,4,   POLE(1,2)=1,0,1,
NSFEM(1)=1,1.   KSECEM(1,1)=1,   KSECEM(1,2)=1,
KSIDEM(1,1)=1,   KSIDEM(1,2)=2,   TEMP(1)=300,300,
DELTAE=.001.   DEPRT=.1.   LRFN=8$
```
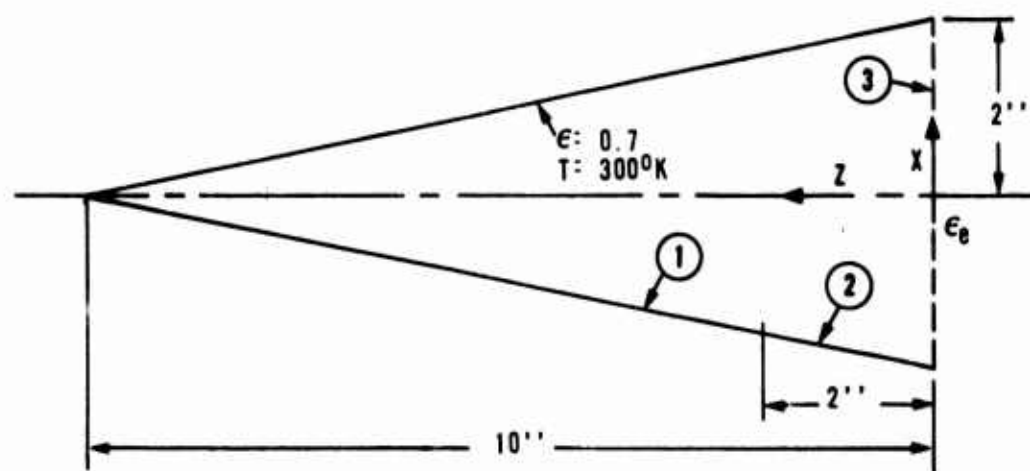
FIGURE 9-3. CONICAL CAVITY

The values given to NSFACE, ISFACE, KCOEF and ISFTP are clear in reference to the figure. Radiant energy is to be accumulated at the opening, so surface 3 is made the important surface. While the rays from surface 1 are split toward the important surface, those from surface 2 are allowed to select random directions. The latter are not split because they are so close to the important surface that the large variation of the important ray energy can cause significant error; see Subsection 4.4. Furthermore, since the rays have a high probability of selecting the directions toward the opening, there is no need to importance sample.

The area of surface 3 is comparable to the square of the shortest distant from surface 1 to surface 3 so it is advisable to partition the important surface. It is divided into 5 segments.

Surfaces 1 and 2 have an absorption of 0.7 and a diffuse reflectance of 0.3.

Parameters for internal emission are specified in NMEMSN. Since rays from surface 2 have a high probability of striking the exit, more rays should be generated there than called for by the area ratio. This is

achieved by placing two poles in the system. The first pole is placed near the center (0, 0 4) and the second near surface 2 (1, 0, 1). The latter is placed one inch off-axis for the purpose of generating rays from surface 2 with various levels of energy.

There is one emitting surface associated with each pole. Both surfaces are in section 1. Surface 1 is associated with pole 1 while surface 2 with pole 2. Both interior surfaces are at the uniform temperature of 300° K.

The distance of a typical pilot ray, the ray from a pole to a corresponding emitting point, is in the order of 3 inches. Assuming 0.7 for a typical value of cos ϕ, see Figure 3-2, the energy of a ray at emission is in the order of

$$e = \frac{2\pi s^2 \epsilon \sigma T^4}{(\cos \phi)}$$

or

$$e = \frac{2\pi \times 3^2 \times 0.7 \times 3.657 \times 10^{-11} \times 300^4}{0.7} \quad \text{watts}$$

$$= 16.7 \text{ watts}$$

The cut-off energy level of 10^{-3} watts is sufficiently small compared with the above value. The ray tracing is limited to 8 reflections.

Tracing 200 pilot rays from each pole, we obtain an emissive power of 3.24 watts at the exit, giving an equivalent cavity emittance of 0.871. This compares favorably with a value of 0.879 obtained from an independent source (Reference 3).

9.4 EXAMPLE 4

The conical cavity in Example 3 was chosen so that comparison can be made with the result of an independent solution. We will now proceed to analyze a cavity and demonstrate that the GUERAP program can be used in solving a wide variety of problems on thermal radiation of which solutions are heretofore unavailable.

As shown in Figure 9-4, the cavity is a circular cone of 10-inch depth and 22.5 degrees half-angle. The front end is covered by a plane with a perfect circular aperture of 2.5 inches radius. Both interior surfaces are gray bodies with 0.7 emittance and at a uniform temperature of 300° K. As in
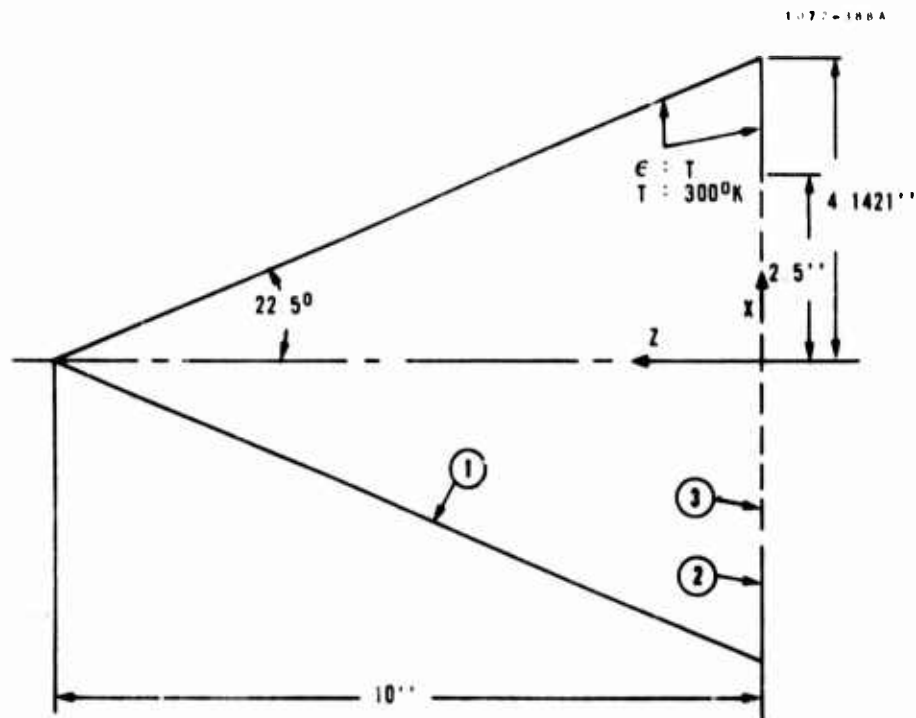
FIGURE 9-4. MODIFIED CONICAL CAVITY

the last example, we are looking for the total radiant energy leaving the
cavity and the equivalent emittance at the exist aperture.

The input data given in Table 9-5 are rather straightforward. The exit
aperture is the important surface for surface 1 while rays from surface 2
are allowed to be randomly distributed.

No particular emphasis seems necessary for emission from any part of
the interior and a pole in the middle of the system is sufficient. There are
two surfaces, surfaces 1 and 2, associated with the pole and both are in
section 1.

The cut-off energy level is set at 10^{-7}, substantially lower than necessary.
However, this will not significantly prolong the calculations because, all
the rays are limited to eight reflections.

With 100 pilot rays, the result shows that energy is leaving the exit
aperture at a rate of 4.58 watts, giving an equivalent opening emittance of
0.788. The latter is substantially lower than that of the last example
because of higher ratio of the opening radius to the cavity depth.

9-13

TABLE 9-5. INPUT DATA OF EXAMPLE 4

```
CONE CAVITY WITH REDUCED EXIT OPENING
ENDTITLE
                       1
 $NAME1 NSEC=1,  RMAP=2.5,  ISEXT=3$
 $NAME2 $
 $NMGEOM IPLANE(1)=2,3,  ICONE(1)=1,
 PTLCTR(1,1)=0,0,10,0,0,0,0,4.1421,
 PTLCTR(1,2)=0,0,0,0,0,1,4.1421,2.5,
 PTLCTR(1,3)=0,0,0,0,0,1,2.5,0$
 $NAME3 $
 $NAME4 NSFACE(1)=3,  ISFACE(1,1)=1,2,3,  KCOEF(1,1)=0,1,1,
 ISFTP(1,1)=5,5,2,  IMPSF(1,1)=1,0,0,  NIMPS(1)=1,
 IMPORT(1,1)=3,  NRING(1,1)=1,  NSEG(1,1)=1$
 $NMCOAT COAT(1,1)=.7,0,.3,  COAT(1,2)=.7,0,.3$
 $NMEMSN NPOLE=1, LEMIT=100, POLE(1,1)=0,0,4, NSFEM(1)=2,
 KSECEM(1,1)=1,1, KSIDEM(1,1)=1,2, TEMP(1)=300,300,
 DELTAE=1.E-7, DEPRT=1.E-7, LRFN=8$
```

9.5 EXAMPLE 5

We now consider an optical system illustrated in Figure 9-5. The input data is simplified by the fact that the system is axially symmetric around the Z-axis. Sun-light with a quarter degree divergence enters the system at 45 degrees from the axis. The first six sections consist of a series of baffles aimed at attenuating the off-axis energy. From the seventh section on there are an aspheric corrector lens, two meniscus lenses and one spherical mirror on the right hand end. The on-axis energy is specularly reflected by the mirror and focused onto the detector, surface 56.

All the required dimensions are clearly indicated in the figure. Also shown are surface numbers, numbers in small circles. Most of them are either real surfaces or apertures, while some are imaginary surfaces used exclusively for importance sampling. We will first briefly describe the surfaces in each of the sections. It should be emphasized here that boundaries of sections are chosen chiefly for convenience in the handling of data and efficiency in the execution.

Section 1 is bounded by a cylinder, a plane baffle, a conical baffle, and two apertures. Referring to Figures 2-4 and 2-5, we see that if we assign 7 and 11 to the surface numbers of the baffle knife edges, the baffles will consist of surfaces 7 through 14. All of these surfaces except 9, 12 and 14 are invluded in the section. Surfaces 49 and 50 are, respectively, the entrance and the exit apertures, of the section. In addition we place a plane annular ring with a larger inner constraint, surface 46, directly in front of surface 10. The purpose of this surface, which is to be used for importance sampling, will become clear later.

Sections 2, 3, 5 and 6 are essentially similar to section 1 except that no additional surface like 46 is created.

Section 4 is bounded by a cone, two conical baffles and two apertures. Similar to section 1, we place a cone with larger inner constraint, surface 47, directly in front of surface 22.

The small circular cylinder in the middle of the system is black coated on all sides. Surfaces of section 7 thus include cylinders 4, 41, and 43, planes 35, 42 and 43, baffle surfaces 31, 32 and 34, and aperture 55.

Section 8 is the interior of the aspheric corrector bounded by planes 35 and 36, and cylinders 41 and 43. Section 9 is the space between the first two lenses. It is bounded by planes 36 and 42, cylinders 41 and 43, and sphere 37.
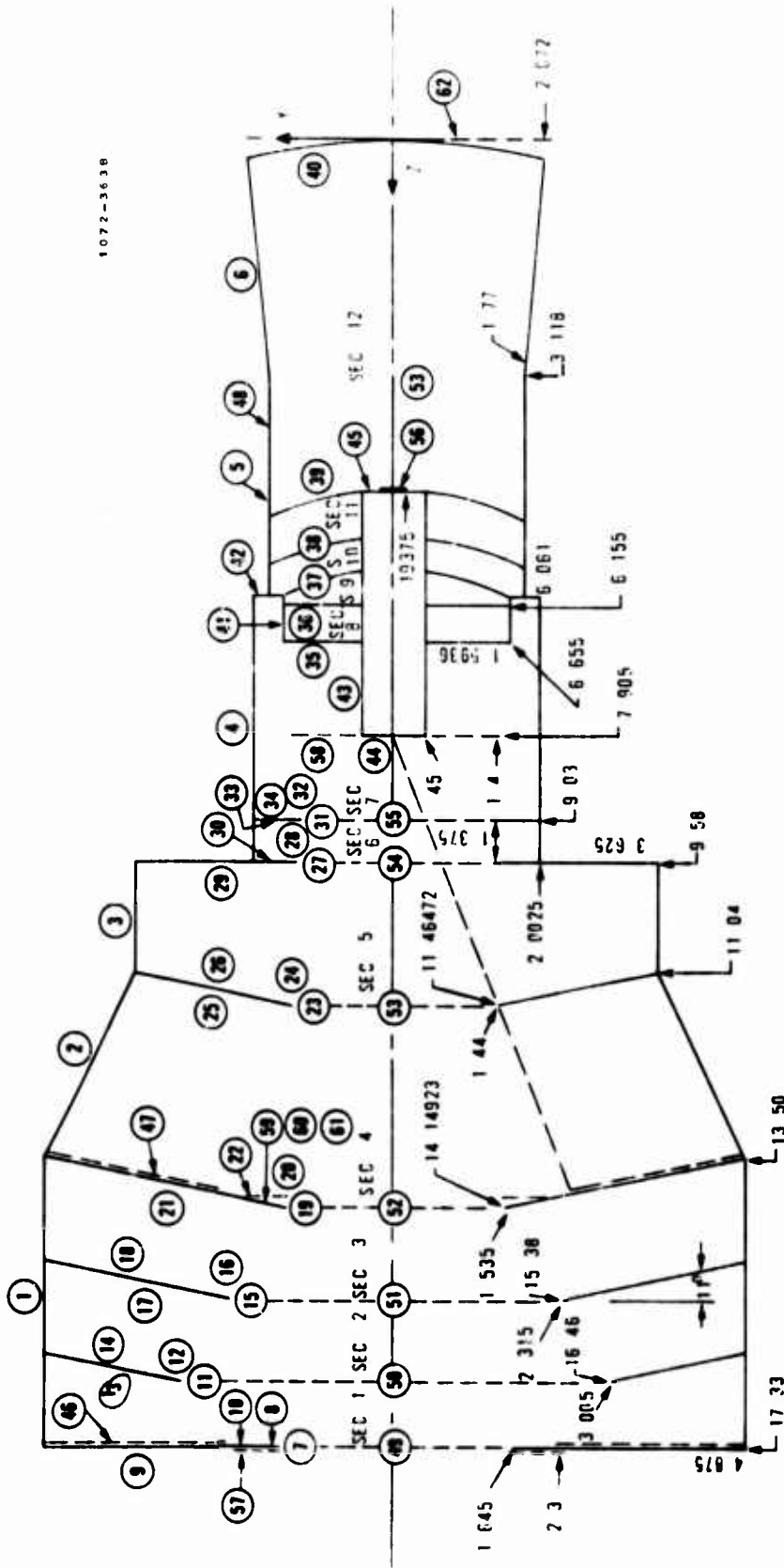
FIGURE 9-5. OPTICAL SYSTEM OF EXAMPLE 2

Section 10 is the interior of the first meniscus lens bounded by plane 42, cylinders 5 and 43, and spheres 37 and 38. Section 11 is the interior of the second meniscus lens bounded by cylinders 5 and 43, and spheres 38 and 39.

Section 12 is the space between the second meniscus lens and the spherical mirror. It is bounded by planes 45 and 56, cylinders 5 and 48, cone 6, and spheres 39 and 40. Surface 56 is a circular detector, where energy is to be collected, placed inside the annular ring 45. Surfaces 5 and 48 are the same cylinder divided by a plane constraint at $Z = 4.5$ inches for importance sampling purposes.

In addition, there are seven more planes to be used as important surfaces. 57 is on the first baffle. In the vicinity of the fourth baffle, there are planes 59, 60 and 61. In section 7, there is the annular ring 58 surrounding circle 44. In section 12, we have 62 approximately coinciding with the mirror and 63 right on the detector. Dimensions for these surfaces are not clearly indicated in the figure. However, they can be easily resolved from the input data, shown in Table 9-6.

Sun-light with a quarter degree divergence comes into the system at 45 degrees from the normal. So we have SUNAGD = 45 and SUNDVD = 0.25. Since the system is axially symmetrical, the incident beam can be in any direction and the azimuthal angle SUNAZD assumes the default value zero.

To estimate the minimum energy level DELTAE, we first assume an extremely small value and generate a small number of rays with reasonable number of interceptions LRFN. The result of the above trial computation will show the desirable level of DELTAE.

Surfaces 49 and 56 are, respectively, the entrance and the exit apertures.

Plane surfaces are 35, 36, 42, 44, 45, 46 and 49 through 63. The inside radius of 42 is obtained from the intersection of the surface with sphere 37. Enough accuracy should be maintained in this value to assure that no gap exists between the two surfaces. It is advisable to use surface 37 as the inner constraint of surface 42.

Plane 46 of inner constraint 2.3 inches is placed closely in front of plane 10. It will thus intercept all the rays that come within its boundary. This will allow the command to follow the instruction concerning importance sampling under surface 46 instead of 10. Surfaces 49 through 55 are a series of circular apertures. Their inside radii are all zero.

TABLE 9-6.   INPUT DATA OF EXAMPLE 5

```
EXAMPLE 5
ENDTITLE
                      1
 $NAME1 SUNAGD=45.,SUNDVD=.25,DELTAE=1.E-15,DEPRI=1.E-12,LEMIT=50.
 LRFN=30,ISEEDP=10,NPRINT=300,VERR=100,NSEC=12,HMAP=.19375,KPRINT=0,
 ISENT=49,ISEXT=56$
 $NAME2 RINDEX(1)=1.,1.,1.,1.,1.,1.,1.,1.4618,1.,1.,625,1.625,1$
 $NMGEOM IPLANE(1)=35,36,42,44,45,46,49,50,51,52,53,54,55,56,57,58,
 59,60,61,62,63,
 PTLCTR(1,35)=2*0.,6.655,2*0.,1.,1.5936,.45,
 PTLCTR(1,36)=2*0.,5.155,2*0.,1.,1.5936,.45,
 PTLCTR(1,42)=2*0.,6.061,2*0.,1.,2.0025,1.54854,
 PTLCTR(1,44)=2*0.,7.905,2*0.,1.,.45,0.,
 PTLCTR(1,45)=2*0.,4.6294,2*0.,1.,.45,.19375,
 PTLCTR(1,46)=2*0.,17.2R999,2*0.,1.,4.875,2.3,
 PTLCTR(1,49)=2*0.,17.33,2*0.,1.,1.645,0.,
 PTLCTR(1,50)=2*0.,16.46,2*0.,1.,3.005,0.,
 PTLCTR(1,51)=2*0.,15.38,2*0.,1.,2.315,0.,
 PTLCTR(1,52)=2*0.,14.14923,2*0.,1.,1.535,0.,
 PTLCTR(1,53)=2*0.,11.46472,2*0.,1.,1.44,0.,
 PTLCTR(1,54)=2*0.,9.58,2*0.,1.,1.375,0.,
 PTLCTR(1,55)=2*0.,9.03,2*0.,1.,1.375,0.,
 PTLCTR(1,56)=2*0.,4.6294,2*0.,1.,.19375,0.,
 PTLCTR(1,57)=0,0,17.33,0,0,-1,2.3,1.645,
 PTLCTR(1,58)=0,0,7.905,0,0,1,1.4,.45,
 PTLCTR(1,59)=0,0,15.38,0,0,1,2.315,0,
 PTLCTR(1,60)=0,0,14.14923,0,0,1,1.535,0,
 PTLCTR(1,61)=0,0,13.9,0,0,-1,2.47,1.535,
 PTLCTR(1,62)=0,0,0,0,0,1,1.76,0,
 PTLCTR(1,63)=C,0,4.6294,0,0,-1,.19375,0,
 ICONE(1)=1,2,3,4,5,6,41,43,47,48,
 PTLCTR(1,1)=0,0,17.33,0,0,13.5,2*4.875,
 PTLCTR(1,2)=0,0,13.5,0,0,11.04,4.875,3.625,
 PTLCTR(1,3)=0,0,11.04,0,0,9.58,2*3.625,
 PTLCTR(1,4)=0,0,9.58,0,0,6.061,2*2.0025,
 PTLCTR(1,5)=0,0,6.061,0,0,4.5,2*1.77,
 PTLCTR(1,6)=0,0,3.118,0,0,.2418,1.77,2.072,
 PTLCTR(1,41)=0,0,6.655,0,0,6.061,2*1.5936,
 PTLCTR(1,43)=0,0,7.905,0,0,4.6294,2*.45,
 PTLCTR(1,47)=0,0,13.91657,0,0,13.49990,2.47,4.875,
 PTLCTR(1,48)=0,0,4.5,0,0,3.118,2*1.77,
 ISPHER(1)=37,38,39,40,
 PTLCTR(1,37)=0,0,9,0,0,5.678,1.54854,.45,
 PTLCTR(1,38)=0,0,9.638,0,0,5.278,1.77,.45,
 PTLCTR(1,39)=0,0,9,0,0,4.6063,1.77,.45,
 PTLCTR(1,40)=0,0,9,0,0,0,2.072,0,
```

TABLE 9-6. INPUT DATA OF EXAMPLE 5

```
IBAFF(1)=7,11,15,19,23,27,31,
PTLCTR(1,7)=0,0,17.33,0,0,1,1.645,0,
PTLCTR(1,11)=0,0,16.46,0,0,1,3.005,11,
PTLCTR(1,15)=0,0,15.38,0,0,1,2.315,11,
PTLCTR(1,19)=0,0,14.14923,0,0,1,1.535,11,
PTLCTR(1,23)=0,0,11.46472,0,0,1,1.44,11,
PTLCTR(1,27)=0,0,9.58,0,0,1,1.375,0,
PTLCTR(1,31)=0,0,9.03,0,0,1,1.375,0,
RKNIFE=.00003,TBAFF=.05,DBAFF=.001,ABAFFD=15$
$NAME3 NSTRT(1)=0,0,0,0,2,1,2,2,0,1,2,2,1,1,2,2,1,1,2,2,
NSTRT(21)=1,1,2,2,1,1,2,2,1,1,2,2,1,1,2,0,2,0,0,0,
NSTRT(41)=1,2,2,1$
$NAME4 NSFACE(1)=9,8,8,9,8,8,10,4,5,5,4,7,
ISFACE(1,1)=1,7,8,10,11,13,46,49,50,
ISFACE(1,2)=1,11,12,14,15,17,50,51,
ISFACE(1,3)=1,15,16,18,19,21,51,52,
ISFACE(1,4)=2,19,20,22,23,25,47,52,53,
ISFACE(1,5)=3,23,24,26,27,29,53,54,
ISFACE(1,6)=4,27,28,30,31,33,54,55,
ISFACE(1,7)=4,31,32,34,35,41,42,43,44,55,
ISFACE(1,8)=35,36,41,43,
ISFACE(1,9)=36,37,41,42,43,
ISFACE(1,10)=37,38,42,5,43,
ISFACE(1,11)=38,39,5,43,
ISFACE(1,12)=39,40,5,6,45,48,56,
KCOEF(1,1)=0,0,0,1,0,1,0,0,1,
KCOEF(1,2)=0,0,0,0,0,1,0,1,
KCOEF(1,3)=0,0,0,0,0,0,1,0,1,
KCOEF(1,4)=0,0,0,0,0,0,1,0,0,1,
KCOEF(1,5)=0,0,0,0,0,1,0,1,
KCOEF(1,6)=0,0,0,1,0,1,0,1,
KCOEF(1,7)=0,0,0,1,1,1,1,1,1,0,
KCOEF(1,8)=0,1,0,1,
KCOEF(1,9)=0,0,0,1,1,
KCOEF(1,10)=1,0,0,0,1,
KCOEF(1,11)=1,0,0,1,
KCOEF(1,12)=1,0,0,0,0,0,0,
ISFTP(1,1)=7*5,1,2,
ISFTP(1,2)=6*5,1,2,
ISFTP(1,3)=6*5,1,2,
ISFTP(1,4)=7*5,1,2,
ISFTP(1,5)=6*5,1,2,
ISFTP(1,6)=6*5,1,2,
ISFTP(1,7)=4*5,4,4*5,1,
ISFTP(1,8)=3,4,5,5,
ISFTP(1,9)=3,4,5,5,5,
```

TABLE 9-6. INPUT DATA OF EXAMPLE 5

```
ISFTP(1,10)=3,4,5,5,5,
ISFTP(1,11)=3,4,5,5,
ISFTP(1,12)=3,5*5,2,
IMPSF(1,1)=1,2,2,2,1,1,0,2,1,
IMPSF(1,2)=0,1,1,1,2,2,1,0,
IMPSF(1,3)=0,1,1,1,0,0,1,0,
IMPSF(1,4)=1,2,2,2,1,1,0,2,1,
IMPSF(1,5)=0,1,1,1,0,0,1,0,
IMPSF(1,6)=0,1,1,1,0,0,1,0,
IMPSF(1,7)=0,1,1,1,0,0,0,0,0,1,
IMPSF(1,12)=1,2,1,4,1,4,0,
NIMPS(1)=2,2,1,2,1,1,1,0,0,0,0,2,
```

IMPORT(1,1)=57,58,	NRING(1,1)=1,3,	NSEG(1,1)=4,1,
IMPORT(1,2)=59,57,	NRING(1,2)=1,1,	NSEG(1,2)=4,4,
IMPORT(1,3)=60,	NRING(1,3)=1,	NSEG(1,3)=4,
IMPORT(1,4)=61,58,	NRING(1,4)=1,3,	NSEG(1,4)=4,1,
IMPORT(1,5)=54,	NRING(1,5)=1,	NSEG(1,5)=4,
IMPORT(1,6)=55,	NRING(1,6)=1,	NSEG(1,6)=4,
IMPORT(1,7)=35,	NRING(1,7)=1,	NSEG(1,7)=4,
IMPORT(1,12)=62,63,	NRING(1,12)=1,1,	NSEG(1,12)=4,1$

```
$NMCOAT COAT(1,1)=.96,0,.04, COAT(1,2)=.96,0,.04, COAT(1,3)=.96,0,.04,
COAT(1,4)=.96,0,.04, COAT(1,5)=.96,0,.04, COAT(1,6)=.96,0,.04,
COAT(1,7)=.96,0,.04, COAT(1,8)=.96,0,.04, COAT(1,9)=.96,0,.04,
COAT(1,10)=.96,0,.04, COAT(1,11)=.96,0,.04, COAT(1,12)=.96,0,.04,
COAT(1,13)=.96,0,.04, COAT(1,14)=.96,0,.04, COAT(1,15)=.96,0,.04,
COAT(1,16)=.96,0,.04, COAT(1,17)=.96,0,.04, COAT(1,18)=.96,0,.04,
COAT(1,19)=.96,0,.04, COAT(1,20)=.96,0,.04, COAT(1,21)=.96,0,.04,
COAT(1,22)=.96,0,.04, COAT(1,23)=.96,0,.04, COAT(1,24)=.96,0,.04,
COAT(1,25)=.96,0,.04, COAT(1,26)=.96,0,.04, COAT(1,27)=.96,0,.04,
COAT(1,28)=.96,0,.04, COAT(1,29)=.96,0,.04, COAT(1,30)=.96,0,.04,
COAT(1,31)=.96,0,.04, COAT(1,32)=.96,0,.04, COAT(1,33)=.96,0,.04,
COAT(1,34)=.96,0,.04, COAT(1,41)=.96,0,.04, COAT(1,42)=.96,0,.04,
COAT(1,43)=.96,0,.04, COAT(1,44)=.96,0,.04, COAT(1,45)=.96,0,.04,
COAT(1,46)=.96,0,.04, COAT(1,47)=.96,0,.04, COAT(1,48)=.96,0,.04,
COAT(1,35)=.01,.02,.01,0,0,.95,.01, COAT(1,36)=.01,.02,.01,0,0,.95,.01,
COAT(1,37)=.01,.02,.01,0,0,.95,.01, COAT(1,38)=.01,.02,.01,0,0,.95,.01,
COAT(1,39)=.01,.02,.01,0,0,.95,.01, COAT(1,40)=.01,.97,.01,.01,
COAT(14,40)=59,59$
$NMEMSN LEMIT=0$
```

Cone and cylinder surfaces are 1 through 6, 41, 43, 47 and 48. Sphere surfaces are 37 through 40. The parameters of the above surfaces are obvious with reference to Figures 2-1 through 2-6.

All the baffles have an edge radius of 0.00003 inch, a thickness of 0.05 inch, and a blade angle of 15 degrees. For the plane baffles, we assume a halfwidth of 0.001 inch for the hyperboloid; see Figure 2-5.

As mentioned in Section 2, there are four surfaces for each baffle. Parameters are read in for the knife edge surfaces 7, 11, 15, 19, 23, 27 and 31. 7, 27, and 31 are plane baffles and the rest are conical. These are indicated by the last argument of each group. As is given, the inclination angles for the conical baffles are 11 degrees.

The standard constraints given by the calculation of basic configurations are satisfactory for most surfaces. However, slight modifications of certain constraints are sometimes necessary. Each of the conical surfaces 1 through 4 has two standard constraints. It is clear, however, that these cones can be allowed to extend indefinitely and the rays in a section will not be falsely intercepted by the extended portion of the cones. The rays will be intercepted by other surfaces because these are at closer distances. Thus, we can remove all the constraints from these surfaces. This is achieved by specifying NSTRT(I) = 0 for I = 1, 2, 3 and 4.

Similarly, no constraint is required on the right hand side of conical surface 6. A constraint is required for the left hand side, however, because the conical surface would have extended into the section. Referring to Paragraph 2.1.2 and the array PTLCTR for surface 6, we see that the first standard constraint is a plane on the left at Z = 3.118 while the second one is a plane on the right at Z = 0.2418. To eliminate the second constraint while keeping the first one, it is necessary only to specify NSTRT(6) = 1.

Referring to Subsection 2.1.5, we see that surface 10, surface 4 of Figure 2-5, is constrained only by the knife edge. It is clear that the surface can be allowed to extend indefinitely on the outside. Thus the number of constraints remains at 1.

Surface numbers for each section are clearly indicated in Figure 9-5. Considering section 7, we have 10 surfaces, that is 4, 31, 32, 34, 35, 41, 42, 43, 44 and 55.

The arrays KCOEF and ISFTP are arranged in the same way as the surface numbers. We will again consider section 7. Surface 4 is a cylinder with the region inside so KCOEF is zero. Surface 31 is a hyperboloid with the region on the side including the center so KCOEF is zero. (See Figure 2-7.)

Surface 35 is a transmitting lens toward the exit so ISFTP is 4. Surface 55 is an aperture toward the entrance so ISFTP is 1. The rest of the surfaces in the section are all non-transmitting surfaces so ISFTP is 5 for each of them.

Important surfaces are 57 and 58 for section 1, 59 and 57 for section 2, etc. The first important surface of section 1, surface 57, is divided into five rings and three segments, etc.

An understanding of the characteristics of the system will assist in the selection of important surfaces. The incident beam 45 degrees off-axis is intercepted by surfaces 15, 17 or 21. We are concerned with the energy that after many transmissions and reflections eventually reaches the detector. As it appears then, we will be interested in the energy that goes into the aperture toward the detector. For example, if we use surface 50 as the important surface for surfaces 7, 8, 10 and 49, we will obtain the energy entering section 2. By repeating the process for all the sections, we will arrive at the energy that reaches the detector.

As we learned from experience, however, we do not obtain the best result using this procedure. For example, when a ray is reflected off surface 10, the portion of the energy going through aperture 50 is rather small. After so many reflections and splitting the energy for the ray is so small when it reaches the detector that it is insignificant when compared with the total energy at the detector. Thus, automatic choice of exit aperture of a section as the important surface is not necessarily the best approach.

Consider a ray being reflected off surface 17. The "shortest" way for this ray to reach the detector is by a single reflection off surface 10 and straight down through the lenses. The energy of this ray will be reduced by importance sampling splitting at surfaces 17 and 10, and absorption and scattering at the lenses and the mirror. Because the ray will hit the mirror off-axis, the energy that reaches the detector will be further reduced by the mirror scattering coefficient. However, the resulting energy of such a ray can be significantly higher than the one described above.

Considering section 1 then, we chose the first important surface, surface 57, as the important surface for surfaces 1, 11, 13 and 50. Thus, every ray from any of these surfaces will be split toward surface 10.

The second important surface of section 1 is the ring 58, in front of the aspheric collector. By assigning this as the important surface for surfaces 7, 8, 10 and 49, we focus our attention on the energy that is going toward the lenses. Note that surface 10 occupies only the middle portion of the baffle surface. When a ray hits the baffle in the outer area, the surface number will be 46 and there will be no splitting. Hence, the values of IMPSF are 0 for surface 46, 1 for surfaces 1, 11, 13 and 50, and 2 for surfaces 7, 8, 10 and 49.

There are three kinds of surfaces in terms of radiation properties. Surfaces 1 through 34 and 41 through 48 are black coated structural surfaces. They have a 96 percent absorptance and a 4 percent diffuse reflectance. Surfaces 35 through 39, the lens surfaces, have 1 percent absorptance, 2 percent specular reflectance, 1 percent diffuse reflectance, 95 percent specular transmittance and 1 percent diffuse forward scattering coefficient. The mirror, surface 40, has 1 percent absorptance, 97 percent specular reflectance, 1 percent diffuse reflectance, and 1 percent near specular reflectance. The angle constant of the exponential decay for the near specular reflectance is obtained from an analysis of the mirror scattering measurement.

The user is warned that an execution of this example requires a relatively large amount of computing time due to its complexity: approximately 15 minutes on a CDC-6600 computer. This problem was taken from an actual analysis performed during the development stage of the GUERAP program. It is included to show the procedure for setting up an input data set for a practical problem.

3366-008

REFERENCES

1. "Use of Expected Value Techniques to Reduce Computer Time Requirements for Multi-stage Baffle/Optical Systems" Appendix 1, Unwanted Energy Rejection Technique Development (UERTD) Progress Report No. 2, 10 September 1971, Honeywell Document 3366-PR2.

2. ibid, "Diffraction Modeling", Appendix 2.

3. "GUERAP User's Manual", T. S. Chou and B. K. Likeness, 6 April 1972, Honeywell Document UERTD TM 3366-007.

4. "Fundamentals of Optics", Jenkins and White, McGraw-Hill, 1957.

5. 'Principles of Optics", Born and Wolf, Pergamon Press, 1959.